Aus dem Institut für Experimentelle Pädiatrische Endokrinologie
der Medizinischen Fakultät Charité – Universitätsmedizin Berlin

Dissertation

Funktionelle Selektivität von G-Protein gekoppelten Rezeptoren in der Energiehomöostase

zur Erlangung des akademischen Grades
Doctor rerum medicinalium (Dr. rer. medic.)

vorgelegt der Medizinischen Fakultät
Charité – Universitätsmedizin Berlin

von

Juliane Dinter (geb. Pratzka)
aus Rodewisch

Datum der Promotion: 30.05.2015

Inhaltsverzeichnis

Inhaltsverzeichnis I

Abbildungsverzeichnis II

Abkürzungsverzeichnis III

1.1 Abstract (deutsch) 1

1.2 Abstract (englisch) 2

2 Einleitung 3
- 2.1 G-Protein gekoppelte Rezeptoren und ihre Rolle in der Energiehomöostase . 3
- 2.2 G-Protein gekoppelter Rezeptor 83 (GPR 83) 6
- 2.3 Melanocortin-4 Rezeptor (MC4R) 6
- 2.4 *Trace amine*-assoziierter Rezeptor 1 (TAAR 1) 6
- 2.5 Beta-adrenerge Rezeptoren 1 und 2 (ADRB 1 und ADRB 2) 7

3 Zielstellungen 8
- 3.1 Aufklärung der Signalisierung des GPR 83 8
- 3.2 Effekte der MC4R-Dimerisierung auf die Signalisierung 8
- 3.3 TAAR 1 Ligandenwirkung an ADRB 1 und ADRB 2 8

4 Methodik 9
- 4.1 G_s- und $G_{i/o}$-Signalweg – cAMP-Assay 9
- 4.2 $G_{q/11}$-Signalweg – IP3-Assay 10
- 4.3 Interaktionsstudien – Sandwich-ELISA 11

5 Ergebnisse 12
- 5.1 Die Aufklärung der $G_{q/11}$ vermittelten Signalisierung des GPR 83 durch konstitutive und Zink (II) induzierte Stimulation 12
- 5.2 Inhibierung der MC4R-Dimerisierung durch Austausch in der intrazellulären Schleife 2 (ICL 2) führt zu Veränderung in der Signalisierung 13
- 5.3 Differentielle Signalmodulation von β-adrenergen Rezeptoren durch TAAR 1 Agonisten 14

6 Diskussion 15
- 6.1 GPR 83 signalisiert via $G_{q/11}$ und kann durch Zink (II) partiell aktiviert werden 15
- 6.2 ICL 2 ist essentiell für die MC4R-Dimerisierung 15
- 6.3 Spurenamine wirken ortho- und allosterisch an ADRB 1 und ADRB 2 16
- 6.4 Schlussbetrachtungen 17

7 Literaturverzeichnis 19

8 Anteilserklärung an den ausgewählten Publikationen 26

9 Druckexemplare der ausgewählten Publikationen **27**
9.1 Publikation 1: G-Protein Coupled Receptor 83 (GPR83) Signaling Determined by Constitutive and Zinc(II)-Induced Activity 27
9.2 Publikation 2: Inhibition of melanocortin-4 receptor dimerization by substitutions in intracellular loop 2 37
9.3 Publikation 3: Differential Modulation of Beta-Adrenergic Receptor Signaling by Trace Amine-Associated Receptor 1 Agonists 48

10 Curriculum Vitae **59**

11 Publikationsliste **64**

12 Eidesstattliche Erklärung **66**

13 Danksagung **67**

Abbildungsverzeichnis

1 Die vier Hauptsignalwege der GPCRs 5
2 Messprinzip cAMP-Assay mittels AlphaScreen Technology® 9
3 Reportergenassay zur IP3-Messung 10
4 Prinzip des Sandwich-ELISA für GPCR-Interaktionsstudien 11
5 Graphische Zusammenfassung zur Aufklärung des Signalwegs des GPR 83 . . 12
6 Graphische Zusammenfassung zu Interaktionsstudien am MC4R 13
7 Unterschiedliche Effekte auf die G_s-Signalisierung durch Spurenamine. 14

Abkürzungsverzeichnis

α / β / γ	alpha / beta / gamma
AC	Adenylatcyclase
ADRB 1 / ADRB 2	β-adrenerger Rezeptor 1 / β-adrenerger Rezeptor 2
Arg	Arginin
Asp	Asparagin
cAMP	zyklisches Adenosinmonophosphat
CB1R	Cannabinoid-1-Rezeptor (Gen *CNR1*)
COS-7	Nierenzellen der grünen Meerkatze (*Cercopithicus aethiops*)
Cys	Cystein
DAG	Diacylglycerol
DAP	2,3-Diaminophenazin
ECL	extrazelluläre Schleife (*extracellular loop*)
EC_{50}	effektive Konzentration (*effective concentration*)
ELISA	*Enzyme-linked immuno sorbent assay*
FLAG	spezifische Protein-Markierung
GDP / GTP	Guanosindiphosphat / Guanosintriphosphat
GHSR	Ghrelin-Rezeptor (*Growth hormone secretagogue receptor*)
Glu	Glutaminsäure
GPCR	G-Protein gekoppelter Rezeptor (*G-protein coupled receptor*)
GPR 83	G-Protein gekoppelter Rezeptor 83
HA	Hämagglutinin (Protein-Markierung)
His	Histidin
HRP	Meerrettichperoxidase (*horseradish peroxidase*)
IBMX	3-Isobutyl-1-methylxanthin
ICL	intrazelluläre Schleife (*intracellular loop*)
IP3	Inositoltrisphosphat
ISOP	Isoproterenol / Isoprenalin
IUPHAR	*International Union of Basic and Clinical Pharmacology*
Leu	Leucin
MC4R	Melanocortin-4-Rezeptor
MSH	Melanozyten-stimulierendes Hormon
NFAT-RE	Transkriptionsfaktor in aktivierten T-Zellen (Responsives Element)
OA / OAR	Octopamin / Octopaminrezeptor
OPD	o-Phenylendiamin
PEA	β-Phenylethylamin
Phe	Phenylalanin
PIP2	Phosphatidylinositolbisphosphat
PKC	Proteinkinase C
PLC	Phospholipase C
POMC	Proopiomelanocortin
PVN	*Nuclei paraventricularis*
RhoA	*Ras homolog gene family, member A*
RhoGEF	Rho-Guaninnukleotidaustauschfaktor
TAAR 1	*Trace amine*-assoziierter Rezeptor 1
TMH	Transmembranhelix
Trp	Tryptophan
TYR / TAR	Tyramin / Tyraminrezeptor
WT	Wildtyp

1.1 Abstract (deutsch)

G-Protein gekoppelte Rezeptoren (GPCRs) sind an der Steuerung aller grundlegenden Zell- und Körperfunktionen wie Metabolismus, Zelldifferenzierung und Wachstum beteiligt. Die Eigenschaften und Mechanismen der GPCRs sind komplex, wobei jeder einzelne Rezeptor individuell zu betrachten und im Zusammenhang zu untersuchen ist.
In dieser Arbeit wurden Rezeptoren erforscht, die insbesondere in der Energiehomöostase eine Rolle spielen und Lücken im Verständnis ihrer Funktionalität aufweisen. Der Fokus wurde auf fünf ausgewählte GPCRs gelegt, den G-Protein gekoppelten Rezeptor 83 (GPR 83), den Melanocortin-4 Rezeptor (MC4R), die β-adrenergen Rezeptoren 1 und 2 (ADRB 1 und ADRB 2), sowie den *Trace amine*-assoziierten Rezeptor 1 (TAAR 1). Es sollten Signalwege des orphanen (Ligand unbekannt) GPR 83, Interaktions-Regulationsmechanismen des wichtigsten GPCR in der Appetitregulation - MC4R, sowie differentielle Signalisierungsmodulationen an ADRB 1 und ADRB 2 untersucht werden.
Im Rahmen der genannten Projekte und der hier aufgeführten resultierenden Publikationen wurden die wichtigsten Signalwege funktionell mittels zellbasierter Stimulationsversuche charakterisiert. Zum anderen wurden GPCR-GPCR Interaktionen durch die Methode des Sandwich-ELISA überprüft.
Die Untersuchungen zeigten, dass der GPR 83 im Zusammenspiel mit Zink (II) den $G_{q/11}$-Signalweg aktiviert, basal aktiv (Liganden unabhängig) ist, sich für $G_{q/11}$ durch bestimmte Mutationen auch konstitutiv aktivieren lässt und als Homodimer vorliegt. Durch die Studien zum MC4R konnte festgestellt werden, dass die intrazelluläre Schleife 2 und Teile der verbundenen Transmembranhelizes 3 und 4 zur Bildung von MC4R-Homodimeren essentiell sind. Durch eine gezielte Separierung des Homodimers durch Modifikationen an diesen Komponenten wurde eine gesteigerte Liganden unabhängige Basalaktivität erzeugt, was auf einen inhibitorischen Einfluss durch die Dimerisierung schließen lässt. Die Spurenamine Tyramin, β-Phenylethylamin und Octopamin sind nicht nur Agonisten des TAAR 1, sondern wirken auch als partielle Antagonisten oder Agonisten an ADRB 1 und ADRB 2. Die differentielle Modulation zeigte sich entweder in einer Blockade oder in einer Aktivierung des G_s-Signalweges. Strukturmodellbetrachtungen im Zusammenspiel mit den funktionellen Daten führten zu der Schlussfolgerung, dass die gemeinsamen Liganden von TAAR 1, ADRB 1 und ADRB 2 aufgrund einer hohen Aminosäureähnlichkeit in einer bestimmten Ligandenbindungsregion lokalisiert sind und ortho- oder allosterisch wirken.
Zusammenfassend führten alle drei Hauptprojekte zu neuen Erkenntnissen, auf die in weiteren Studien aufgebaut werden kann. Es wurden insbesondere neue Details zur funktionellen Selektivität von GPCRs in der komplexen Regulation gezeigt, die nicht zuletzt helfen können, in das Problem des zunehmenden Übergewichts weiter Teile der Weltbevölkerung zielgerichtet und selektiv pharmakologisch einzugreifen.

1.2 Abstract (englisch)

G-protein coupled receptors (GPCRs) are involved in the control of all basic cellular and physiological functions such as metabolism, cell differentiation and growth. The characteristics and mechanisms of GPCRs are complex, while each individual receptor needs to be investigated individually and considered in context to each other.
Within this paper receptors were ascertained which are particularly involved in the energy homeostasis but which still hold gaps in understanding their functionality. The focus was placed on five selected GPCRs, the G-protein coupled receptor 83 (GPR 83), the melanocortin-4 receptor (MC4R), the β-adrenergic receptors 1 and 2 (ADRB 1 and ADRB 2), and the trace amine-associated receptor 1 (TAAR 1). The aim was to unravel signaling pathways of the orphan (ligand unknown) GPR 83, regulatory interaction mechanisms of the most important GPCR in appetite regulation – the MC4R, and differential signaling modulations of ADRB 1 and ADRB 2.
In the scope of these projects and the resulting publications listed here the most important signaling pathways were functionally characterized using cell-based stimulation assays. On the other hand GPCR-GPCR interactions were investigated using a sandwich-ELISA approach.
The investigations showed that the GPR 83 is activated in combination with zinc (II) in the $G_{q/11}$-signaling pathway, is basally active (ligand independent), can be activated constitutively for $G_{q/11}$ by a certain mutation, and moreover is present as homodimer. Through the MC4R studies it was shown that the intracellular loop 2 and parts of the conjoined transmembrane helices 3 and 4 are essential for MC4R homodimer formation. Modifications of these components led to a selective separation of the homodimers and increased the ligand independent basal activity suggesting an inhibitory influence by the dimerization. The trace amines tyramine, β-phenylethylamine and octopamine are not only agonists at TAAR 1, but also act as partial antagonists or agonists at ADRB 1 and ADRB 2. The differential modulation was exhibited in either a blockade or an activation of the G_s-signaling pathway. Consideration of structure models in combination with the obtained functional data led to the conclusion that the shared ligands of TAAR 1, ADRB 1 and ADRB 2 are localized in a specific ligand binding region due to their high amino acid similarity, thus acting ortho- or allosterically.
In summary, all three main projects led to new insights providing information and knowledge for further studies. New details unraveling the functional selectivity of GPCRs in the complex regulation are shown which may help to reduce the increasing obesity as problem of the world population by intervening with selective pharmaceuticals.

2 Einleitung

2.1 G-Protein gekoppelte Rezeptoren und ihre Rolle in der Energiehomöostase

G-Protein gekoppelte Rezeptoren (GPCRs) sind an der Steuerung lebenswichtiger Körperfunktionen wie dem Metabolismus, neuronaler Transduktion, Sekretion, Zelldifferenzierung und Wachstum, sowie inflammatorischen oder immunologischen Antworten beteiligt (Bouvier, 2001). Sie sind zudem mit ca. 800 Genen die größte Gruppe der membranständigen Proteine beim Menschen (Jassal *et al.*, 2010). Darüber hinaus werden mehr als 90 % der GPCRs im Gehirn exprimiert (Vassilatis *et al.*, 2003), von wo auch die Appetitregulation sowie die Energiehomöostase mitgesteuert werden. Allein rund 40 GPCRs sind direkt in der Appetitregulation involviert (Schioth, 2006), wobei die im Hypothalamus vorkommenden GPCRs eine besondere Rolle in der Appetitregulation spielen (Sainsbury & Zhang, 2012). Gestörtes Körpergewicht weist multifaktorielle Ursachen auf, wobei die generelle Auswirkung in einer Verschiebung von Energieaufnahme und Energieverbrauch liegt (Rui, 2013). Als Folgen können Übergewicht und Adipositas resultieren, die zu den großen globalen Gesundheitsproblemen zählen (OECD, 2010). GPCRs sind aufgrund ihrer zentralen Rolle ideale Angriffsorte für pharmakologische Interventionen (Stallaert *et al.*, 2011), nicht zuletzt auch für die Gegenregulation pathogener Störungen im Metabolismus. Daher besteht die Notwendigkeit der umfassenden Untersuchung involvierter GPCRs und ihrer Funktionalität, um pharmakologische Eingriffe bestmöglich zu erkennen und unter der Minimierung unerwünschter Nebeneffekte zu gestalten.

GPCRs sind eine Superfamilie von membranständigen Rezeptoren, die aus sieben Transmembranhelizes (TMHs) mit drei intra- und drei extrazellulären Schleifen (ICLs bzw. ECLs) bestehen. Diese Superfamilie wird in mehrere Familien unterteilt, wohingegen die Familie A (*rhodopsin-like receptors*) mit etwa 3000 Mitgliedern den größten Anteil darstellt (Kakarala & Jamil, 2014). Neben den Familie A GPCRs existieren fünf weitere Familien.

GPCRs vermitteln zelluläre Reaktionen zumeist durch die Bindung von Liganden, welche die Zelle im extrazellulären Bereich erreichen.

GPCRs werden durch verschiedene Eigenschaften charakterisiert:

i) Etwa 60 Wildtyp (WT) GPCRs weisen eine Liganden unabhängige Signalisierungsaktivität auf (Seifert & Wenzel-Seifert, 2002). Diese Rezeptoren befinden sich in einer dauerhaft teilaktiven Konformation und signalisieren folglich konstitutiv (Rosenbaum *et al.*, 2009).

ii) Zu den Signal-induzierenden Liganden zählen physiologisch zumeist Agonisten, die den Rezeptor aktivieren, aber auch Antagonisten (zumeist synthetisch, nicht endogen), die die Signalisierung blockieren.

Eine klassische Rezeptoraktivierung lässt sich durch Bindung eines Agonisten bewirken. Dieser bindet in der endogenen Ligandenbindungsregion (orthosterisch), bewirkt eine Konformationsänderung des Rezeptors und damit eine Auslösung von Signalisierung (siehe iii). Antagonisten binden ebenfalls an den Rezeptor, ohne dabei eine Signalkaskade auszulösen, inhibieren jedoch auf verschiedene Weise die Wirkung der Agonisten. Das anerkannte Phänomen der allosterischen Liganden bezieht sich auf das Vorkommen mehrerer Bindungsorte für Liganden in einem Rezeptormolekül (Motlagh *et al.*, 2014). Eine besondere Form von Antagonisten sind inverse Agonisten, sie reduzieren auch aktiv die Basal- oder konstitutive Aktivität von GPCRs (siehe i).

iii) Die Anordnung der sieben TMHs liegt in einem dynamischen Zustand vor und wird durch Wasserstoffbrückenbindungen stabilisiert (Stallaert *et al.*, 2011; Teller *et al.*, 2001). Durch Ligandenbindung kommt es schließlich zu einer Veränderung der TMH-Anordnung. Im Zuge der Aufklärung verschiedener Kristallstrukturen des ADRB 2 konnten die TMHs und deren Reaktionen auf Ligandenbindung beschrieben werden, die generell an der Konformationsänderung zwischen in- und aktivem Zustand beteiligt sind. Dabei stellte sich heraus, dass zur Rezeptoraktivierung insbesondere die TMH 6 eine große Bewegung vollziehen muss, während die TMH 5, die ICL 2 und die ICL 3 durch eher kleinere Bewegungen bzw. Verlängerungen den Rezeptor aktivieren (Rasmussen *et al.*, 2011).

iv) Die Aktivierung der vier G-Protein gekoppelten Hauptsignalwege G_s, $G_{i/o}$, $G_{q/11}$ und $G_{12/13}$ und deren nachgeschalteten Signalisierungskaskaden, wird durch die jeweilige Dissoziation der Carboxy-terminalen G-Protein Untereinheit ausgelöst (Abb. 1). Alle G-Protein Subtypen sind Heterotrimere und bestehen aus einer α-, β-, γ-Untereinheit. Durch eine Rezeptor-vermittelte Konformationsänderung und den Austausch von im G-Protein gebunden GDP zu GTP kommt es zur Dissoziation einer der G-Protein Untereinheiten. Die sogenannten G_s-Proteine (s für stimulierend) stimulieren die Adenylatcyclase (AC), was zu einem Anstieg des sekundären Botenstoffes cAMP führt. $G_{i/o}$-Proteine bewirken Gegenteiliges durch die Inhibition der AC und folglich eine Absenkung von intrazellulärem cAMP. $G_{q/11}$-Proteine stimulieren die Phospholipase C (PLC), die Phosphatidylinositolbisphosphat (PIP2) hydrolysiert, was zur Bildung der sekundären Botenstoffe Inositoltriphosphat (IP3) und Diacylglycerol (DAG) führt (Scholz, 1989). IP3 wiederum aktiviert die Freigabe von Calcium im Endoplasmatischen Retikulum, während DAG die Proteinkinase C (PKC) aktiviert (Billington & Penn, 2003). Das vierte wichtige G-Protein ist das $G_{12/13}$-Protein, durch dessen Aktivierung den Rho-Guaninnukleotidaustauschfaktor (RhoGEF) und schließlich das *Ras homolog gene family, member A* (RhoA) aktiviert wird. Ein GPCR kann über einen oder aber auch mehrere Signalwege signalisieren. Darüber hinaus kann ein Rezeptor selektiv für einen Liganden sein, aber auch durch mehrere Agonisten aktiviert werden

und jeweils verschiedene Signalwege aktivieren. In diesem Fall wird von funktioneller Selektivität gesprochen (Stallaert *et al.*, 2011). Alle sekundären Botenstoffe aktivieren ein komplexes Netzwerk von Signalvermittlern, die letztendlich Prozesse wie Zellproliferation, Zellviabilität, Angiogenese oder Differenzierung auslösen oder steuern (Dorsam & Gutkind, 2007).

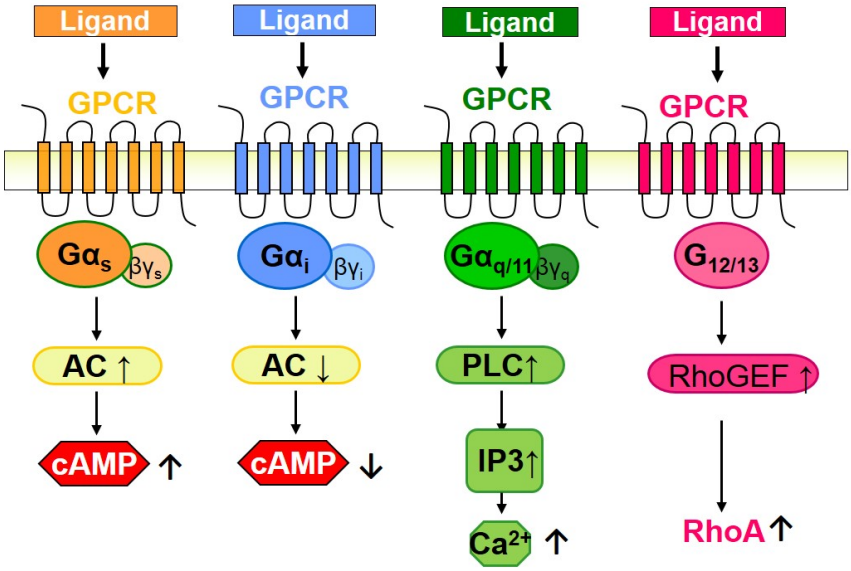

Abb. 1: Die vier Hauptsignalwege der GPCRs.
Die Aktivierung der vier Hauptsignalwege $G_{i/o}$, G_s, $G_{q/11}$ und $G_{12/13}$ und deren nachgeschaltete Signalisierungskaskade: Das heterotrimere G-Protein besteht aus einer α- und einer $\beta\gamma$-Untereinheit durch deren Dissoziation die nachfolgenden Signalwege ausgelöst werden. G_i-Proteine bewirken die Inhibition der AC und folglich eine Absenkung von cAMP. Die G_s-Proteine stimulieren die Adenylatcyclase (AC), was zu einem Anstieg des sekundären Botenstoffes cAMP führt. $G_{q/11}$-Proteine stimulieren die Phospholipase C (PLC), durch die es zur Bildung von Inositoltriphosphat (IP3) kommt, was wiederum die Calcium-Ausschüttung aktiviert. Das $G_{12/13}$-Protein, aktiviert den Rho-Guaninnukleotidaustauschfaktors (RhoGEF) und schließlich den *Ras homolog gene family, member A* (RhoA).

v) Ein weiteres Charakteristikum von GPCRs ist die Möglichkeit zur Formation von Rezeptor-Dimeren (Maggio *et al.*, 1996). Durch die Interaktion des GPCR mit dem gleichen Subtyp (Homooligomerisierung) oder mit einem anderen Subtypen (Heterooligomerisierung) können die Rezeptoreigenschaften erheblich modifiziert werden. Zum einen kann beispielsweise ein weiterer Signalweg in Form von funktioneller Selektivität aktiviert (Rovira *et al.*, 2010) und so das Signalspektrum erweitert werden (Hernanz-Falcon *et al.*, 2004). GPCR-Oligomerisierung kann aber auch die Ligandenbindung beeinflussen und somit zu einer Signalverstärkung führen (George *et al.*, 2002). Weiterhin kann die GPCR-GPCR-Interaktion Änderungen in der Rezeptorfaltung und im Transport der GPCRs zur Zelloberfläche mit sich zu ziehen (George *et al.*, 2002).

Die Eigenschaften der GPCRs sind zusammengefasst sehr komplex. In dieser Arbeit werden Rezeptoren betrachtet, die in der Energiehomöostase eine Rolle spielen und die Lücken im Verständnis ihrer Funktionalität aufzeigen.

2.2 G-Protein gekoppelter Rezeptor 83 (GPR 83)

Bei dem zur Familie A gehörenden G-Protein gekoppelten Rezeptor 83 (GPR 83) handelt es sich um einen orphanen GPCR, von dem der Ligand und / oder die Funktion unbekannt ist (Wise *et al.*, 2004). Der GPR 83 wird überwiegend im Thymus und in diversen hypothalamischen Nuclei exprimiert, die bekannterweise eine Rolle in dem Energiemetabolismus spielen (Nakazato *et al.*, 2001). Weiterhin steht der GPR 83 im Verdacht, eine Rolle in der Hypothalamus-Hypophysen-Nebennierenrinden Achse zu spielen (Müller *et al.*, 2013a). Weiterhin konnte gezeigt werden, dass die Expression von GPR 83 in übergewichtigen Mäusen im Vergleich zu Wildtyp-Mäusen erhöht ist (Müller *et al.*, 2013b). Um die Rolle des GPR 83 in physiologische Regulationen besser einordnen zu können, müssen auch die molekularen Eigenschaften dieses orphanen GPCRs aufgeklärt werden.

2.3 Melanocortin-4 Rezeptor (MC4R)

Ein weiterer Akteur in der Energiehomöostase ist der Melanocortin-4 Rezeptor (MC4R), der zur Familie A der GPCR gehört. Der MC4R spielt eine wichtige Rolle im Leptin-Melanocortin System (Hebebrand *et al.*, 2013). Die Expression von Proopiomelanocortin (POMC) im Hypothalamus wird durch das in Adipozyten synthetisierte Hormon Leptin (Friedman, 2014) hochreguliert und hat die Ausschüttung von α- und β-MSH (Melanozyten-stimulierendes Hormon) zur Folge. Diese aktivieren den im hypothalamischen *Nuclei paraventricularis* (PVN) exprimierten MC4R (Ellacott & Cone, 2006). Der MC4R signalisiert über den G_s-Signalweg und bewirkt durch nachfolgende Signalkaskaden die Ausschüttung von anorexigenen Peptiden und inhibiert orexigene Peptide (Breit *et al.*, 2011). Eine Vielzahl von natürlich vorkommenden inaktivierenden heterozygoten Mutationen ist für den MC4R bekannt, die auch die häufigste genetische Ursache für Übergewicht im Menschen ist (Farooqi *et al.*, 2003). Weiterhin besitzt auch der MC4R die Fähigkeit, Homo- oder Heterooligomere zu bilden (Biebermann *et al.*, 2003; Piechowski *et al.*, 2013). Welche Rolle die Oligomerisierung für die Funktionalität des MC4R spielt, war bislang ungeklärt. Da der MC4R ein Kandidat zur pharmakologischen Intervention gegen Übergewicht ist, muss das Verhalten der Oligomerisierung auf die Signalwirkung geklärt werden.

2.4 *Trace amine*-assoziierter Rezeptor 1 (TAAR 1)

Trace amine-assoziierte Rezeptoren (TAARs) zählen ebenfalls zu den Familie A GPCRs (Borowsky *et al.*, 2001; Bunzow *et al.*, 2001). Der TAAR 1 ist der am besten charakterisierte Subtyp von neun humanen Rezeptor-Varianten (Lindemann *et al.*, 2005). TAAR 1 wird im Menschen in verschiedenen inneren Organen, aber auch in diversen Hirnregionen wie u. a. im Hypothalamus exprimiert (Borowsky *et al.*, 2001; Lewin, 2006; Regard *et al.*, 2007).

TAARs spielen eine Rolle in der Modulation neuronaler und kardiovaskulärer Prozesse und vermutlich auch in der Energiehomöostase (Braulke *et al.*, 2008; Doyle *et al.*, 2007; Fehler *et al.*, 2010; Frascarelli *et al.*, 2008). Der Subtyp TAAR 1 ist promiskuitiv für ein breites Spektrum von Liganden und wird im G_s-Signalweg durch Spurenamine (*trace amines*) wie Tyramin (TYR), β-Phenylethylamin (PEA), Octopamin (OA), aber auch durch Schilddrüsenhormonderivate oder Neurotransmitter aktiviert (Kleinau *et al.*, 2011). Das Spurenamin OA zeigte in Adipozyten eine durch β-adrenerge Rezeptoren vermittelte Induktion der Lipolyse (Carpene *et al.*, 1999). Weiterhin spielen Spurenamine eine Rolle im Energiemetabolismus, da beispielsweise verringerte OA-Werte bei anorektischen Patienten und erhöhte TYR-Werte bei an Bulimie erkrankten gefunden wurden (D'Andrea *et al.*, 2008).
Der Zusammenhang zwischen TAAR 1, seiner Sequenz- / Strukturähnlichkeit zu adrenergen Rezeptoren und seinem breiten Ligandenprofil ist bisher lückenhaft, kann aber für das Verständnis seiner Rolle in der Energiehomöostase essentiell sein.

2.5 Beta-adrenerge Rezeptoren 1 und 2 (ADRB 1 und ADRB 2)

Die adrenergen Rezeptoren sind eine sehr intensiv erforschte Gruppe von GPCRs und kommen ebenfalls in neun verschiedenen Varianten vor (Kobilka, 1992). Diese werden generell den α- und β-adrenerge Rezeptoren zugeteilt (IUPHAR Datenbank 12.8.14). In der vorliegenden Arbeit wurde der Fokus auf die β 1- und β 2-adrenergen Rezeptoren (ADRB 1 und ADRB 2) gelegt, ausgehend von den bereits erwähnten starken Ähnlichkeiten der Aminosäuresequenzen zu TAAR 1 (siehe 2.4). Für ADRB 1 und ADRB 2 ist jeweils eine Vielzahl von Liganden bekannt. Hauptsächlich handelt es sich um zwei endogene Agonisten, Adrenalin und Noradrenalin, und um synthetische Agonisten wie Isoproterenol. Antagonisten wie Propranolol sind ebenfalls synthetischer Natur. Beide untersuchten GPCRs signalisieren über die Aktivierung des G_s-Proteins. ADRB 1 und ADRB 2 werden beide im Auge und in der Lunge exprimiert, während der ADRB 1 zusätzlich im Hypothalamus vorkommt (Regard *et al.*, 2008). Beta-adrenerge Rezeptoren besitzen eine Vielzahl von Angriffspunkten durch die Beeinflussung kardiovaskulärer Funktionen, die wiederum die Energiehomöostase beeinflussen (Chruscinski *et al.*, 1999). Da ADRB 1 und ADRB 2 auch in Prä-Adipozyten exprimiert werden, beide in der Lipolyse involviert sind und Studien zeigten, dass β-adrenerge Rezeptoren an Adipositas und Lipideinlagerung beteiligt sind (Robidoux *et al.*, 2004), liegen weitere Indizien für eine Rolle in der Energiehomöostase vor. Da Agonisten von β-adrenergen Rezeptoren auch TAAR 1 aktivieren können, stellte sich zudem die umgekehrte Frage, ob TAAR 1 Agonisten (Spurenamine) auch Effekte an ADRB 1 und ADRB 2 auslösen.

3 Zielstellungen

Die vorliegende Arbeit sollte helfen, wichtige bislang ungeklärte Aspekte von GPCRs aufzuklären, die in der Energiehomöostase involviert sind. Hierfür wurde Fokus auf fünf spezielle GPCRs gelegt, GPR 83, MC4R, ADRB 1 und ADRB 2 sowie TAAR 1. Mit dieser Arbeit sollten Signalwege eines orphanen GPCRs, GPCR-GPCR-Dimerbildungscharakteristika, sowie differentielle Signalisierungsmechansimen untersucht werden.

3.1 Aufklärung der Signalisierung des GPR 83

Ziel dieser Arbeit war es Einblicke in die molekulare Grundlage der GPR 83-Signalisierung zu erlangen. Dies sollte durch eine mutationsbasierte Aktivierung realisiert werden. Zum anderen ist von einigen GPCRs bereits bekannt, dass sich diese durch Metallionen aktivieren oder in ihrer Signalisierung modifizieren lassen: Eine Wirkung von Zink (II)-Ionen und weiteren 2-wertigen Metallionen sollte daher am GPR 83 getestet werden. Eine weitere bemerkenswerte Eigenschaft von G-Protein gekoppelten Rezeptoren ist die Fähigkeit der direkten Interaktion miteinander durch die Dimerisierung oder auch Oligomerisierung. Daher sollte auch der GPR 83 auf die Formation von Homodimeren untersucht werden, um diesen Kandidaten in der Energiehomöostase vollständig funktionell zu charakterisieren.

3.2 Effekte der MC4R-Dimerisierung auf die Signalisierung

Im Fokus dieser Arbeit stand die Entschlüsselung des Zusammenhanges zwischen Signalisierung und MC4R-Dimerisierung. Dafür sollten zuerst die Dissoziation des Dimerzustandes in Monomere erreicht und dessen Auswirkung auf die Signalisierung im Vergleich charakterisiert werden. Hierzu sollten modifizierte MC4R Varianten generiert werden, die durch den Austausch von speziellen Strukturbereichen des Cannabinoid-1-Rezeptors (CB1R) kein Dimer mehr bilden können. Dieser ist ebenfalls ein GPCR, der eine Rolle in der Energiehomöostase spielt und keine Interaktion mit dem MC4R eingeht. Die funktionellen Parameter von Wildtyp (WT) und der natürlich vorkommenden MC4R Variante H158R sollten mit diesen Chimären MC4R / CB1R Varianten verglichen werden.

3.3 TAAR 1 Ligandenwirkung an ADRB 1 und ADRB 2

Ziel dieser Arbeit war die Untersuchung der Effekte von speziellen TAAR 1 Liganden auf die Signalisierung der homologen ADRB 1 und ADRB 2. TAAR 1 kann nicht nur von den Spurenaminen TYR, PEA und OA aktiviert werden, sondern auch durch β-adrenerge Agonisten wie ISOP. Die Spurenamine sollten daher in Hinblick auf ihre Effekte auf die Signalisierung von ADRB 1 und ADRB 2 mittels Ko-Stimulationsversuchen getestet werden. Weiterhin wurden vergleichende Strukturmodell-Analysen zwischen homologen Rezeptoren durchgeführt.

4 Methodik

Zur Untersuchung von GPCRs stehen eine Vielzahl von molekularbiologischen *in vitro* Methoden zur Verfügung. Zum einen kann die Signalisierung mittels zellbasierter Stimulationsversuche bestimmt werden und zum anderen gibt es Möglichkeiten zur Charakterisierung von GPCR-GPCR-Interaktionen. Im Rahmen dieser Arbeit wurden die GPCRs auf die drei unterschiedlichen Signalwege G_s, $G_{i/o}$ und $G_{q/11}$ funktionell charakterisiert. Die Interaktionsstudien wurden mit der biochemischen Methode des Sandwich-ELISA durchgeführt.
Besonderes Augenmerk sollte an dieser Stelle auf ein Mitführen geeigneter Kontrollen liegen. In den funktionellen Assays wurde der zu untersuchende GPCR stets ohne oder mit Ligand (basal bzw. stimuliert) getestet. Außerdem wurde stets eine Negativkontrolle basal und stimuliert, sowie Positivkontrollen mitgeführt. Auch bei dem Sandwich-ELISA wurden Negativ- und Positivkontrollen, sowie eine Nicht-Interaktion für den zu untersuchenden Rezeptor gezeigt.

4.1 G_s- und $G_{i/o}$-Signalweg – cAMP-Assay

Für die durchgeführten Experimente wurden die eukaryotischen *Human embryonic kidney* (HEK 293)- oder die von Meerkatzen-abgeleiteten Nierenzellen (COS-7-Zellen) genutzt (Müller *et al.*, 2013a; Piechowski *et al.*, 2013). Diese wurden transient mit der entsprechenden Plasmid-DNA transfiziert und ohne bzw. mit Ligand in Anwesenheit des Phosphodiesterase-Hemmers 3-Isobutyl-1-methylxanthin (IBMX), zur Inhibition des cAMP-Abbaus, inkubiert. Zur Analyse von $G_{i/o}$-koppelnden Rezeptoren wurden die Zellen mit Forskolin inkubiert, um die allgemeine Adenylatcyclase zu stimulieren. Im Falle eines $G_{i/o}$-signalisierenden Rezeptors kommt es mit einem Agonisten zur Absenkung des cAMP-Levels.

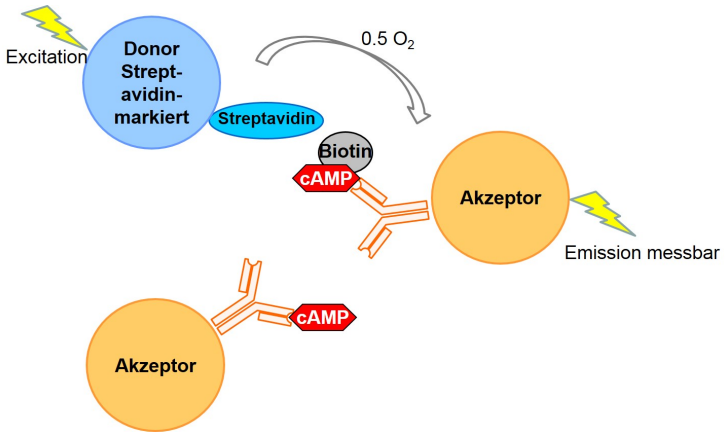

Abb. 2: Messprinzip cAMP-Assay mittels AlphaScreen Technology®.
Es handelt sich um einen kompetitiven Immunoassay, bei dem biotinyliertes cAMP mit dem cAMP der Probe um die Bindungsstelle eines Anti-cAMP-Antikörpers konkurriert, der an Akzeptorkügelchen gebunden ist. Im Falle einer Bindung mit dem Kompetitor koppeln die mit Streptavidin-markierten Donorkügelchen die Biotinmarkierung. Nach Excitation der Donorkügelchen kommt es zur Energieübertragung auf die Akzeptorkügelchen, wodurch eine messbare Emission von Lichtwellen resultiert.

Nach Ligandeninkubtion wurden die Zellen lysiert und mittels der AlphaScreen Technology® (Perkin Elmer Inc.) gemessen. Dabei handelt es sich um einen kompetitiven Immunoassay, bei dem biotinyliertes cAMP mit dem cAMP der Probe um die Bindungsstelle eines Anti-cAMP-Antikörpers konkurriert (Abb. 2). Im Falle der Bindung mit dem Kompetitor bindet der mit Streptavidin-markierte Donor die Biotinmarkierung. Nach Excitation der Donorkügelchen kommt es zur Energieübertragung auf die Akzeptorkügelchen, was in einer messbaren Emission von Lichtwellen resultiert. Je höher das Signal, desto niedriger ist die cAMP-Menge. Mittels einer Standardreihe kann der cAMP-Gehalt der Probe genau ermittelt werden.

4.2 $G_{q/11}$-Signalweg – IP3-Assay

Die Charakterisierung des $G_{q/11}$-Signalwegs wurde mit einem Reportergenassay in HEK 293-Zellen durchgeführt (Müller *et al.*, 2013a). Dafür wurden die Zellen mit einem Reporterkonstrukt und der entsprechenden Rezeptorplasmid-DNA ko-transfiziert. Das Reporterkonstrukt besteht aus dem Gen für die Firefly-Luciferase unter der Kontrolle eines responsiven Elements für den *Transkriptionsfaktor in aktivierten T-Zellen (nuclear factor of activated T-cells,* NFAT) (Abb. 3). Durch die $G_{q/11}$-Signalisierung kommt es intrazellulär zur Bildung von IP3, was durch weitere Schritte einen Anstieg von Calcium bewirkt. Calcium bindet und aktiviert Calmodulin, das wiederrum Calcineurin bindet. Calcineurin dephosphoryliert NFAT, welches schließlich im Nucleus das entsprechende responsive Element (NFAT-RE) bindet. Dadurch wird die Luciferase exprimiert. Zur Messung wurde das Substrat Oxyluciferin hinzugegeben, um die bei der Substratumsetzung entstandenen Lichtwellen zu messen.

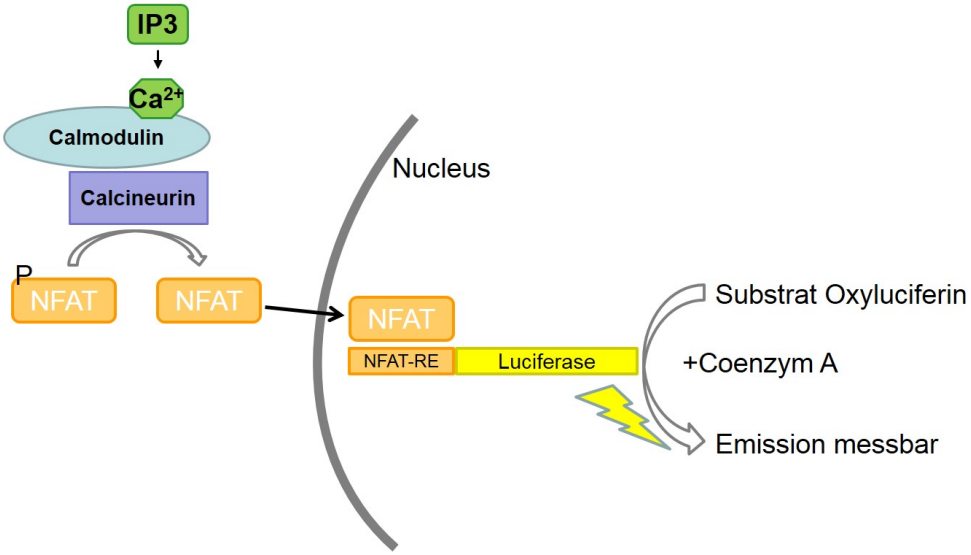

Abb. 3: Reportergenassay zur IP3-Messung.
Die Bildung von Inositoltriphosphat bewirkt einen Anstieg von Calcium (Ca^{2+}). Dieses bindet und aktiviert Calmodulin, das wiederrum Calcineurin bindet. Calcineurin dephosphoryliert den nukleären *Transkriptionsfaktor in aktivierten T-Zellen (nuclear factor of activated T-cells*, NFAT), welches schließlich im Nucleus das entsprechende responsive Element (NFAT-RE) bindet. Dadurch wird die Luciferase exprimiert, die durch die Umsetzung des Substrates Oxyluciferin messbare Lichtwellen entstehen.

4.3 Interaktionsstudien – Sandwich-ELISA

Für den Sandwich-*Enzyme-linked immuno sorbent assay* (ELISA) wurden COS-7-Zellen mit zwei auf verschiedene Weise markierten Konstrukten transfiziert (Piechowski *et al.*, 2013). Ein Rezeptor ist dabei N-terminal Hämagglutinin (HA) markiert und der weitere zu untersuchende Rezeptor wird Carboxy-terminal Flag-markiert (Abb. 4).
Durch eine besondere Zusammensetzung des Lysepuffers und optimierten Zentrifugationsschritten können Dimere aus der Zellmembran gelöst werden, ohne dabei die Interaktion zu zerstören. Die isolierte Proteinsuspension wurde auf eine mit Anti-Flag-Antikörper beschichtete Multiwell-Platte gegeben und mit einem Biotin markierten Anti-HA-Antikörper behandelt. Als nächsten Schritt wurde eine Meerrettichperoxidase (HRP) mit Streptavidin-Markierung hinzugegeben, die das Biotin hochspezifisch bindet. Mit dem Substrat o-Phenylendiamin (OPD) bewirkt die HRP eine Farbreaktion. Diese Farbentwicklung wurde mit einem Photometer (Anthos Labtec Instruments, Wals, Österreich) durch die Messung der optischen Dichte (OD 0,02 - 1,0) bei den Wellenlängen 492 nm / 620 nm bestimmt.

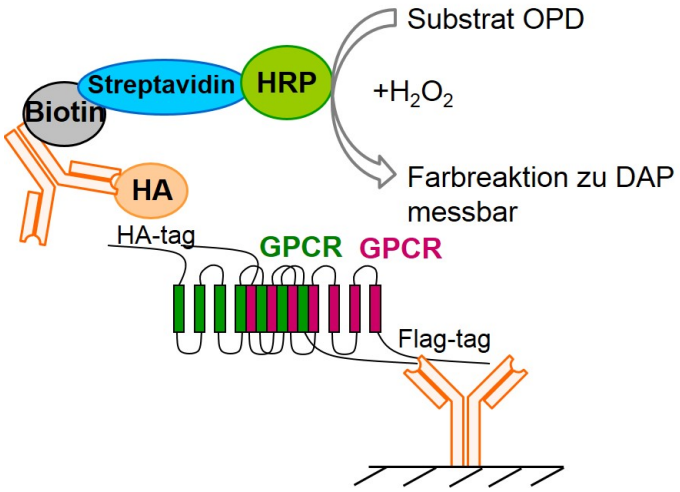

Abb. 4: Prinzip des Sandwich-ELISA für GPCR-Interaktionsstudien.
Ein GPCR wird N-terminal Hämagglutinin (HA) markiert und ein weiterer GPCR wird Carboxy-terminal Flag-markiert. Das Dimer wird mit einer mit Anti-Flag-Antikörper beschichteten Multiwell-Platte inkubiert und mit einem mit Biotin-markierten Anti-HA-Antikörper behandelt. Als nächster Schritt wurde eine Meerrettichperoxidase (HRP) mit Streptavidin-Markierung hinzugegeben, die hochspezifisch Biotin bindet. HRP bewirkt mit dem Substrat o-Phenylendiamin (OPD) in Anwesenheit von Wasserstoffperoxid eine Farbreaktion zu 2,3-Diaminophenazin (DAP), die bei 492 nm/ 620 nm gemessen wird.

5 Ergebnisse

5.1 Die Aufklärung der $G_{q/11}$ vermittelten Signalisierung des GPR 83 durch konstitutive und Zink (II) induzierte Stimulation

Publikation 1: Müller, A.*, Kleinau G.*, ... Pratzka J. *et al.* (2013): G-Protein Coupled Receptor 83 (GPR83) Signaling Determined by Constitutive and Zinc(II)-Induced Activity. PLoS One. [15. Januar 2013]

In dieser Arbeit wurde zum ersten Mal gezeigt, dass der Maus-GPR83 (mGPR 83) eine erhöhte basale $G_{q/11}$-Aktivität aufwies, die mit 2,3-facher Signalisierung signifikant über der Negativkontrolle lag. Dabei wurden weder die $G_{i/o}$- noch die G_s-Signalwege beeinflusst. Eine weitere Möglichkeit der Rezeptoraktivierung wurde in dieser Arbeit mittels eines Aminosäureaustausches an einer hochkonservierten Aminosäure in der Transmembranhelix (TMH) 6 realisiert (C304W). Somit konnte eine zusätzliche Aktivierung von 21 % gegenüber der Basalaktivität des WT erzielt werden. Weiterhin wurden Zink (II)-Ionen als Aktivatoren für GPR 83 identifiziert. Weitere getestete 2-wertige Ionen wie Calcium (II)- oder Magnesium (II)-Ionen erzielten hingegen keine Wirkung. Zink (II) reagierte als Agonist in physiologischen Konzentrationsbereichen, was sich durch einen 4-fachen Anstieg der IP3-Formation zeigte. Eine Konzentrations-Wirkungs-Kurve lieferte mit einem EC_{50}-Wert von 10.2±1.4 µM Zink (II) einen biphasischen Verlauf, der auf verschiedene Bindungsstellen hindeutet. Im Zuge dieser Erkenntnisse wurde ein Bereich von Ionenbindungs-sensitiven Aminosäuren (His145, His204, Cys207, Glu217 und Asp227) in einer für Aktivierung sensiblen Region des GPR 83, identifiziert, da die Sensitivität für Zink (II) bei Mutation dieser Aminosäuren vermindert wurde. Ein weiteres Charakteristikum des GPR 83 ist die Fähigkeit Homodimere zu bilden.

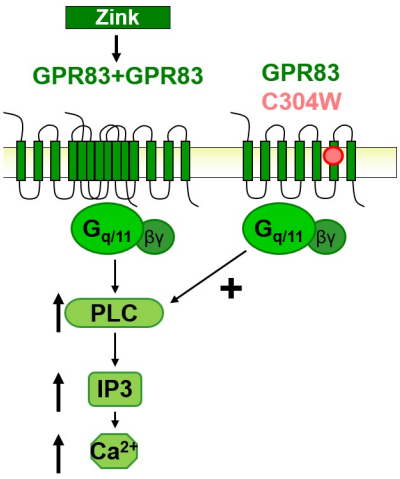

Abb. 5: Graphische Zusammenfassung zur Aufklärung des Signalwegs des GPR 83. Der als Homodimer vorliegende GPR 83 signalisiert über den $G_{q/11}$-Signalweg mit Stimulation der Phospholipase C (PLC) und Bildung von Inositoltriphosphat (IP3), wodurch es zur Freisetzung von Calcium (Ca^{2+}) kommt. Die $G_{q/11}$-Signalkaskade am GPR 83 wird durch eine Liganden unabhängige Basalaktivität, durch Zink (II)-Ionen oder auch durch die konstitutiv aktivierende Mutation C304W ausgelöst.

5.2 Inhibierung der MC4R-Dimerisierung durch Austausch in der intrazellulären Schleife 2 (ICL 2) führt zu Veränderung in der Signalisierung

Publikation 2: Piechowski C.L., ..., Pratzka J. *et al.* (2013): Inhibition of melanocortin-4 receptor dimerization by substitutions in intracellular loop 2.
Journal of Molecular Endocrinology. [2013. 51, 109-118]
Ziel dieser Arbeit war die Verhinderung der Bildung von MC4R-Dimeren, also der Forcierung der Monomerbildung. Dies wurde erreicht, indem einzelne oder mehrfache Substitutionen in dem intrazellulären Bereich des Rezeptors der interazellulären Schleife 2 (ICL 2) und den benachbarten Regionen TMH 3 und TMH 4 vorgenommen wurden. Durch die Generierung von zahlreichen Chimären aus MC4R und CB1R, zeigte sich, dass die ICL 2 von großer Bedeutung für die Dimerbildung ist, bzw. Modifikationen hier zur Separierung in Monomere beiträgt. Die Chimären mit vollständigem Austausch der TMH 3 und/oder TMH 4 wurden von dezidierten Funktionsuntersuchungen ausgeschlossen, da sie schon eine stark verminderte Fähigkeit zur Oberflächenexpression aufwiesen, was eine Charakterisierung stark beeinträchtigt. Die monomerisierten Chimären mit WT vergleichbarer Oberflächenexpression zeigten eine erhöhte konstitutive Aktivität im G_s-Signalweg. Interessanterweise spielt die ICL 2 auch eine entscheidende Rolle für die Signalisierung des MC4R, was sich auch an einer natürlich vorkommenden inaktivierenden MC4R Mutante (His158Arg, H158R, ebenfalls im Bereich der ICL 2) zeigte (Abb. 6). Hier ist das cAMP-Signal um 68 % erhöht im Vergleich zum WT, wobei die Rezeptorexpression unverändert blieb. Der Aktivitätszugewinn der dissoziierten Rezeptoren deutet darauf hin, dass ein Bezug zwischen Rezeptordimerisierung und Signalisierungseigenschaften besteht. Spezifizierte Interaktionsuntersuchungen zeigten, dass es auch in der Mutante H158R zur Dimer-Dissoziation kam. Somit wurde zusätzlich in einer natürlich vorkommenden aktivierenden MC4R Mutation in der ICL 2 beobachtet, dass dieser Bereich höchstwahrscheinlich entscheidend für die Dimerisierung des MC4R ist.

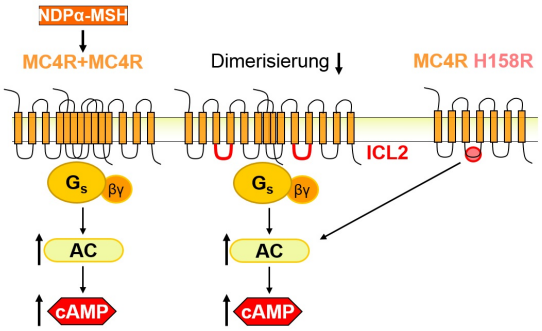

Abb. 6: Graphische Zusammenfassung zu Interaktionsstudien am MC4R.
MC4R liegen als Homooligomere vor und signalisieren über den G_s-Signalisierungsweg nach NDP α-MSH (synthetisches α-MSH) Stimulation. Durch Aktivierung der G_s-Proteine wird die Adenylatcylase (AC) stimuliert, was die Bildung von cAMP bewirkt. Aminosäureaustausch in der intrazellulären Schleife 2 (ICL 2) bewirkt eine Verminderung der Homooligodimerisierung des MC4R, was jedoch die cAMP-Signalisierung konstitutiv aktivierte.

5.3 Differentielle Signalmodulation von β-adrenergen Rezeptoren durch TAAR 1 Agonisten

Publikation 3: Kleinau G.* und Pratzka J.* *et el.*: Differential Modulation of β-Adrenergic Receptor Signaling by Trace Amine-Associated Receptor 1 Agonists.
PLoS One. [31. Oktober 2011]
Ziel dieser Arbeit war es, die TAAR 1 Agonisten TYR, PEA und OA an den auch evolutionär verwandten adrenergen Rezeptoren ADRB 1 und ADRB 2 zu untersuchen. Ko-Stimulation einer konstanten Konzentration von Isoproterenol (ISOP) mit steigenden Konzentrationen von TYR, PEA oder OA zeigte, dass TYR und PEA als partielle allosterische Antagonisten am ADRB 1 und ADRB 2 wirken können, was durch eine Verminderung des maximalen cAMP-Signals im Vergleich zu ISOP allein gemessen wurde. OA hingegen zeigte sich als schwacher ADRB 1 Agonist und als partieller orthosterischer ADRB 2 Antagonist, was durch eine Verschiebung des EC_{50}-Wertes gekennzeichnet ist. Um die molekularen Gründe für die TAAR1 Liganden Promiskuität und die herausgefundenen Signalisierungsunterschiede an den speziellen aminergen Rezeptoren zu spezifizieren, wurden in der vorliegenden Publikation Sequenzvergleiche ausgewählter homologer Rezeptoren durchgeführt. Dafür wurden die Aminosäuresequenzen von TAARs, ADRB 1 und ADRB 2, Tyramin- (TAR), Octopamin- (OAR), und Dopaminrezeptoren verwendet. Daraus ergab sich, dass die für TAAR 1 bemerkenswerte Ligandenpromiskuität auf einer hohen Aminosäureähnlichkeit zu anderen aminergen Rezeptoren in der Ligandenbindungsregion beruhen könnte. Die für die aminerge Ligandenbindung spezifischen Seitenketten sind auch in den TAARs konserviert. Weiterhin zeigten spezifische Eigenschaften im Bereich der Ligandenbindung am TAAR auch Unterschiede, die möglicherweise die Unterschiede in den Liganden-induzierten Effekten an ADRB 1 und ADRB 2 (wie z. B. Antagonismus) erklären könnten.

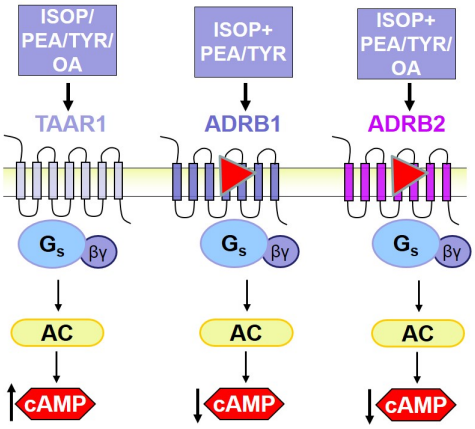

Abb. 7: Unterschiedliche Effekte auf die G_s-Signalisierung durch Spurenamine.
Isoproterenol (ISOP), β-Phenylethylamin (PEA), Tyramin (TYR) und Octopamin (OA) aktivieren den *Trace amine*-assoziierten Rezeptor 1 (TAAR 1) im G_s-Signalweg. Ko-Stimulation von ISOP mit PEA oder TYR bzw. OA blockierten die β-adrenergen Rezeptoren 1 und 2 (ADRB 1, ADRB 2), wodurch die cAMP Level sanken. Die zwei Bindungstaschen (einschließlich *Minor Pocket*) im ADRB 1 und ADRB 2 werden durch das rote Dreieck symbolisiert.

6 Diskussion

6.1 GPR 83 signalisiert via $G_{q/11}$ und kann durch Zink (II) partiell aktiviert werden

In der vorliegenden Publikation wurde gezeigt, dass der GPR 83 über $G_{q/11}$ signalisieren kann und sich durch Zink (II)-Ionen aktivieren lässt. Weiterhin wurde herausgefunden, dass dieser Rezeptor als Homodimer vorliegt und basalkonstitutiv aktiv ist. Ein wichtiger Schritt zur Deorphanisierung des GPR 83 wurde durch die Aufklärung des Signalweges geleistet.
Bekannt war von weiteren GPCRs, dass eine Aktivierung durch die Bindung von zweiwertigen Metallionen erreicht werden kann. In erster Linie wurde Zink (II) bisher als Agonist für diverse GPCRs beschrieben, wie für den α-adrenergen Rezeptor 1A (Ciolek *et al.*, 2011) oder den ADRB 2 (Swaminath *et al.*, 2003), aber auch für den MC1R bzw. den MC4R (Holst *et al.*, 2002) oder den Zink-*sensing* Rezeptor (Asraf *et al.*, 2014). Außerdem fungiert es als endogener Verstärker der α-MSH Wirkung am MC4R (Holst & Schwartz, 2003). Zink-Ionen befinden sich u. a. im Gehirn und sind an der Modulation neuronaler Steuerungsprozesse beteiligt, wobei Konzentrationen mit bis zu 300 µM im synaptischen Spalt vorkommen (Assaf & Chung, 1984). Bereits niedrige Konzentrationen von Zink (II) im physiologischen Nanomolar-Bereich aktivierten den GPR 83. Die aufgeführten Gründe weisen tatsächlich darauf hin, dass Zink (II) auch ein endogener Ligand des GPR 83 sein kann. Die Entdeckung einer N-terminalen extrazellulären Zink (II)-Bindungsstelle untermauerte zudem erstmals die Wichtigkeit dieser Region für die Signalregulation des GPR 83. Die Bildung von GPR 83 Homodimeren erweitert zudem die molekularen Eigenschaften der GPR 83 Signalisierung. Es wurde interessanterweise kürzlich berichtet, dass der GPR 83 mit einem weiteren GPCR aus der Regulation des Energiemetabolismus heterodimerisiert, dem Ghrelin Rezeptor (GHSR, *Growth hormone secretagogue receptor*) (Müller *et al.*, 2013b), was neben einer verminderten GHSR-Basalaktivität auch bedeutende Änderungen der einzelnen Rezeptoreigenschaften zur Folge haben kann (siehe Einleitung).
Zusammenfassend bieten die vorgestellten Untersuchungen wichtige molekulare Informationen, die zum Verständnis der physiologischen Rolle des GPR 83 beitragen. GPR 83 ist Teil des GPCR-Netzwerkes, welches in der Gewichtsregulation beteiligt ist. Um mehr Einblicke in das Zusammenspiel dieses Netzwerkes zu gewinnen, wurde ein weiterer GPCR aus der Appetitregulation untersucht.

6.2 ICL 2 ist essentiell für die MC4R-Dimerisierung

Der MC4R ist ein wichtiger Regulator in der Energiehomöostase. Er bildet Homodi- bzw. oligomere, wobei die Kenntnisse über molekulare Mechanismen und Auswirkungen auf die Rezeptoreigenschaften noch lückenhaft sind.

Im Rahmen dieser Publikation wurde erstmals ermittelt, dass die ICL 2 und die benachbarten TMH 3 und TMH 4 einen essentiellen Beitrag zum Homodimerisierungsprozess des MC4Rs leisten. Dadurch wurden neue Details zu strukturellen Voraussetzungen der MC4R Homooligomerisierung aufgeklärt. Es kann nicht ausgeschlossen werden, dass auch weitere Bereiche des Rezeptors eine Rolle für die MC4R-MC4R-Interaktion spielen.
In anderen Arbeiten wurde ebenfalls gezeigt, dass die TMH 4 bedeutend für die Dimerbildung, wie dem Chemokinrezeptor 5, ist (Hernanz-Falcon *et al.*, 2004). Bei dem Heterodimer zwischen dem metabotropen Glutamat 2 Rezeptor und dem Serotonin Rezeptor 2A wurde *in vitro* und *in vivo* (in isolierten Geweben) gefunden, dass mindestens drei Aminosäuren im intrazellulären Teil der TMH 4 des metabotropen Glutamat 2 Rezeptors wichtige Kontaktpunkte für die Dimerbildung sind (Moreno *et al.*, 2012).
Bemerkenswert ist die erhöhte G_s-Basalaktivität durch die Separierung des MC4R-MC4R-Homodimers. Bei dieser speziellen Form von differentieller Signalisierung ergab sich keine Änderung des Signalweges, wie es beispielsweise für Modifikationen in der TMH 3 bekannt ist (Mo *et al.*, 2012). Möglicherweise liegen Gründe für die konstitutive Aktivität bei einem unterschiedlichen Verhältnis zwischen Anzahl MC4R (Monomer oder Dimer) und dem intrazellulären G-Protein. Ein weiterer Grund kann auch eine Konformationsänderung der Rezeptoren sein, der sich durch die Dimerbildung ergeben.
Die vorgestellten Untersuchungen haben insgesamt ergeben, dass die ICL 2 essentiell für die Homooligomerisierung des MC4R ist, wobei andere Studien, wie bereits oben aufgeführt, auch darauf hinweisen, dass angrenzende TMHs bedeutend für die Rezeptor-Rezeptor-Interaktion sein können.

6.3 Spurenamine wirken ortho- und allosterisch an ADRB 1 und ADRB 2

TAAR1, ADRB 1 und ADRB 2 besitzen Gemeinsamkeiten hinsichtlich ihrer Liganden und ihrer Aminosäuresequenzen. Interessanterweise fungieren die OAR und die TAR in Invertebraten als Gegenstück zu den adrenergen Rezeptoren in Vertebraten, die auch einen zeitigen evolutionären Ursprung zu haben scheinen (Roeder, 2005). Dies stärkt die aufgeführten Ergebnisse, dass es tatsächlich einen physiologisch relevanten Zusammenhang zwischen β-adrenergen und Spurenaminrezeptoren gibt. Unterstützend zu dieser These zeigten Untersuchungen an Erythrozyten, dass nach ISOP-Stimulation ein antagonistischer Effekt durch das Schilddrüsenhormonmetabolit (Thyronamin) T3AM auftrat, wobei TYR keine Inhibition der β-adrenergen Bindung hervorrief (Cody *et al.*, 1984). Die Thyronamine T0AM und T1AM hingegen aktivieren den TAAR 1 (Scanlan *et al.*, 2004). Weiterhin wirken die beschriebenen Spurenamine sympatomimetisch, jedoch mit anderen Eigenschaften als die Catecholamine, was auf eine direkte Bindung an den β-adrenergen Rezeptoren oder eine Verdrängung von endogenen Agonisten zurückzuführen sein könnte (Chiba, 1976; Frascarelli *et al.*, 2008).

Gründe für die unterschiedliche Wirkung von OA gegenüber anderen Spurenaminen könnte die zusätzliche Hydroxylgruppe sein, die PEA und TYR fehlen. Diese Hydroxylgruppe interagiert möglicherweise über eine Wasserstoffbrücke mit dem Asparagin in der TMH 7 (Position 7.39 nach (Ballesteros & Weinstein, 1995)), vergleichbar den Catecholaminen an adrenergen Rezeptoren. Somit sind PEA und TYR wahrscheinlich in einer anderen Orientierung als OA in der allosterischen Bindungstasche. Interessanterweise ist diese Position auch am TAAR1 als ligandenbindungsrelevant beschrieben (Tan *et al.*, 2008). Außerdem zeigt die Kristallstruktur des ADRB 1 mit ISOP einen freien Bereich nahe der Ligandenbindungstasche. Aufgrund der hier gefundenen Allo- / Orthosterie und der Strukturmodellbetrachtungen kann vermutet werden, dass sich im ADRB 1 und ADRB 2 eine zweite (allosterische) Bindungstasche befindet. Diese zweite Bindungsregion wurde als *Minor Pocket* bezeichnet und befindet sich zwischen TMH 2, 3, 6 und 7. Die Möglichkeiten eines pharmakologischen Einsatzes vergrößert sich aufgrund dieser funktionellen Selektivität erheblich (Rosenkilde *et al.*, 2010). Dieser Bereich ist in den Kristallstrukturen des ADRB 1 nicht von ISOP besetzt, bzw. auch nicht von dem Antagonisten Carazolol in der Kristallstruktur des ADRB 2 (Kleinau *et al.*, 2011; Rosenkilde *et al.*, 2010).

6.4 Schlussbetrachtungen

Die vorliegenden Publikationen weisen erneut darauf hin, dass das vollständige molekulare Verständnis essentieller GPCRs in der Physiologie sehr komplex gestaltet sein kann.
Die fünf betrachteten GPCRs spielen jeweils eine definierte Rolle in der Regulation der Energiehomöostase bzw. in der Appetitregulation. Bei der aktuell ansteigenden Problematik von Übergewicht und damit verbundenen erhöhten Risiken für Erkrankungen des Herzkreislaufsystems, Diabetes oder Krebs, wird es immer wichtiger Möglichkeiten zum pharmakologischen Eingreifen zu finden, um das System der Gewichtsregulation gerichtet beeinflussen zu können. Daher ist es essentiell alle Wirkmechanismen der daran beteiligten GPCRs zu kennen und auch alle bekannten Charakteristika des für eine Therapie zu modulierenden GPCRs für die Wirkstoffsuche in Betracht zu ziehen.
Die Herangehensweise die Basalaktivität zu betrachten oder die mutationsbedingte Erhöhung der basalen Signalisierung, um den Signalweg zu identifizieren oder den Rezeptor mit Metallionen zu stimulieren, kann als Grundlage für das Deorphanisieren weiterer GPCRs dienen, wie für den GPR 83 gezeigt.
Die Ergebnisse der Dimerdissoziation des MC4R bieten einen Ausgangspunkt zum besseren Verständnis natürlich vorkommender Mutationen und deren Phänotyp. Die Dimerseparierung dient ebenfalls als Therapieoption gegen Übergewicht, indem die MC4R-Homodimere mit Hilfe von Peptiden zerstört werden, wodurch der MC4R besser signalisiert. Die Erkenntnisse bieten außerdem eine Grundlage für eine pharmakologische Intervention weiterer pathogener Veränderungen.

Das durch die Untersuchungen erworbene Wissen über Rezeptoraktivierung oder –blockade durch promiskutive Liganden liefert bisher unbekannte Kenntnisse über die sehr gut erforschten β-adrenergen Rezeptoren. Da β-adrenerge Rezeptoren Angriffspunkt in der Behandlung von beispielsweise kardiovaskulären Krankheiten eingesetzt werden (Rockman *et al.*, 2002), sind die hier beschriebenen Effekte von Spurenaminen von großer Bedeutung, nicht zuletzt, weil sie in Nahrungsmitteln wie Käse, Schokolade oder Wein vorkommen (Huang *et al.*, 2011). Die differentielle Modulation von Spurenaminen bietet neuen Raum bezüglich des Wissens über die Fähigkeiten von Liganden an einem Rezeptor als Agonist zu wirken, während er an einem anderen Rezeptor als Antagonist agieren kann. Die gezeigten Untersuchungen bieten ebenfalls Grundlage für die Herangehensweise mittels Strukturstudien. Sie können kritische Befunde erklären und somit zum besseren Verständnis beitragen.
Da es sich in den beschriebenen Untersuchungen um *in vitro* Versuche handelt, können Anhaltspunkte geliefert werden, um physiologische Abläufe zu erklären oder zu prognostizieren, doch müssen sie auch *in vivo* verifiziert werden. Weiterhin handelt es sich bei den GPR 83 Ergebnissen um die Maus-Rezeptorvariante, weil die *in vivo* Effekte auch an Mausstudien gesehen wurden (Müller *et al.*, 2013b). Hier besteht die offene Frage der Übertragbarkeit auf den Menschen und den physiologischen Zusammenhang zwischen GPR 83 und der Gewichtsregulation.
Zusammenfassend bieten alle drei Untersuchungen fundamentale und fortgeschrittene Erkenntnisse, auf die in weiteren Studien zur Erforschung der GPCRs aufgebaut werden kann. Es wurden neue Details zum Zusammenhang der funktionellen Selektivität von GPCRs in der komplexen Regulation der Energiehomöostase gezeigt, die nicht zuletzt helfen sollen, um in das Problem des zunehmenden Übergewichts pharmakologisch einzugreifen.

7 Literaturverzeichnis

Asraf H, Salomon S, Nevo A, Sekler I, Mayer D, Hershfinkel M (2014) The ZnR/GPR39 interacts with the CaSR to enhance signaling in prostate and salivary epithelia. Journal of cellular physiology 229: 868-877

Assaf SY, Chung SH (1984) Release of endogenous Zn2+ from brain tissue during activity. Nature 308: 734-736

Ballesteros JA, Weinstein H (1995) [19] Integrated methods for the construction of three-dimensional models and computational probing of structure-function relations in G protein-coupled receptors. In Methods in Neurosciences, Stuart CS (ed), Vol. Volume 25, pp 366-428. Academic Press

Biebermann H, Krude H, Elsner A, Chubanov V, Gudermann T, Gruters A (2003) Autosomal-dominant mode of inheritance of a melanocortin-4 receptor mutation in a patient with severe early-onset obesity is due to a dominant-negative effect caused by receptor dimerization. Diabetes 52: 2984-2988

Billington CK, Penn RB (2003) Signaling and regulation of G protein-coupled receptors in airway smooth muscle. Respiratory research 4: 2

Borowsky B, Adham N, Jones KA, Raddatz R, Artymyshyn R, Ogozalek KL, Durkin MM, Lakhlani PP, Bonini JA, Pathirana S, Boyle N, Pu X, Kouranova E, Lichtblau H, Ochoa FY, Branchek TA, Gerald C (2001) Trace amines: identification of a family of mammalian G protein-coupled receptors. Proceedings of the National Academy of Sciences of the United States of America 98: 8966-8971

Bouvier M (2001) Oligomerization of G-protein-coupled transmitter receptors. Nature reviews Neuroscience 2: 274-286

Braulke LJ, Klingenspor M, DeBarber A, Tobias SC, Grandy DK, Scanlan TS, Heldmaier G (2008) 3-Iodothyronamine: a novel hormone controlling the balance between glucose and lipid utilisation. Journal of comparative physiology B, Biochemical, systemic, and environmental physiology 178: 167-177

Breit A, Buch TR, Boekhoff I, Solinski HJ, Damm E, Gudermann T (2011) Alternative G protein coupling and biased agonism: new insights into melanocortin-4 receptor signalling. Molecular and cellular endocrinology 331: 232-240

Bunzow JR, Sonders MS, Arttamangkul S, Harrison LM, Zhang G, Quigley DI, Darland T, Suchland KL, Pasumamula S, Kennedy JL, Olson SB, Magenis RE, Amara SG, Grandy DK (2001) Amphetamine, 3,4-methylenedioxymethamphetamine, lysergic acid diethylamide, and metabolites of the catecholamine neurotransmitters are agonists of a rat trace amine receptor. Molecular pharmacology 60: 1181-1188

Carpene C, Galitzky J, Fontana E, Atgie C, Lafontan M, Berlan M (1999) Selective activation of beta3-adrenoceptors by octopamine: comparative studies in mammalian fat cells. Naunyn-Schmiedeberg's archives of pharmacology 359: 310-321

Chiba S (1976) Pharmacologic analysis of positive chronotropic and inotropic responses to octopamine. The Tohoku journal of experimental medicine 118: 247-253

Chruscinski AJ, Rohrer DK, Schauble E, Desai KH, Bernstein D, Kobilka BK (1999) Targeted disruption of the beta2 adrenergic receptor gene. The Journal of biological chemistry 274: 16694-16700

Ciolek J, Maiga A, Marcon E, Servent D, Gilles N (2011) Pharmacological characterization of zinc and copper interaction with the human alpha(1A)-adrenoceptor. European journal of pharmacology 655: 1-8

Cody V, Meyer T, Dohler KD, Hesch RD, Rokos H, Marko M (1984) Molecular structure and biochemical activity of 3,5,3'-triiodothyronamine. Endocrine research 10: 91-99

D'Andrea G, Ostuzzi R, Bolner A, Francesconi F, Musco F, d'Onofrio F, Colavito D (2008) Study of tyrosine metabolism in eating disorders. Possible correlation with migraine. Neurological sciences : official journal of the Italian Neurological Society and of the Italian Society of Clinical Neurophysiology 29 Suppl 1: S88-92

Dorsam RT, Gutkind JS (2007) G-protein-coupled receptors and cancer. Nature reviews Cancer 7: 79-94

Doyle KP, Suchland KL, Ciesielski TM, Lessov NS, Grandy DK, Scanlan TS, Stenzel-Poore MP (2007) Novel thyroxine derivatives, thyronamine and 3-iodothyronamine, induce transient hypothermia and marked neuroprotection against stroke injury. Stroke; a journal of cerebral circulation 38: 2569-2576

Ellacott KL, Cone RD (2006) The role of the central melanocortin system in the regulation

of food intake and energy homeostasis: lessons from mouse models. Philosophical transactions of the Royal Society of London Series B, Biological sciences 361: 1265-1274

Farooqi IS, Keogh JM, Yeo GS, Lank EJ, Cheetham T, O'Rahilly S (2003) Clinical spectrum of obesity and mutations in the melanocortin 4 receptor gene. The New England journal of medicine 348: 1085-1095

Fehler M, Broadley KJ, Ford WR, Kidd EJ (2010) Identification of trace-amine-associated receptors (TAAR) in the rat aorta and their role in vasoconstriction by beta-phenylethylamine. Naunyn-Schmiedeberg's archives of pharmacology 382: 385-398

Frascarelli S, Ghelardoni S, Chiellini G, Vargiu R, Ronca-Testoni S, Scanlan TS, Grandy DK, Zucchi R (2008) Cardiac effects of trace amines: pharmacological characterization of trace amine-associated receptors. European journal of pharmacology 587: 231-236

Friedman J (2014) 20 YEARS OF LEPTIN: An overview. The Journal of endocrinology

George SR, O'Dowd BF, Lee SP (2002) G-protein-coupled receptor oligomerization and its potential for drug discovery. Nature reviews Drug discovery 1: 808-820

Hebebrand J, Hinney A, Knoll N, Volckmar AL, Scherag A (2013) Molecular genetic aspects of weight regulation. Deutsches Arzteblatt international 110: 338-344

Hernanz-Falcon P, Rodriguez-Frade JM, Serrano A, Juan D, del Sol A, Soriano SF, Roncal F, Gomez L, Valencia A, Martinez AC, Mellado M (2004) Identification of amino acid residues crucial for chemokine receptor dimerization. Nature immunology 5: 216-223

Holst B, Elling CE, Schwartz TW (2002) Metal ion-mediated agonism and agonist enhancement in melanocortin MC1 and MC4 receptors. The Journal of biological chemistry 277: 47662-47670

Holst B, Schwartz TW (2003) Molecular mechanism of agonism and inverse agonism in the melanocortin receptors: Zn(2+) as a structural and functional probe. Annals of the New York Academy of Sciences 994: 1-11

Huang KJ, Jin CX, Song SL, Wei CY, Liu YM, Li J (2011) Development of an ionic liquid-based ultrasonic-assisted liquid-liquid microextraction method for sensitive determination of biogenic amines: application to the analysis of octopamine, tyramine and phenethylamine in beer samples. Journal of chromatography B, Analytical technologies in the biomedical and

life sciences 879: 579-584

Jassal B, Jupe S, Caudy M, Birney E, Stein L, Hermjakob H, D'Eustachio P (2010) The systematic annotation of the three main GPCR families in Reactome. Database : the journal of biological databases and curation 2010: baq018

Kakarala KK, Jamil K (2014) Sequence-structure based phylogeny of GPCR Class A Rhodopsin receptors. Molecular phylogenetics and evolution 74: 66-96

Kleinau G, Pratzka J, Nürnberg D, Grüters A, Führer-Sakel D, Krude H, Köhrle J, Schöneberg T, Biebermann H (2011) Differential modulation of Beta-adrenergic receptor signaling by trace amine-associated receptor 1 agonists. PloS one 6: e27073

Kobilka B (1992) Adrenergic receptors as models for G protein-coupled receptors. Annual review of neuroscience 15: 87-114

Lewin AH (2006) Receptors of mammalian trace amines. The AAPS journal 8: E138-145

Lindemann L, Ebeling M, Kratochwil NA, Bunzow JR, Grandy DK, Hoener MC (2005) Trace amine-associated receptors form structurally and functionally distinct subfamilies of novel G protein-coupled receptors. Genomics 85: 372-385

Maggio R, Barbier P, Fornai F, Corsini GU (1996) Functional role of the third cytoplasmic loop in muscarinic receptor dimerization. The Journal of biological chemistry 271: 31055-31060

Mo XL, Yang R, Tao YX (2012) Functions of transmembrane domain 3 of human melanocortin-4 receptor. Journal of molecular endocrinology 49: 221-235

Moreno JL, Muguruza C, Umali A, Mortillo S, Holloway T, Pilar-Cuellar F, Mocci G, Seto J, Callado LF, Neve RL, Milligan G, Sealfon SC, Lopez-Gimenez JF, Meana JJ, Benson DL, Gonzalez-Maeso J (2012) Identification of three residues essential for 5-hydroxytryptamine 2A-metabotropic glutamate 2 (5-HT2A.mGlu2) receptor heteromerization and its psychoactive behavioral function. The Journal of biological chemistry 287: 44301-44319

Motlagh HN, Wrabl JO, Li J, Hilser VJ (2014) The ensemble nature of allostery. Nature 508: 331-339

Müller A, Kleinau G, Piechowski CL, Müller TD, Finan B, Pratzka J, Grüters A, Kru-

de H, Tschöp M, Biebermann H (2013a) G-protein coupled receptor 83 (GPR83) signaling determined by constitutive and zinc(II)-induced activity. PloS one 8: e53347

Müller TD, Müller A, Yi CX, Habegger KM, Meyer CW, Gaylinn BD, Finan B, Heppner K, Trivedi C, Bielohuby M, Abplanalp W, Meyer F, Piechowski CL, Pratzka J, Stemmer K, Holland J, Hembree J, Bhardwaj N, Raver C, Ottaway N, Krishna R, Sah R, Sallee FR, Woods SC, Perez-Tilve D, Bidlingmaier M, Thorner MO, Krude H, Smiley D, DiMarchi R, Hofmann S, Pfluger PT, Kleinau G, Biebermann H, Tschöp MH (2013b) The orphan receptor Gpr83 regulates systemic energy metabolism via ghrelin-dependent and ghrelin-independent mechanisms. Nature communications 4: 1968

Nakazato M, Murakami N, Date Y, Kojima M, Matsuo H, Kangawa K, Matsukura S (2001) A role for ghrelin in the central regulation of feeding. Nature 409: 194-198

OECD (2010) Obesity and the Economics of Prevention: Fit not Fat: OECD Publishing.

Piechowski CL, Rediger A, Lagemann C, Mühlhaus J, Müller A, Pratzka J, Tarnow P, Grüters A, Krude H, Kleinau G, Biebermann H (2013) Inhibition of melanocortin-4 receptor dimerization by substitutions in intracellular loop 2. Journal of molecular endocrinology 51: 109-118

Rasmussen SG, DeVree BT, Zou Y, Kruse AC, Chung KY, Kobilka TS, Thian FS, Chae PS, Pardon E, Calinski D, Mathiesen JM, Shah ST, Lyons JA, Caffrey M, Gellman SH, Steyaert J, Skiniotis G, Weis WI, Sunahara RK, Kobilka BK (2011) Crystal structure of the beta2 adrenergic receptor-Gs protein complex. Nature 477: 549-555

Regard JB, Kataoka H, Cano DA, Camerer E, Yin L, Zheng YW, Scanlan TS, Hebrok M, Coughlin SR (2007) Probing cell type-specific functions of Gi in vivo identifies GPCR regulators of insulin secretion. The Journal of clinical investigation 117: 4034-4043

Regard JB, Sato IT, Coughlin SR (2008) Anatomical profiling of G protein-coupled receptor expression. Cell 135: 561-571

Robidoux J, Martin TL, Collins S (2004) Beta-adrenergic receptors and regulation of energy expenditure: a family affair. Annual review of pharmacology and toxicology 44: 297-323

Rockman HA, Koch WJ, Lefkowitz RJ (2002) Seven-transmembrane-spanning receptors and heart function. Nature 415: 206-212

Roeder T (2005) Tyramine and octopamine: ruling behavior and metabolism. Annual review of entomology 50: 447-477

Rosenbaum DM, Rasmussen SG, Kobilka BK (2009) The structure and function of G-protein-coupled receptors. Nature 459: 356-363

Rosenkilde MM, Benned-Jensen T, Frimurer TM, Schwartz TW (2010) The minor binding pocket: a major player in 7TM receptor activation. Trends in pharmacological sciences 31: 567-574

Rovira X, Pin JP, Giraldo J (2010) The asymmetric/symmetric activation of GPCR dimers as a possible mechanistic rationale for multiple signalling pathways. Trends in pharmacological sciences 31: 15-21

Rui L (2013) Brain regulation of energy balance and body weight. Reviews in endocrine & metabolic disorders 14: 387-407

Sainsbury A, Zhang L (2012) Role of the hypothalamus in the neuroendocrine regulation of body weight and composition during energy deficit. Obesity reviews : an official journal of the International Association for the Study of Obesity 13: 234-257

Scanlan TS, Suchland KL, Hart ME, Chiellini G, Huang Y, Kruzich PJ, Frascarelli S, Crossley DA, Bunzow JR, Ronca-Testoni S, Lin ET, Hatton D, Zucchi R, Grandy DK (2004) 3-Iodothyronamine is an endogenous and rapid-acting derivative of thyroid hormone. Nature medicine 10: 638-642

Schioth HB (2006) G protein-coupled receptors in regulation of body weight. CNS & neurological disorders drug targets 5: 241-249

Scholz J (1989) [Inositol trisphosphate, a new second messenger for positive inotropic effects on the heart?]. Klinische Wochenschrift 67: 271-279

Seifert R, Wenzel-Seifert K (2002) Constitutive activity of G-protein-coupled receptors: cause of disease and common property of wild-type receptors. Naunyn-Schmiedeberg's archives of pharmacology 366: 381-416

Stallaert W, Christopoulos A, Bouvier M (2011) Ligand functional selectivity and quantitative pharmacology at G protein-coupled receptors. Expert opinion on drug discovery 6: 811-825

Swaminath G, Lee TW, Kobilka B (2003) Identification of an allosteric binding site for Zn2+ on the beta2 adrenergic receptor. The Journal of biological chemistry 278: 352-356

Tan ES, Groban ES, Jacobson MP, Scanlan TS (2008) Toward deciphering the code to aminergic G protein-coupled receptor drug design. Chemistry & biology 15: 343-353

Teller DC, Okada T, Behnke CA, Palczewski K, Stenkamp RE (2001) Advances in determination of a high-resolution three-dimensional structure of rhodopsin, a model of G-protein-coupled receptors (GPCRs). Biochemistry 40: 7761-7772

Vassilatis DK, Hohmann JG, Zeng H, Li F, Ranchalis JE, Mortrud MT, Brown A, Rodriguez SS, Weller JR, Wright AC, Bergmann JE, Gaitanaris GA (2003) The G protein-coupled receptor repertoires of human and mouse. Proceedings of the National Academy of Sciences of the United States of America 100: 4903-4908

Wise A, Jupe SC, Rees S (2004) The identification of ligands at orphan G-protein coupled receptors. Annual review of pharmacology and toxicology 44: 43-66

8 Anteilserklärung an den ausgewählten Publikationen

Publikation 1: Müller A.*, Kleinau G.*, ..., Pratzka J. *et al.*, G-Protein Coupled Receptor 83 (GPR83) Signaling Determined by Constitutive and Zinc(II)-Induced Activity.
PLoS One, 2013
***gleichberechtigte Erstautoren**
(Impact Factor (2013): 3,534)

Anteil experimenteller Arbeit: 20 % | Anteil Schreibarbeit: 10 %

Die Qualität der Experimente profitierte von Frau Dinters experimenteller Expertise. Sie war an der Durchführung der funktionellen Charakterisierungsversuche, sowie an der Datenanalyse und dem Schreibprozess involviert.

Publikation 2: Piechowski C.L., ..., Pratzka J. *et al.*, Inhibition of melanocortin-4 receptor dimerization by substitutions in intracellular loop 2.
Journal of Molecular Endocrinology, 2013
(Impact Factor (2013): 3,621)

Anteil experimenteller Arbeit: 10 % | Anteil Schreibarbeit: 20 %

Frau Dinter wirkte unterstützend bei der Durchführung der Dimerisierungsversuche mit. Frau Dinter war an der Datenanalyse und Auswertung beteiligt. Sie war ebenfalls aktiv bei dem Schreibprozess tätig.

Publikation 3: Kleinau G.* und Pratzka J.* *et al.*, Differential Modulation of Beta-Adrenergic Receptor Signaling by Trace Amine-Associated Receptor 1 Agonists.
PLoS One, 2011
***gleichberechtigte Erstautoren**
(Impact Factor (2013): 3,534)

Anteil experimenteller Arbeit: 90 % | Anteil Schreibprozess: 50 %

Frau Dinter war an dem Großteil der experimentellen Arbeiten beteiligt mit anschließender Datenanalyse und Auswertung. Die dazugehörigen Abbildungen und statistischen Auswertungen wurden gänzlich von ihr umgesetzt. Am Schreibprozess war sie ebenfalls stark involviert.

Datum Juliane Dinter

9 Druckexemplare der ausgewählten Publikationen

9.1 Publikation 1: G-Protein Coupled Receptor 83 (GPR83) Signaling Determined by Constitutive and Zinc(II)-Induced Activity

A. Müller*, G. Kleinau*, C. L. Piechowski, T. D. Müller, B. Finan, J. Pratzka, A. Grüters, H. Krude, M. Tschöp, H. Biebermann (2013)
PLoS One. 2013;8(1):e53347.
doi: 10.1371/journal.pone.0053347. Epub 2013 Jan 15.

***gleichberechtigte Erstautoren**

OPEN ACCESS Freely available online

PLOS | ONE

G-Protein Coupled Receptor 83 (GPR83) Signaling Determined by Constitutive and Zinc(II)-Induced Activity

Anne Müller[1], **Gunnar Kleinau[1]**, **Carolin L. Piechowski[1]**, **Timo D. Müller[2]**, **Brian Finan[2]**, **Juliane Pratzka[1]**, **Annette Grüters[1]**, **Heiko Krude[1]**, **Matthias Tschöp[2,3]**, **Heike Biebermann[1]***

1 Institute of Experimental Pediatric Endocrinology, Charité Universitätsmedizin Berlin, Berlin, Germany, **2** Institute of Diabetes and Obesity, Helmholtz Center Munich, German Research Center for Environmental Health (GmbH), Munich, Germany, **3** Department of Metabolic Diseases, Technical University, Munich, Germany

Abstract

The G-protein coupled receptor 83 (GPR83) is an orphan G-protein coupled receptor for which the natural ligand(s) and signaling pathway(s) remain to be identified. Previous studies suggest a role of GPR83 in the regulation of thermogenesis and the control of circulating adiponectin. The aim of this study was to gain insights into the molecular underpinnings underlying GPR83 signaling. In particular, we aimed to assess the underlying G-protein activated signaling pathway of GPR83 and how this pathway is affected by mutational activation and zinc(II) challenge. Finally, we assessed the capacity of GPR83 for homodimerization. Our results show for the first time that mouse (m) GPR83 has high basal Gq/11 activity without affecting Gi or Gs signaling. Furthermore, we found that, under physiological conditions, zinc(II) (but not calcium(II) and magnesium(II)) potently activates mGPR83, thus identifying zinc(II) as an endogenous molecule with agonistic capability to activate mGPR83. In line with the observation that zinc(II)-ions activate mGPR83, we identified a cluster of ion-binding sensitive amino acids (e.g. His145, His204, Cys207, Glu217) in an activation sensitive receptor region of mGPR83. The occurrence of a constitutive activating mutant and a zinc(II)-binding residue at the N-terminal part corroborate the importance of this region in mGPR83 signal regulation. Finally, our results indicate that mGPR83 forms homodimers, which extend the current knowledge and molecular facets of GPR83 signaling.

Citation: Müller A, Kleinau G, Piechowski CL, Müller TD, Finan B, et al. (2013) G-Protein Coupled Receptor 83 (GPR83) Signaling Determined by Constitutive and Zinc(II)-Induced Activity. PLoS ONE 8(1): e53347. doi:10.1371/journal.pone.0053347

Editor: Roland Seifert, Medical School of Hannover, United States of America

Received September 24, 2012; **Accepted** November 27, 2012; **Published** January 15, 2013

Copyright: © 2013 Müller et al. This is an open-access article distributed under the terms of the Creative Commons Attribution License, which permits unrestricted use, distribution, and reproduction in any medium, provided the original author and source are credited.

Funding: This work was supported by the Deutsche Forschungsgemeinschaft (DFG; www.dfg.de): BI893/5-1, 893/6-2, KL2334/2-1 and Graduate College 1208: Hormonal Regulation of Energy Metabolism, Body Weight and Growth (www.endogk.de/en/), TP1. The funders had no role in study design, data collection and analysis, decision to publish, or preparation of the manuscript.

Competing Interests: The authors have declared that no competing interests exist.

* E-mail: heike.biebermann@charite.de

These authors contributed equally to this work.

Introduction

G-protein coupled receptor 83 (GPR83), previously identified as JP05, GPR72 or the glucocorticoid-induced receptor (GIR) is an orphan G-protein coupled receptor (GPCR) belonging to the rhodopsin-like class A GPCRs [1]. GPR83 was originally identified as a stress responsive transcript isolated from the murine thymoma cell line WEHI-7TG after stimulation with glucocorticoids or forskolin [2-4]. Furthermore, induction of GPR83 mRNA expression upon dexamethasone [5] or amphetamine [6] treatment suggests a potential role in the regulation of the hypothalamus-pituitary adrenal (HPA) axis. To this extent, GPR83 is most abundantly expressed in the murine brain and the thymus [3]. Former studies showed a selective upregulation of GPR83-expression in regulatory T cells (Treg) suggesting a role in development and function of these cells which are important for maintaining immunological tolerance. However recently it was shown, that GPR83 is dispensable for Treg cell development and activity [7]. Within the mouse brain, GPR83 is highly expressed within forebrain limbic system structures, the striatum and different hypothalamic regions [8]. Of appreciable importance, GPR83 expression patterns are similar between rodents and humans [6,9], and there is 87% sequence identity amongst the two species [10].

Unlike the well-characterized anatomical location of GPR83 expression, the endogenous ligand(s) and molecular underpinnings of ligand-activated signaling remain to be identified. GPR83 has previously been suggested to play a regulatory role in thermogenesis and also to be involved in the control of circulating adiponectin levels [11]. Other reports suggest GPR83 belongs to the neuropeptide Y (NPY) receptor family, based on the nearly 35% sequence identity GPR83 shares with various members of the NPY receptor family and that the C-terminal fragment of NPY binds to GPR83 at a lower affinity as compared to NPY receptor subtypes [10]. Despite these implicated roles in the neuroendocrine control of energy balance and structural similarities to other neuropeptide receptors, the signaling properties of murine GPR83 (mGPR83) have yet to be characterized.

To identify G-protein signaling cascades initiated by mGPR83 signaling, we first tested the capacity to induce a basal tone of the different G-proteins (Gs, Gi, Gq/11). Subsequently, to confirm the identified pathway, a specific mutation was introduced at a highly conserved amino acid in transmembrane helix 6 (TMH6) [12,13] to constitutively activate the receptor. In the thyroid stimulating hormone receptor (TSHR) pathogenic mutants at Cys636 (e.g.

Cys636Trp) in TMH6 were characterized as constitutive activating mutations (CAMs) [14,15]. This position is localized in the highly conserved $Cys^{6.47}$-$Trp^{6.48}$-Leu/$Ala^{6.49}$-$Pro^{6.50}$ motif of family A GPCR [16] (the numbers are according to the unified system suggested for family A GPCRs by Ballesteros & Weinstein [17]). Assuming similar micro-switch mechanisms in conserved family A GPCRs [18,19], this cysteine at mGPR83 position 304 was also mutated to tryptophan (Cys304Trp) and tested for constitutive G-protein activation. In addition, we evaluated other hallmark GPCR-specific signaling features, including the capacity for homodimerization and capability of zinc(II)-activated downstream signaling [20]. It is reported that zinc(II) can behave as an agonist, allosteric modulator or inverse agonist at numerous GPCRs and, thus, can diversely affect signaling [20-26]. To specify zinc(II)-action on mGPR83, activation by two further divalent cations, calcium(II) and magnesium(II), was also tested. Several GPCRs like the calcium-sensing receptor [27] are known to bind Ca(II).

Altogether, this study aimed to establish new molecular details of mGPR83 signaling in order to contribute further insights into the physiological and pharmacological characteristics of mGPR83.

Materials and Methods

Construction of Wild type and Mutant Receptors

Gpr83 was amplified from murine hypothalamic cDNA, *TSHR* (thyroid stimulating hormone receptor) from human thyroid cDNA, *MC3R* (melanocortin 3 receptor) and *5HTR1B* (5-hydroxytryptamine 1B receptor) from human genomic DNA and *GHSR* (ghrelin receptor) from human cDNA purchased from UMR cDNA Resource Center, Rolla, MO, USA [28,29]. Receptor-DNAs were cloned into the pcDps expression vector. Hemagglutinin tags were either cloned at the aminoterminal end (NHA) or subsequent to the signal peptide sequence (SP-HA). FLAG-tags were generated at the carboxyterminal ends (C-FLAG). The pcDps[NHA-rM3R (rat muscarinic receptor 3)] construct was kindly provided by Torsten Schöneberg (Institute of Biochemistry, University of Leipzig) and served as basis for all other cloned rM3R-constructs.

Mutant *Gpr83* were generated by site directed mutagenesis with wild type *Gpr83*- or *SP-HA-Gpr83*-pcDps as template.

The correctness of all PCR-derived products was proven by automatic sequencing. The pGL4.30[luc2P/NFAT-RE/Hygro] reporter construct, co-transfected for IP_3 determination was purchased from Promega (Madison, WI).

Cell Culture and Transfection

HEK293 (human embryonic kidney) and COS-7 cells were grown in Earls minimum essential medium (Earls MEM; Biochrom, Berlin, Germany) and in Dulbeccos modified Eagles medium (DMEM, Biochrom), respectively, supplemented with 10% fetal bovine serum (PAA Laboratories GmbH, Cölbe, Germany), 100 U/ml penicillin, 100 µg/ml streptomycin (Biochrom, Berlin, Germany) and 2 mM L-glutamine (Invitrogen, Paisley, UK) at 37°C and 5% CO_2.

For measurement of intracellular IP_3 via reporter gene assay, HEK293 cells were seeded into 48-well plates (5×10^4 cells/well), coated with poly-L-lysin (Biochrom). For cAMP accumulation assays, COS-7 cells were seeded into 48-well plates (3.75×10^4 cells/well). Transfection was performed with 83.3 ng of receptor plasmid-DNA/well and 0.9 µl Metafectene^{TM}/well (Biontex, Martinsried, Germany). For IP_3 measurement equal amounts of a reporter construct containing a response element and the firefly luciferase gene under control of the nuclear factor of activated T-cells (NFAT) (Promega, Mannheim, Germany) was co-transfected. Cell surface expression studies were carried out in COS-7 cells, seeded into 48-well plates (3.75×10^4 cells/well) using 166.7 ng DNA/well and 1.0 µl Metafectene^{TM}/well for transfection. Sandwich ELISA for dimerization studies were carried out in COS-7 cells seeded into 6cm-dishes (7×10^5 cells). Transfection was performed using 3 µg DNA and 8 µl Metafectene^{TM} per dish.

Investigation of Different Signaling Pathways

Intracellular cAMP levels for determination of Gs or Gi activation were measured in COS-7 cells by AlphaScreen technology [30]. Cells were transfected 24 h after seeding. One day later, transfection mixture was replaced with medium. The hTSHR stimulated with 100 mU/ml bovine thyroid stimulating hormone (bTSH, Sigma-Aldrich, Taufkirchen, Germany) served as Gs positive control [31,32]. To investigate Gi activity, stimulation with 50 µM forskolin (Sigma-Aldrich) was performed 48 h after transfection. Cells were incubated for 45′ at 37°C and 5% CO_2 in serum-free DMEM containing 1 mM 3-isobutyl-1-methylxanthine (IBMX, Sigma-Aldrich), in the absence or presence of forskolin. The h5HTR1B co-stimulated with forskolin and 100 nM serotonin (Sigma-Aldrich) served as Gi positive control [33]. After stopping the reaction by aspiration of medium, cells were lysed at 4°C for 2 h on a shaking platform in 100 µl/well lysis buffer containing 5 nM HEPES, 0.1% BSA, 0.3% Tween20 and 1 mM IBMX. 5 µl of each sample were transferred to a 384-well plate. Acceptor and donor beads were added according to the manufacturers' protocol (Perkin Elmer Life Science, Zaventem, Belgium).

Intracellular IP_3 levels were determined in HEK293 cells using a luciferase reporter assay. One day after seeding, receptor plasmids and the reporter construct were co-transfected. Transfection mixture was replaced with medium 18 h to 20 h after transfection. Two days after transfection, cells were incubated in serum-free Earls MEM in the absence or presence of increasing concentrations of $ZnCl_2$ (Sigma-Aldrich), $CaCl_2$ and $MgCl_2$ (Merck, Darmstadt, Germany; stock solutions were prepared in HPLC Gradient Grade water (J.T.Baker, Deventer, the Netherlands) [34]) at 37°C and 5% CO_2. Medium without additives contains 1.8 mM Ca(II) and 0.4 mM Mg(II). After stimulation cells were lysed with 100 µl/well 1× Passive Lysis Buffer (Promega). IP_3 was determined by luciferase activity according to the manufacturer's instructions (Promega) (Gq/11 positive control hTSHR stimulated with 100 mU/ml bTSH [31,32]).

Cell Surface Expression Studies

To investigate cell surface expression in an ELISA system, HA-tagged receptors were transfected one day after seeding. The tag-less GPR83 served as a negative control. Transfection mixture was replaced with medium 18 h to 20 h after transfection. Three days later, cells were washed, paraformaldehyde-fixed and probed with a biotin-labeled anti-HA antibody (Roche Applied Science, Mannheim, Deutschland). Bound biotin anti-HA-antibody was detected by peroxidase-labeled streptavidin (BioLegend, London, UK) in a substrate/chromogen reaction as described [35].

Homodimerization Studies

Dimerization was measured using the method of sandwich ELISA. Therefore HA- and FLAG-tagged constructs were co-transfected. Cells were harvested 3 days after transfection and solubilized at 4°C (10 mM Tris/HCl, pH 7.4, 150 mM NaCl, 1 mM EDTA, 1 mM DTT, 1% desoxycholat-Na, 1% NP-40 and 0,2 mM PMSF) over night. Lysates were incubated in anti-FLAG antibody (Sigma-Aldrich)-coated 96-well plates for 2 hours. The

HA epitope was detected as described above. Total protein concentration of lysates was measured using a bicinchoninic acid (BCA) based protein assay (Thermo Scientific, Bonn, Germany). Heterodimerization of the NHA-tagged hMC3R and FLAG-tagged hGHSR served as positive [28] and the NHA-tagged hGHSR as negative control.

Statistical analyses were performed using the statistical tools implemented in Graph Pad Prism (GraphPad Software, San Diego, California, USA).

Molecular Homology Modeling of mGPR83

As a result of advanced experimental methods [36] a large number of GPCR crystal structures, among other rhodopsin variants in the group of dopamine, chemokine, adenosine or acetylcholine receptors, have been published in recent years [37]. These crystal structures represent different receptor conformations [36,38], served as templates for GPCR homology modeling [39] and are also useful tools to improve pharmacological approaches [40-43].

The bovine rhodopsin structure was suggested as a template for mGPR83 modeling by already published algorithms concerning best-template selections [44,45]. The structural mGPR83 homology model described here is based on an inactive rhodopsin conformation (Protein Data Bank entry code 2I35). Amino acid sequences between mGPR83 and rhodopsin overlap especially in biophysical properties and length at the extracellular loop (ECL) 2 (Electronic supplementary material, Fig. S1). The general modeling procedure was performed as recently described [46].

Gaps of missing residues in the loops of the template structure were completed by the 'Loop Search' tool in Sybyl 8.1 (Tripos Inc., St. Louis, Missouri, 63144, USA). Side-chains and loops of homology models were subjected to conjugate gradient minimizations (until converging at a termination gradient of 0.05 kcal/mol*Å) and molecular dynamics simulation (2 ns) by fixing the backbone of the TMHs. Finally, the model was minimized without constraints using the AMBER 7.0 Force field. Structure images were produced using PyMOL software (The PyMOL Molecular Graphics System, Version 1.3 Schrödinger, LLC).

Results

Identification of the mGPR83 Signaling Pathway

cAMP accumulation in mGPR83 transiently-transfected HEK293 cells was measured to determine the basal G-protein constituents for mGPR83 signaling. The results revealed that mGPR83 did not alter Gs- or Gi-mediated signal activation compared to the negative empty vector control, the Gs positive control (bovine TSH stimulated hTSHR) or the Gi positive control (forskolin and serotonin co-stimulated h5HTR1B) (Electronic supplementary material, Fig. S2). However, mGPR83 showed a basal Gq/11 signal activity of 2.3 fold compared to mock transfection, as indicated by ligand-independent accumulation of IP_3 ($p<0.001$; Tab. 1, Fig. 1 and 2). In support of this notion, the Cys304Trp mutant increased the accumulation of IP_3 2.7 fold compared to mock and by 21% compared to baseline levels of wild type mGPR83 ($p<0.001$; Fig. 1), thus confirming the constitutive activity of this mGPR83 mutant. Furthermore, challenge of wild type mGPR83 with 100 µM zinc(II) further increased IP_3 formation to a maximum of 4.0 fold compared to mock and by 79% compared to the baseline of mGPR83 wild type ($p<0.001$; Fig. 1 and 2). This increase in IP_3 formation (Fig.1 and 2) was consistent with an EC_{50} of 10.2 ± 1.4 µM by treatment with 1 nM – 1 mM zinc(II) (Fig.1 and 2). Interestingly, we observed a biphasic shape of the concentration-response curve (Fig. 2), suggesting binding of zinc(II)-ions at two binding sites and potential allosteric modulation. One first activation step is reached significantly with 100 nM of zinc(II) ($p<0.05$; Fig. 2). The highest activation level occurs with 100 µM zinc(II) ($p<0.01$; Fig. 2). Notably, this zinc(II)-mediated activity is strong, with 79% increase over basal mGPR83 signaling compared to zinc(II)-mediated stimulation of other GPCRs (MC4R about 25% referred to mock transfection [23]). Zn(II)-concentrations above 1 mM lead to cell death.

Stimulation with Ca(II) more than 1.8 mM and with a Mg(II) concentration more than 0.4 mM did not lead to further mGPR83 signaling activity (supplementary material, Fig. S3).

Identification of Zinc(II)-binding Sites at mGPR83

The amino acids potentially involved in zinc(II)-binding at mGPR83 were identified from analyses of the mGPR83 sequence (Electronic supplementary material, Fig. S1) and the structural mGPR83 homology model (Fig. 3). According to previous insights on GPCRs [23,25,26,47], zinc(II) is suggested to bind to extracellular domains including the N-terminal tail (Ntt), the ECLs and the extracellular segments of the transmembrane helices. Amino acids were chosen for mutagenesis (Tab. 1) according to known zinc(II)-ion binding motifs from different protein super-families, which included Cys-Cys-Cys-Cys, Cys-His-Cys, His-His-His or His-Glu-His sequences [48]. To specifically impair zinc(II)-binding capacity, Cys, Glu, Asp and/or His residues in the extracellular region (Fig. 3) were mutated to alanine, and these mGPR83 mutants were functionally characterized for cell surface expression, basal activity and zinc(II)-induced signaling properties. Zinc(II)-stimulation was also performed in concentration-response curves using 1 nM – 1 mM Zn(II). Results of 100 µM and 1 mM Zn(II) were identically in proportion to wild type mGPR83. Therefore and due to the lowest standard error in this saturation region (Fig. 2), only data for 1 mM Zn(II)-stimulation were displayed in table 1. The results revealed that alanine mutations at six residues, His42, His145, His204, Cys207, Glu217 and Asp227, dampened zinc(II)-ion sensitivity or completely ablated zinc(II)-stimulation capacity (Tab. 1).

Cell Surface Expression of Mutated mGPR83

The majority of the mGPR83 variants exhibited a 70% or more cell surface expression compared with wild type mGPR83 (Tab. 1). However, three of the eleven mutants (Glu217Ala, His204Ala and His321Ala) were only moderately expressed, with expression levels between 30-50% as compared to wild type mGPR83. In comparison, the constitutively active Cys304Trp mutant in TMH6 was characterized by an expression level of 87.9 ± 6.0% in comparison to 100% wild type (Tab. 1).

Constitutive Activation of mGPR83 by Mutations

Surprisingly, the alanine mutagenesis at potential zinc(II) binding sites ultimately led to the identification of several constitutively active mutants, in particular His27Ala, Asp218Ala, Glu230Ala and His321Ala. All of these mutations increased the basal signaling level (IP_3 formation) by 133-150% compared to wild type (Tab. 1). Mapping of these amino acids to the structural mGPR83 homology model revealed a spatial clustering of these amino acids in a region between ECL2/ECL3 and TMH6 (Fig. 3). This spatial receptor region is well characterized for other GPCRs to be sensitive for signaling activity, especially in their interplay [49-53]. However, this spatial region's regulatory role for mGPR83 activity is determined in detail for the first time here. Specifically, substitution of His27Ala increased basal activity by

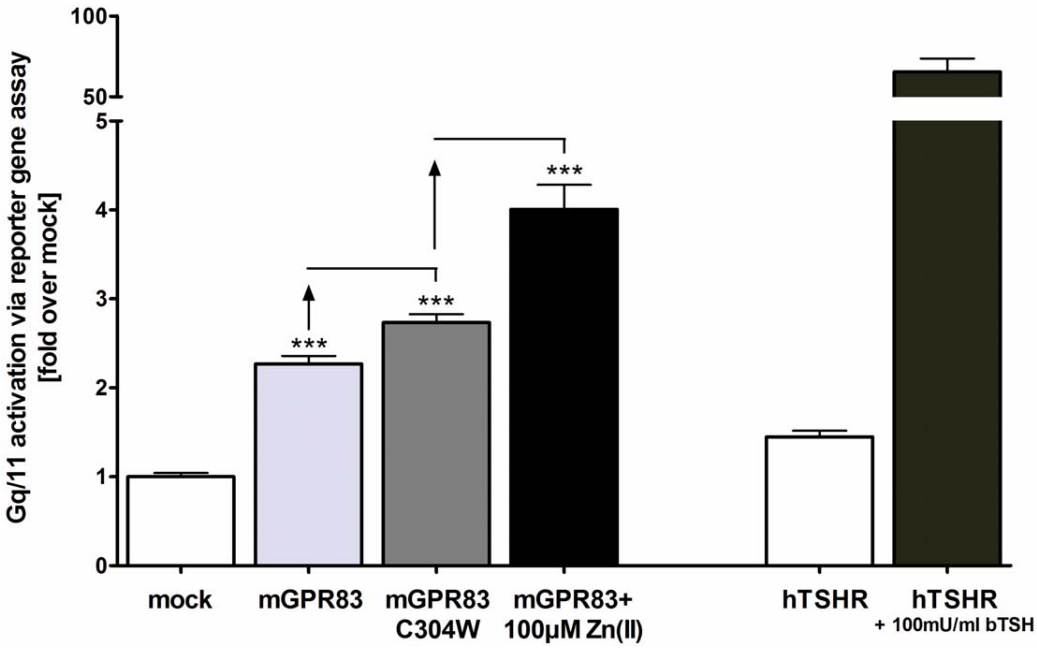

Figure 1. mGPR83 signals via the Gq/11 pathway revealed by basal signaling activity, CAMs and zinc(II)-stimulation. HEK293 cells were transiently transfected with the empty expression vector pcDps (mock) or pcDps carrying the wild type *Gpr83* or the *Gpr83 C304W* mutant, respectively. Two days after transfection, stimulation with $ZnCl_2$ (1 nM – 1 mM; stimulation curve in Fig. 2; black column: 100 µM) was carried out and cells were lysed. IP_3-accumulation was measured in a reporter gene assay. The hTSHR stimulated with 100 mU/ml bTSH functions as assay control [31,32]. Data were assessed from a minimum of 3 independent experiments, each performed at least in triplicates and represent mean ± SEM calculated fold over basal mock transfection with 19775.4 ± 2259.9 relative light units, set to 1. *** $p<0.001$ (unpaired t-test, two-tailed).
doi:10.1371/journal.pone.0053347.g001

133% compared to wild type (Tab. 1). This residue is located at the extreme N-terminus in close proximity to the signal peptide (positions 1-16) and is not included in the structural homology model because a structural fragment template is lacking. This is the first indication that the N-terminus of mGPR83 participates in signaling regulation.

Homodimerization of mGPR83

Finally, we assessed the capacity of mGPR83 to form homodimeric complexes, which is an important and common feature of GPCRs [54,55]. To analyze the capacity of mGPR83 to homodimerize, a sandwich ELISA was performed. A homodimeric association of mGPR83 (dark grey column, Fig. 4) was observed, which is comparable to the control heterodimer of hMC3R/hGHSR (black column, Fig. 4). For verification, we analyzed the interaction with the rat M3R (light grey column, Fig. 4). This signal is comparable to the negative control (white column, Fig. 4), thus corroborating significant mGPR83 dimer formation.

Discussion

The major aim of this study was to gain novel insights into the molecular underpinnings of mGPR83 signaling pathway(s) without existing knowledge of an endogenous ligand. Our results demonstrate that mGPR83 is characterized by a basal level of Gq/11 mediated accumulation of inositol trisphosphate. This information is of particular importance for future studies regarding the directed potential in pharmacological interventions targeting this receptor. Of important note, our finding that mGPR83 is an Gq/11 signaling GPCR was also confirmed by identification of several CAMs and the capacity to be activated by zinc(II)-ions.

GPR83 Activates the Gq/11 Mediated Pathway by Zinc(II)-ion Binding at Specific Signaling Sensitive Amino Acids

Zinc(II) is one of the most abundant trace elements in the human body, plays a prominent role in human health and interact with many GPCRs. Zinc(II)-ions are stored in glutamatergic synaptic vesicles and are co-released with neurotransmitters into the synaptic cleft where zinc(II) concentrations up to 300 µM can be obtained [56,57]. Within the neuronal expressed GPCRs it could be shown that zinc(II) activates and/or potentiates MC4R, β2-adrenergic receptor and tachykinin NK3 receptor signaling, also by engineered metal ion sites [20,23,25,26]. In contrast, the µ-opioid receptor and the D_2 or D_4 dopamine receptors are inhibited by zinc(II)-ions [47,58]. Zinc(II)-ions can act as signaling molecules by catalytic and structural effects and it is known that different cell-surface proteins, notably in neurons are effected by metal-ions like transporters for neurotransmitters, ion channels or even GPCRs [59,60].

Strikingly, we here show for the first time that zinc(II) acts agonistically in a micro-molar range on mGPR83. Already concentrations of 1nM Zn(II) lead to a first slight increase in mGPR83-signaling which is maintained until concentrations up to 10 µM zinc(II). From this first activation-level a strong and steeply stimulation of mGPR83 can be reached (Fig.2) in accordance to the obtained physiological concentrations in the synaptic cleft at around 100 µM Zn(II). Extracellular Zn(II)-concentrations above 1 mM lead in cell culture to cell-death. In multicellular organisms virtually all zinc is intracellularly located and appears in complexes with proteins and nucleic acids [61]. In accordance with the fact that physiologically only 1% of all Zn(II) occurs extracellular, to high concentrations of administered Zn(II) lead to a modified pH value of the medium and therefore to cell death *in vitro*.

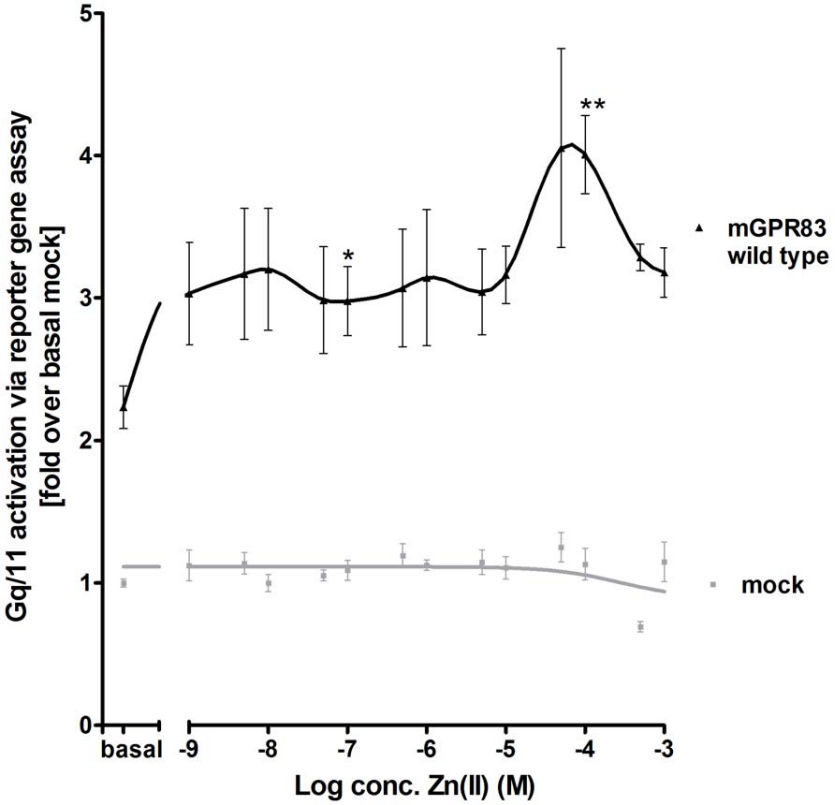

Figure 2. Concentration-response curve of zinc(II)- stimulation at mGPR83. HEK293 cells were transiently transfected with the empty expression vector pcDps (mock) or pcDps encoding the wild type *Gpr83*. Two days after transfection, stimulation with 1 nM – 1 mM $ZnCl_2$ was carried out, cells were lysed and IP_3-accumulation was measured in a reporter gene assay. The hTSHR stimulated with 100 mU/ml bTSH functioned as assay control [data not shown, [31,32]. The EC_{50} value of the wild type mGPR83 is 10.2 ± 1.4 µM zinc(II) and was obtained from the concentration-response curve (1 nM – 1 mM Zn(II)) using GraphPad Prism. First asterisk indicates a significant increase in IP_3 formation in comparison to basal wild type. Second asterisks indicate significance in comparison to the first asterisk. Data were evaluated from a minimum of 3 independent experiments, each performed at least in triplicates and calculated fold over the mock transfection, with 24718.3 ± 3958.7 relative light units, set to 1. Shown data represent mean ± SEM. * $p<0.05$, ** $p<0.01$ (unpaired t-test, two-tailed).
doi:10.1371/journal.pone.0053347.g002

By site-directed mutagenesis, the zinc(II)-sensitive amino acids in the extracellular domain, which were predicted according to known binding motifs and implications from a structural homology model, were explored. Typical zinc(II)-ion binding motifs are constituted by combinations of Cys-Cys-Cys-Cys, Cys-His-Cys, His-His-His or His-Glu-His side-chains [48]. Our studies elucidated a few specific amino acids (His42, His145, His204, Cys207, Glu217, Asp227) participating in zinc(II)-binding. Alanine mutations at these positions led to a loss of zinc(II)-mediated activity. Furthermore, the identification of six zinc(II)-sensitive positions opens the possibility that zinc(II) binds at two different clusters within the spatial region between the Ntt, ECL2, and TMH3/4. This finding is in accordance to a biphasic stimulation curve of zinc(II) at mGPR83 (Fig. 2).

In accordance to our structural homology model, side-chains of residues Glu217 and Asp227 are keeping the ECL2 in its conformation, presumably through hydrogen bonds within the backbone of this loop (Fig. 3). Binding of zinc(II) between those residues likely causes an interruption of stabilizing intramolecular interactions in the inactive state. Consequently, zinc(II)-binding induces structural shifts between the ECL2 and may alter its interaction with other domains. This potentially can modify the precise juxtaposition of ECL2, which has been identified as a crucial activation step for other family A GPCRs [49-53,62,63]. A potential relationship between homodimeric mGPR83 variants and zinc(II)-binding properties have yet to be elucidated because details of the homodimer interface are uncharacterized. However, the aspect of zinc(II)-induced mGPR83 activation might be of high future interests. This includes the physiological impact of GPR83 in relation to zinc(II)-ion availability, but also a potential modulatory function of zinc(II) on other ligand-receptor interactions. Zinc(II) could be of catalytic or structural impact for an undiscovered physiological mGPR83-ligand. Additionally, potential interactions of mGPR83 with other proteins (for example GPCRs) could be influenced structural and/or functional by zinc(II).

In addition to our findings of Zn(II)-stimulation on mGPR83 we have shown that calcium(II) and magnesium(II) did not induce Gq/11-signaling when administered in physiological concentrations (as occurring in the synaptic cleft) [64-66]. This finding might be related to missing binding motifs for other divalent ions than zinc and support an exclusive stimulation of GPR83 by zinc."

First Identification of Structural Components Important for Signaling Regulation

Several mutated mGPR83 variants (e.g. Asp218Ala, Glu230Ala, His321Ala) exhibited varying degrees of ligand-independent basal activity. The mutated residues are distributed

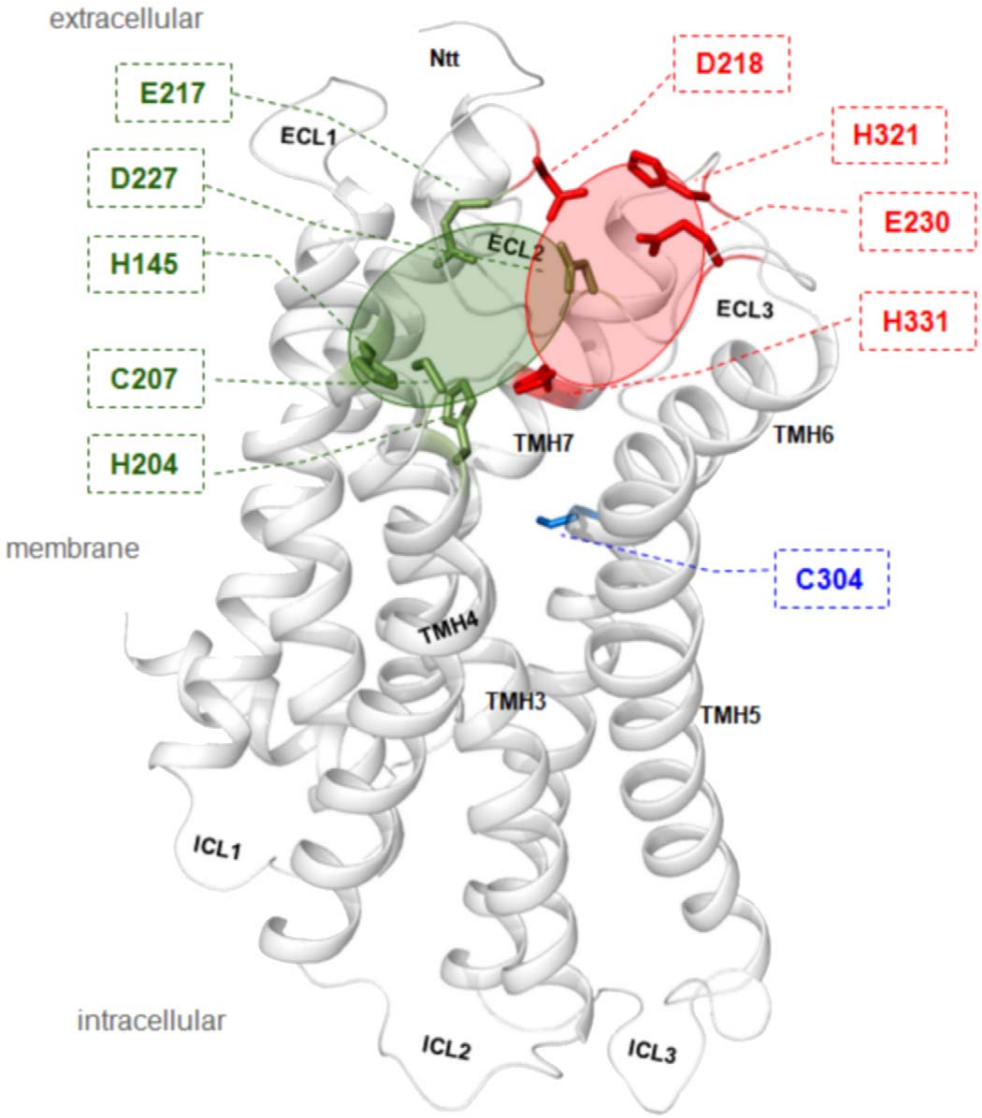

Figure 3. Structural mGPR83 homology model with sensitive positions for constitutive receptor activation and zinc(II)-stimulation. This structual GPR83 homology model is based on the crystal structure of rhodopsin in the inactive state. Highlighted wild type amino acids were depicted from this model for experimental approaches, because they are located extracellularly at the ECLs or at the extracellular ends of the TMHs and those amino acids are known as putative determinants of metal-ion binding motifs: histidine, glutamate, asparagine or cysteine. Arranged in defined spatial arrangements they can interact e.g. with zinc(II)-ions. Interestingly, six side-chain substitutions abolished stimulation by zinc(II) (green sticks) and five substitutions at different positions expressed an increase in constitutive signaling activity of mGPR83 (red sticks). The are spatially clustered in two different regions – red cycle (CAMs) and green (zinc(II)-binding) full cycle. In summary, they are indicating the extracellular region of the mGPR83 as highly sensitive for activation. Cysteine 304 (blue stick) at TMH6 is one of the highly conserved family A GPCR residues and it was reported for several receptors that mutations here are leading almost always to constitutive receptor activation. Indeed, also the mGPR83 Cys304Trp mutation causes a slight ligand independent (constitutive) activation of Gq/11 mediated signaling pathways.
doi:10.1371/journal.pone.0053347.g003

in a cluster-like manner in a spatial region between ECLs 2/3 and TMH7 (Fig. 3). Of an important note, the level of constitutive signaling did not allow further stimulation by zinc(II) (Tab. 1). This implies that the CAM positions identified here could participate in zinc(II)-binding and receptor activation and that loss-of-function mutations cannot be induced because of the overriding constitutive activity. However, these CAMs indicate a region of sensitivity for receptor activation that is located in the extracellular domain and TMH7, which is close to the identified zinc(II)-binding sites.

Interestingly, the occurrence of a CAM (His27Ala) and a zinc(II)-binding sensitive residue (His42Ala) at the extreme extracellular N-terminus of mGPR83 highlights this region as a determinant for signaling regulation. This region of mGPR83 is composed of nearly 70 amino acids that are conserved among species (Electronic supplementary material, Fig. S1). Furthermore, these structural findings support a potential domain-like fold in this region. It is of future interest to take these first hints into consideration for studying signaling mechanisms of the GPR83 in detail. This N-terminal part might function as a tethered inverse agonist that switches to an intramolecular agonist during activation or may function as a signal transmitter. Such scenario

Table 1. Functional characterization of amino acids that could be involved in zinc(II)-binding.

Construct	Localization	Cell surface expression	IP_3 accumulation (Zn(II)-stimulation) fold over basal mock transfection	
		% of wild type	basal	stimulated (1mM Zn(II))
mock transfection		8 ± 1	1 ± 0.1	1.2 ± 0.1
wild type mGPR83		100 ± 6	2.2 ± 0.1	3.1 ± 0.2
E217A	ECL2	39 ± 2	2.0 ± 0.1	2.0 ± 0.2
D218A	ECL2	74 ± 4	3.2 ± 0.2 ***	3.2 ± 0.2
D227A	ECL2	84 ± 5	2.0 ± 0.1	1.8 ± 0.1
E230A	ECL2	94 ± 7	3.2 ± 0.3 **	2.9 ± 0.3
H27A	Ntt	105 ± 6	3.0 ± 0.1 ***	2.5 ± 0.2
H42A	Ntt	94 ± 6	2.6 ± 0.2	2.6 ± 0.2
H145A	TMH3	74 ± 5	2.0 ± 0.2	2.2 ± 0.2
H204A	TMH4	31 ± 2	1.8 ± 0.1	2.0 ± 0.1
H321A	ECL3	48 ± 4	3.4 ± 0.2 ***	3.3 ± 0.1
H331A	TMH7	68 ± 4	3.2 ± 0.2 **	3.9 ± 0.2
C207A	ECL2	121 ± 7	2.8 ± 0.3	2.5 ± 0.2

For cell surface expression studies COS-7 cells were transiently transfected with the empty expression vector pcDps (mock), *Gpr83* wild type or *Gpr83* mutants. HEK293 cells were used for functional characterization. Data were evaluated from three or four independent experiments, each performed at least in triplicates. IP_3 accumulation performed as reporter gene assay was calculated fold over the basal mock transfection with 24718.3 ± 3958.7 relative light units, set to 1. The hTSHR stimulated with 100 mU/ml bTSH functioned as control for Gq/11 activation [data not shown, [31,32]]. Shown data represent mean ± SEM. The mutated aminoacid residues are grouped into extracellular located Ds (Asp) and Es (Glu), Hs (His) and one C (Cys) that could be involved in Zn(II)-binding. Asteriks indicate significant higher basal activity in comparison to wild type. ** $p<0.01$, *** $p<0.001$ (unpaired t-test, two-tailed); Ntt – N-terminal tail.
doi:10.1371/journal.pone.0053347.t001

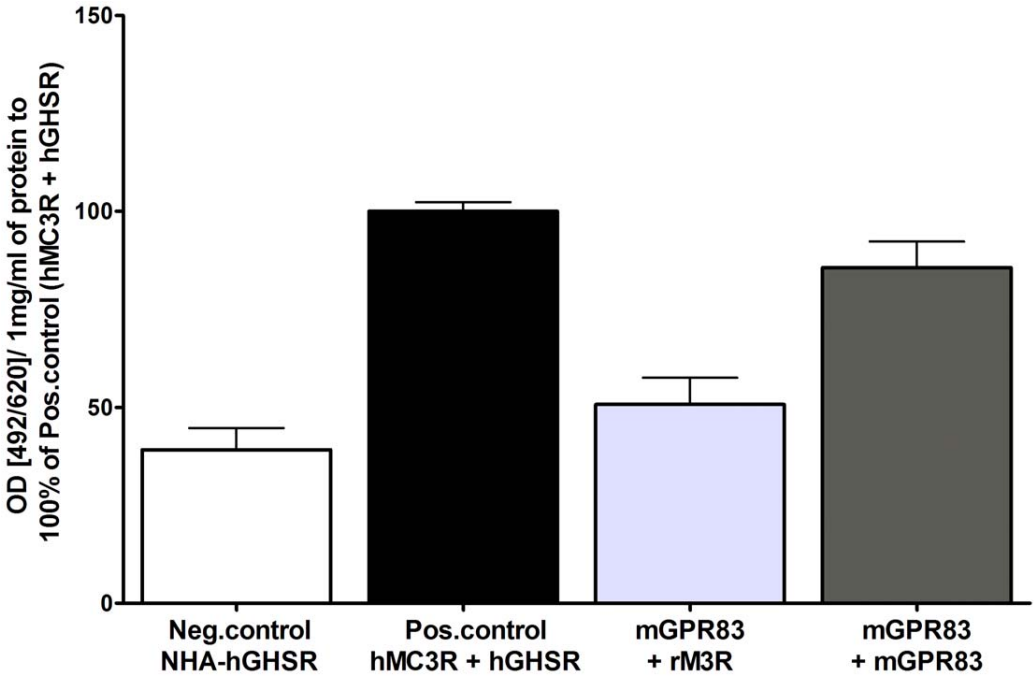

Figure 4. Homodimerization of mGPR83. Dimerization studies were performed using sandwich ELISA. COS-7 cells were transiently transfected. As negative control serves the NHA-hGHSR (white column) and as positive control the co-transfection of NHA-tagged hMC3R and FLAG-tagged hGHSR (black column, [28]). The light grey column represents the average of the HA- respectively FLAG-tagged mGPR83 in combination with the correspondent tagged rM3R. The dark grey column represents co-transfection of HA-tagged mGPR83 and FLAG-tagged mGPR83. Dimerization was measured via the HA epitope. The mean absorption (492 nm/620 nm) is calculated per 1 mg/ml of protein and shown as percentage of the hMC3R/hGHSR heterodimer (absorption (492/620)/ 1mg/ml of protein: 0.3 ± 0.04). Data were assessed from 3 independent experiments, each performed in triplicates and represent mean ± SEM.
doi:10.1371/journal.pone.0053347.g004

for a family A GPCR has been investigated at the extracellular part of glycoprotein hormone receptors (reviewed in [67]).

The mGPR83 Forms Higher Order Complexes

Knowledge concerning the determinants important for GPR83 activation, modulatory or agonistic effects of metal-ions, and mechanisms of signal transformation from an extracellular stimulus to initiation of an intracellular cascade is a prerequisite to estimate its full functional and pharmacological capacity. This includes the identification of protein-protein interactions for example with other GPCRs. Our data indicate mGPR83 forms homodimeric, or higher order, complexes but the exact identity of these complexes have yet to be characterized. It is well reported that oligomeric associations could have dramatic influences on signaling properties or pharmacological features of GPCRs [54,55]. For instance, the orientation of transmembrane helix 4 is modified during activation of dopamine receptor homodimers [68]. Additionally, activation of a single constituent of a heterodimeric complex of α2-adrenergic and μ-opioid receptors can trans-incativate the second receptor [69]. Activation of the dimeric metabotropic glutamate receptor is related to helical intersubunit re-arrangements [70]. In many scenarios of dimeric GPCR-GPCR interrelation the ligand binding capacity is especially influenced [55]. Reflecting the enormous potential impact of dimerization on structure and function of GPCRs, this characteristic might also be considered a prominent mechanistic feature for GPR83. Future studies should tackle specifically this issue more detailed.

In conclusion, this study revealed that mGPR83 exhibits a basal level of Gq/11 meditated IP_3 signaling, which can be increased by mutations at certain positions in the transmembrane region. Furthermore, we show that mGPR83 can be stimulated by zinc(II)-ions, and we identified detailed binding site residues within the N-terminal domain, which suggests a regulatory role for signal transformation. In addition, mGPR83 is able to form homodimeric or oligomeric complexes, which can have profound pharmacological prospective. This feature also suggests that GPR83 has an interplay capacity with other GPCRs. Ultimately, we believe this study opens the field for further studies to unravel the physiological role of GPR83. Additionally, the study design described herein, which is the first to investigate ligand-independent signaling mechanisms, may serve as a roadmap to characterize other orphan GPCRs.

Supporting Information

Figure S1 Sequence alignment comparison between particular family A GPCRs. The amino acid sequences of GPR83 from different species are represented in comparison with bovine rhodopsin and the human beta-2 adrenergic receptor. The crystal structure of rhodopsin was used as a template for structural GPR83 homology model. Based on the crystal structures of rhodopsin and the beta-2 adrenergic receptor the structural dimensions of the helices and loops are assigned (lilac boxes). Similar residues regarding biophysical properties are marked with gray background (blossum 62 matrix). Color code: black – proline, blue – positively charged, cyan/green – aromatic and hydrophobic, green – hydrophobic, red – negatively charged, gray – hydrophilic, dark-red – cysteines, magenta – histidine. The extracellular CAM H27A was identified in this project.
(TIF)

Figure S2 mGPR83 shows no basal activity in Gs or Gi. COS-7 cells were transiently transfected with the empty expression vector pcDps (mock), pcDps carrying the wild type mGpr83, the mGpr83 C304W mutant, the hTSHR or the h5HTR1B. Two days after transfection, stimulation with 50 μM forskolin, 100 mU/ml bTSH and 100 nM serotonin was carried out, cells were lysed and cAMP-accumulation was measured. The bTSH stimulated hTSHR serves as Gs positive control (dark grey column, [23,24]), the forskolin serotonin co-stimulated h5HTR1B as Gi positive control (light grey column, [25]). Data were evaluated from 3 independent experiments, each performed at least in triplicates and calculated fold over the (basal) mock transfection with 2.6 ± 0.1 nM cAMP set to 1. Shown data represent mean ± SEM.
(TIF)

Figure S3 Concentration-response curve of calcium(II)- and magnesium(II)- stimulation at mGPR83. HEK293 cells were transiently transfected with the empty expression vector pcDps (mock) or pcDps encoding the wild type *Gpr83*. Medium without additives contains 1.8 mM Ca(II) and 0.4 mM Mg(II) (matches the basal values). Two days after transfection, stimulation with calcium(II) up to 4.8 mM **(A)** and magnesium(II) up to 8 mM **(B)** was carried out, cells were lysed and IP_3-accumulation was measured in a reporter gene assay. The hTSHR stimulated with 100 mU/ml bTSH functioned as assay control (data not shown, [31,32]). Data were evaluated from 3 independent experiments, each performed at least in triplicates and calculated fold over the mock transfection, with 10496.7 ± 484.2 for Ca(II) and 16206.7 ± 1784.8 for Mg(II) relative light units, set to 1. Shown data represent mean ± SEM.
(TIF)

Author Contributions

Conceived and designed the experiments: AM GK CLP JP HK HB. Performed the experiments: AM GK CLP JP HB. Analyzed the data: AM GK CLP TDM BF JP AG HK MHT HB. Contributed reagents/materials/analysis tools: GK HB. Wrote the paper: AM GK CLP TDM BF JP AG HK MHT HB.

References

1. Alexander SP, Mathie A, Peters JA (2011) Guide to Receptors and Channels (GRAC), 5th edition. Br J Pharmacol 164 Suppl 1: S1-324.
2. Baughman G, Harrigan MT, Campbell NF, Nurrish SJ, Bourgeois S (1991) Genes newly identified as regulated by glucocorticoids in murine thymocytes. Mol Endocrinol 5: 637-644.
3. Harrigan MT, Baughman G, Campbell NF, Bourgeois S (1989) Isolation and characterization of glucocorticoid- and cyclic AMP-induced genes in T lymphocytes. Mol Cell Biol 9: 3438-3446.
4. Harrigan MT, Campbell NF, Bourgeois S (1991) Identification of a gene induced by glucocorticoids in murine T-cells: a potential G protein-coupled receptor. Mol Endocrinol 5: 1331-1338.
5. Adams F, Grassie M, Shahid M, Hill DR, Henry B (2003) Acute oral dexamethasone administration reduces levels of orphan GPCR glucocorticoid-induced receptor (GIR) mRNA in rodent brain: potential role in HPA-axis function. Brain Res Mol Brain Res 117: 39-46.
6. Brezillon S, Detheux M, Parmentier M, Hokfelt T, Hurd YL (2001) Distribution of an orphan G-protein coupled receptor (JP05) mRNA in the human brain. Brain Res 921: 21-30.
7. Lu LF, Gavin MA, Rasmussen JP, Rudensky AY (2007) G protein-coupled receptor 83 is dispensable for the development and function of regulatory T cells. Mol Cell Biol 27: 8065-8072.
8. Pesini P, Detheux M, Parmentier M, Hokfelt T (1998) Distribution of a glucocorticoid-induced orphan receptor (JP05) mRNA in the central nervous system of the mouse. Brain Res Mol Brain Res 57: 281-300.
9. Sah R, Pritchard LM, Richtand NM, Ahlbrand R, Eaton K, et al. (2005) Expression of the glucocorticoid-induced receptor mRNA in rat brain. Neuroscience 133: 281-292.

10. Sah R, Parker SL, Sheriff S, Eaton K, Balasubramaniam A, et al. (2007) Interaction of NPY compounds with the rat glucocorticoid-induced receptor (GIR) reveals similarity to the NPY-Y2 receptor. Peptides 28: 302-309.
11. Dubins JS, Sanchez-Alavez M, Zhukov V, Sanchez-Gonzalez A, Moroncini G, et al. (2012) Downregulation of GPR83 in the hypothalamic preoptic area reduces core body temperature and elevates circulating levels of adiponectin. Metabolism in press.
12. Parnot C, Miserey-Lenkei S, Bardin S, Corvol P, Clauser E (2002) Lessons from constitutively active mutants of G protein-coupled receptors. Trends Endocrinol Metab 13: 336-343.
13. Schoneberg T, Schulz A, Biebermann H, Hermsdorf T, Rompler H, et al. (2004) Mutant G-protein-coupled receptors as a cause of human diseases. Pharmacol Ther 104: 173-206.
14. Biebermann H, Winkler F, Handke D, Teichmann A, Gerling B, et al. (2012) New pathogenic thyrotropin receptor mutations decipher differentiated activity switching at a conserved helix 6 motif of family A GPCR. J Clin Endocrinol Metab 97: E228-232.
15. Winkler F, Kleinau G, Tarnow P, Rediger A, Grohmann L, et al. (2010) A new phenotype of nongoitrous and nonautoimmune hyperthyroidism caused by a heterozygous thyrotropin receptor mutation in transmembrane helix 6. J Clin Endocrinol Metab 95: 3605-3610.
16. Schwartz TW, Frimurer TM, Holst B, Rosenkilde MM, Elling CE (2006) Molecular mechanism of 7TM receptor activation–a global toggle switch model. Annu Rev Pharmacol Toxicol 46: 481-519.
17. Ballesteros JA, Weinstein H (1995) Integrated Methods for the Construction of Three-Dimensional Models and Computational Probing of Structure-Function Relationships in G-Protein Coupled Receptors. Methods Neurosci 25: 366-428.
18. Ahuja S, Smith SO (2009) Multiple switches in G protein-coupled receptor activation. Trends Pharmacol Sci 30: 494-502.
19. Nygaard R, Frimurer TM, Holst B, Rosenkilde MM, Schwartz TW (2009) Ligand binding and micro-switches in 7TM receptor structures. Trends Pharmacol Sci 30: 249-259.
20. Rosenkilde MM, Lucibello M, Holst B, Schwartz TW (1998) Natural agonist enhancing bis-His zinc-site in transmembrane segment V of the tachykinin NK3 receptor. FEBS Lett 439: 35-40.
21. Ciolek J, Maiga A, Marcon E, Servent D, Gilles N (2011) Pharmacological characterization of zinc and copper interaction with the human alpha(1A)-adrenoceptor. Eur J Pharmacol 655: 1-8.
22. Elling CE, Frimurer TM, Gerlach LO, Jorgensen R, Holst B, et al. (2006) Metal ion site engineering indicates a global toggle switch model for seven-transmembrane receptor activation. J Biol Chem 281: 17337-17346.
23. Holst B, Elling CE, Schwartz TW (2002) Metal ion-mediated agonism and agonist enhancement in melanocortin MC1 and MC4 receptors. J Biol Chem 277: 47662-47670.
24. Storjohann L, Holst B, Schwartz TW (2008) Molecular mechanism of Zn2+ agonism in the extracellular domain of GPR39. FEBS Lett 582: 2583-2588.
25. Swaminath G, Lee TW, Kobilka B (2003) Identification of an allosteric binding site for Zn2+ on the beta2 adrenergic receptor. J Biol Chem 278: 352-356.
26. Swaminath G, Steenhuis J, Kobilka B, Lee TW (2002) Allosteric modulation of beta2-adrenergic receptor by Zn(2+). Mol Pharmacol 61: 65-72.
27. Thiel G, Lesch A, Keim A (2012) Transcriptional response to calcium-sensing receptor stimulation. Endocrinology 153: 4716-4728.
28. Rediger A, Tarnow P, Bickenbach A, Schaefer M, Krude H, et al. (2009) Heterodimerization of hypothalamic G-protein-coupled receptors involved in weight regulation. Obes Facts 2: 80-86.
29. Biebermann H, Schoneberg T, Krude H, Schultz G, Gudermann T, et al. (1997) Mutations of the human thyrotropin receptor gene causing thyroid hypoplasia and persistent congenital hypothyroidism. J Clin Endocrinol Metab 82: 3471-3480.
30. Staubert C, Tarnow P, Brumm H, Pitra C, Gudermann T, et al. (2007) Evolutionary aspects in evaluating mutations in the melanocortin 4 receptor. Endocrinology 148: 4642-4648.
31. Van Sande J, Raspe E, Perret J, Lejeune C, Maenhaut C, et al. (1990) Thyrotropin activates both the cyclic AMP and the PIP2 cascades in CHO cells expressing the human cDNA of TSH receptor. Mol Cell Endocrinol 74: R1-6.
32. Allgeier A, Offermanns S, Van Sande J, Spicher K, Schultz G, et al. (1994) The human thyrotropin receptor activates G-proteins Gs and Gq/11. J Biol Chem 269: 13733-13735.
33. Siegel GJ, Agranoff BW, Albers RW, Fisher SK, Uhler MD (1999) "Chapter 13: Serotonin Receptors". In: Siegel GJ, editor. Basic Neurochemistry: Molecular, Cellular, and Medical Aspects. Philadelphia: Lippincott-Raven. 263-292.
34. Holst B, Egerod KL, Schild E, Vickers SP, Cheetham S, et al. (2007) GPR39 signaling is stimulated by zinc ions but not by obestatin. Endocrinology 148: 13-20.
35. Schulz A, Grosse R, Schultz G, Gudermann T, Schoneberg T (2000) Structural implication for receptor oligomerization from functional reconstitution studies of mutant V2 vasopressin receptors. J Biol Chem 275: 2381-2389.
36. Kobilka B, Schertler GF (2008) New G-protein-coupled receptor crystal structures: insights and limitations. Trends Pharmacol Sci 29: 79-83.
37. Zhao Q, Wu BL (2012) Ice breaking in GPCR structural biology. Acta Pharmacol Sin 33: 324-334.
38. Hanson MA, Stevens RC (2009) Discovery of new GPCR biology: one receptor structure at a time. Structure 17: 8-14.
39. Costanzi S (2010) Modeling G Protein-Coupled Receptors: a Concrete Possibility. Chim Oggi 28: 26-31.
40. Carlsson J, Coleman RG, Setola V, Irwin JJ, Fan H, et al. (2011) Ligand discovery from a dopamine D3 receptor homology model and crystal structure. Nat Chem Biol 7: 769-778.
41. Kontoyianni M, Liu Z (2012) Structure-based design in the GPCR target space. Curr Med Chem 19: 544-556.
42. Mason JS, Bortolato A, Congreve M, Marshall FH (2012) New insights from structural biology into the druggability of G protein-coupled receptors. Trends Pharmacol Sci 33: 249-260.
43. Shoichet BK, Kobilka BK (2012) Structure-based drug screening for G-protein-coupled receptors. Trends Pharmacol Sci 33: 268-272.
44. Worth CL, Kleinau G, Krause G (2009) Comparative sequence and structural analyses of G-protein-coupled receptor crystal structures and implications for molecular models. PLoS One 4: e7011.
45. Worth CL, Kreuchwig A, Kleinau G, Krause G (2011) GPCR-SSFE: a comprehensive database of G-protein-coupled receptor template predictions and homology models. BMC Bioinformatics 12: 185.
46. Costanzi S (2012) Homology modeling of class a g protein-coupled receptors. Methods Mol Biol 857: 259-279.
47. Schetz JA, Chu A, Sibley DR (1999) Zinc modulates antagonist interactions with D2-like dopamine receptors through distinct molecular mechanisms. J Pharmacol Exp Ther 289: 956-964.
48. Vallee BL, Auld DS (1990) Zinc coordination, function, and structure of zinc enzymes and other proteins. Biochemistry 29: 5647-5659.
49. Bokoch MP, Zou Y, Rasmussen SG, Liu CW, Nygaard R, et al. (2010) Ligand-specific regulation of the extracellular surface of a G-protein-coupled receptor. Nature 463: 108-112.
50. Massotte D, Kieffer BL (2005) The second extracellular loop: a damper for G protein-coupled receptors? Nat Struct Mol Biol 12: 287-288.
51. Peeters MC, van Westen GJ, Li Q, Ijzerman AP (2011) Importance of the extracellular loops in G protein-coupled receptors for ligand recognition and receptor activation. Trends Pharmacol Sci 32: 35-42.
52. Wheatley M, Simms J, Hawtin SR, Wesley VJ, Wootten D, et al. (2007) Extracellular loops and ligand binding to a subfamily of Family A G-protein-coupled receptors. Biochem Soc Trans 35: 717-720.
53. Wheatley M, Wootten D, Conner MT, Simms J, Kendrick R, et al. (2012) Lifting the lid on GPCRs: the role of extracellular loops. Br J Pharmacol 165: 1688-1703.
54. Bouvier M (2001) Oligomerization of G-protein-coupled transmitter receptors. Nat Rev Neurosci 2: 274-286.
55. George SR, O'Dowd BF, Lee SP (2002) G-protein-coupled receptor oligomerization and its potential for drug discovery. Nat Rev Drug Discov 1: 808-820.
56. Assaf SY, Chung SH (1984) Release of endogenous Zn2+ from brain tissue during activity. Nature 308: 734-736.
57. Xie X, Smart TG (1994) Modulation of long-term potentiation in rat hippocampal pyramidal neurons by zinc. Pflugers Arch 427: 481-486.
58. Fowler CB, Pogozheva ID, LeVine H 3rd, Mosberg HI (2004) Refinement of a homology model of the mu-opioid receptor using distance constraints from intrinsic and engineered zinc-binding sites. Biochemistry 43: 8700-8710.
59. Elinder F, Arhem P (2003) Metal ion effects on ion channel gating. Q Rev Biophys 36: 373-427.
60. Norgaard-Nielsen K, Gether U (2006) Zn2+ modulation of neurotransmitter transporters. Handb Exp Pharmacol: 1-22.
61. Tapiero H, Tew KD (2003) Trace elements in human physiology and pathology: zinc and metallothioneins. Biomed Pharmacother 57: 399-411.
62. Barwell J, Woolley MJ, Wheatley M, Conner AC, Poyner DR (2012) The role of the extracellular loops of the CGRP receptor, a family B GPCR. Biochem Soc Trans 40: 433-437.
63. Kleinau G, Claus M, Jaeschke H, Mueller S, Neumann S, et al. (2007) Contacts between extracellular loop two and transmembrane helix six determine basal activity of the thyroid-stimulating hormone receptor. J Biol Chem 282: 518-525.
64. Brown EM (1991) Extracellular Ca2+ sensing, regulation of parathyroid cell function, and role of Ca2+ and other ions as extracellular (first) messengers. Physiol Rev 71: 371-411.
65. Nicholson C, Bruggencate GT, Steinberg R, Stockle H (1977) Calcium modulation in brain extracellular microenvironment demonstrated with ion-selective micropipette. Proc Natl Acad Sci U S A 74: 1287-1290.
66. Silver RA, Lubke J, Sakmann B, Feldmeyer D (2003) High-probability uniquantal transmission at excitatory synapses in barrel cortex. Science 302: 1981-1984.
67. Kleinau G, Krause G (2009) Thyrotropin and homologous glycoprotein hormone receptors: structural and functional aspects of extracellular signaling mechanisms. Endocr Rev 30: 133-151.
68. Guo W, Shi L, Filizola M, Weinstein H, Javitch JA (2005) Crosstalk in G protein-coupled receptors: changes at the transmembrane homodimer interface determine activation. Proc Natl Acad Sci U S A 102: 17495-17500.
69. Vilardaga JP, Nikolaev VO, Lorenz K, Ferrandon S, Zhuang Z, et al. (2008) Conformational cross-talk between alpha2A-adrenergic and mu-opioid receptors controls cell signaling. Nat Chem Biol 4: 126-131.
70. Brock C, Oueslati N, Soler S, Boudier L, Rondard P, et al. (2007) Activation of a dimeric metabotropic glutamate receptor by intersubunit rearrangement. J Biol Chem 282: 33000-33008.

9.2 Publikation 2: Inhibition of melanocortin-4 receptor dimerization by substitutions in intracellular loop 2

C. L. Piechowski, A. Rediger, C. Lagemann, J. Mühlhaus, A. Müller, J. Pratzka, P. Tarnow, A. Grüters, H. Krude, G. Kleinau, H. Biebermann.

J Mol Endocrinol. 2013 Jun 29;51(1):109-18.
http://dx.doi.org/10.1530/JME-13-0061. Print 2013.

Inhibition of melanocortin-4 receptor dimerization by substitutions in intracellular loop 2

Carolin L Piechowski, Anne Rediger, Christina Lagemann, Jessica Mühlhaus, Anne Müller, Juliane Pratzka, Patrick Tarnow, Annette Grüters, Heiko Krude, Gunnar Kleinau and Heike Biebermann

Institute of Experimental Pediatric Endocrinology, Charité-Universitätsmedizin Berlin, Humboldt-Universität zu Berlin, Augustenburger Platz 1, 13353 Berlin, Germany

Correspondence should be addressed to H Biebermann
Email
heike.biebermann@charite.de

Abstract

Obesity is one of the most challenging global health problems. One key player in energy homeostasis is the melanocortin-4 receptor (MC4R), which is a family A G-protein-coupled receptor (GPCR). It has recently been shown that MC4R has the capacity to form homo- or heterodimers. Dimerization of GPCRs is of great importance for signaling regulation, with major pharmacological implications. Unfortunately, not enough is yet known about the detailed structural properties of MC4R dimers or the functional consequences of receptor dimerization. Our goal, therefore, was to explore specific properties related to MC4R dimerization. First, we aimed to induce the dissociation of dimers to monomers and to compare the functional parameters of wild-type and MC4R variants. To inhibit homo-dimerization, we designed MC4R chimeras with the cannabinoid-1 receptor, a receptor that does not interact with MC4R. Indeed, we identified several substitutions in the intracellular loop 2 (ICL2) and adjacent regions of transmembrane helix 3 (TMH3) and TMH4 that lead to partial dimer dissociation. Interestingly, the capacity for signaling activity was generally increased in these MC4R variants, although receptor expression remained unchanged. This increase in activity for dissociated receptors might indicate a link between receptor dimerization and signaling capacity. Moreover, dimer dissociation was also observed in a naturally occurring activating MC4R mutation in ICL2. Taken together, this study provides new information on the structural prerequisites for MC4R dimerization and identifies an approach to induce the dissociation of MC4R dimers. This might be useful for further investigation of pharmacological properties.

Key Words

- G-protein-coupled receptor
- melanocortin-4 receptor
- dimerization
- constitutive signaling activity
- dimer dissociation

Journal of Molecular Endocrinology
(2013) **51**, 109–118

Introduction

The melanocortin-4 receptor (MC4R) is encoded by a single-exon gene and is primarily expressed in the hypothalamic paraventricular nucleus, spinal cord, sympathetic preganglionic neurons, brain stem, and penis (Van der Ploeg *et al*. 2002, Tao 2010). Upon activation by the pro-opiomelanocortin-derived peptides α-MSH and β-MSH, the receptor mainly couples to the Gs/adenylyl cyclase system, but also activates a variety of downstream effectors, such as kinases, leading to decreased food intake and increased energy expenditure (Cone 2006). From *in vitro* studies, it is known that MC4R exhibits ligand-independent activity (Nijenhuis *et al*. 2001). Heterozygous

http://jme.endocrinology-journals.org
DOI: 10.1530/JME-13-0061
© 2013 Society for Endocrinology
Printed in Great Britain
Published by Bioscientifica Ltd.

MC4R mutation is the most frequent known genetic cause of obesity in humans (Farooqi *et al.* 2003). Because of its important role in hypothalamic energy metabolism, the MC4R seemed to be a suitable target for pharmacological treatment, although effective targeting in humans has not yet been achieved (reviewed in Biebermann *et al.* (2012)). Currently known MC4R ligands cause decreased food intake in mice but not in humans (Krishna *et al.* 2009).

It has recently been shown that MC4R is able to form homodimers (Biebermann *et al.* 2003, Elsner *et al.* 2006, Nickolls & Maki 2006) and that a few mutations cause dominant-negative effects on wild-type (WT) receptor function (Biebermann *et al.* 2003, Tarnow *et al.* 2008). Furthermore, heterodimerization has been demonstrated between MC4R and other G-protein-coupled receptors (GPCRs), such as GPR7, that are potentially involved in weight regulation (Rediger *et al.* 2009). Heterodimerization of MC4R has not yet been successfully considered in drug design (Rozenfeld & Devi 2010, 2011).

Little is yet known about the structural and biophysical prerequisites for MC4R dimerization (reviewed in Rediger *et al.* (2012)). The impact (if any) on functional properties in comparison to MC4R monomers is still unclear, although it is well established that dimerization of many GPCRs can have a dramatic influence on the signaling properties of the interacting protomers – such as ligand binding (Levoye *et al.* 2006), G-protein coupling selectivity, or signal transduction mechanisms (reviewed in George *et al.* (2002)).

The current study was performed to obtain deeper insights into the prerequisites and consequences of MC4R homodimerization. For simplicity, we will use the term dimerization, although we cannot distinguish between dimers and higher order complexes of oligomers, such as tetramers. The strategy was to inhibit dimerization by modifying putative dimer contacts and to compare the functional properties of modified variants with those of WT MC4R. The strategy of dimer dissociation has also been used several times for other GPCRs and can shift the monomer–dimer equilibrium toward the monomeric state (Lambert 2010, Kasai *et al.* 2011).

Materials and methods

Construction of chimeric MC4R/CB1R receptors and the MC4R variants His158Arg and His158Ala

Mutant receptors were constructed by site-directed mutagenesis and chimeric receptors using PCR with overlapping oligonucleotides, with MC4R and cannabinoid-1 receptor (CB1R) as full-length templates in the pcDps expression vector (kindly provided by Prof. Torsten Schöneberg (University of Leipzig)). Full-length chimeric receptors were then either N-terminally hemagglutinin (HA)-tagged (NHA) or C-terminally FLAG-tagged (FLAG) or received both tags (HAF). Additionally, a naturally occurring MC4R variant His158Arg (Hinney *et al.* 2006) (located in the intracellular loop 2 (ICL2)) was investigated with respect to dimerization. For comparison, we also designed a histidine-to-alanine substitution at this position (His158Ala) by site-directed mutagenesis.

Cell culture and transfection

All functional studies were performed in COS-7 cells. COS-7 cells were maintained in DMEM (Biochrom, Berlin, Germany), supplemented with 10% FCS (PAA Laboratories GmbH, Cölbe, Germany), 2 mM L-glutamine (Invitrogen), 100 units/ml penicillin, and 100 μg/ml streptomycin (Biochrom). Cells were incubated at 37 °C in humidified air containing 5% CO_2. Transfections were carried out 24 h after seeding using metafectene (Biontex, Munich, Germany), according to the manufacturer's protocol. Total receptor expression and receptor interaction were determined by a sandwich ELISA with 5×10^5 cells seeded in 6 cm dishes and transfected with a total of 3 μg DNA and 8 μl metafectene. Cell surface expression assays and cAMP assays were performed in 48-well plates. Cell surface expression was determined with 5×10^4 cells/well transfected with 0.17 μg DNA/well and 1 μl metafectene/well. Intracellular cAMP accumulation was performed with 4×10^4 cells/well, and transfected with 0.08 μg DNA/well and 0.93 μl metafectene/well. Signaling studies were performed with N-terminally HA-tagged constructs. Further tests indicated that the signaling properties are not affected by the addition of tags.

Determination of chimeric and mutant receptor cell surface expression

Seventy-two hours after transfection with N-terminally HA-tagged receptors, cells were washed with Dulbecco's PBS (DPBS, Biochrom) and fixed for 30 min in 4% formaldehyde in DPBS, followed by washing twice in DPBS. After incubation in blocking buffer (10% FCS-supplemented DMEM) for 1 h at 37 °C, cells were incubated for 2 h at 37 °C in blocking buffer with 1 μg/ml biotin-labeled anti-HA MAB (Roche). After four washing steps in DPBS, the samples were incubated at 37 °C overnight in blocking buffer with 1 μg/ml streptavidin-labeled

http://jme.endocrinology-journals.org
DOI: 10.1530/JME-13-0061
© 2013 Society for Endocrinology
Printed in Great Britain
Published by Bioscientifica Ltd.

peroxidase (BioLegend, San Diego, CA, USA). After four washing steps, the samples were stained with 0.1% H_2O_2 and 10 μg *o*-phenylenediamine (Sigma–Aldrich) in substrate buffer (0.1 M citric acid, and 0.1 M Na_2HPO_4 at pH 5.2). The reaction was stopped after 10 min with 1 M Na_2SO_3 in 1 M HCl. Colorimetry was carried out using an *Anthos reader 2001* (Anthos Labtec Instruments GmbH, Salzburg, Austria), employing absorption at 492 nm/620 nm.

Determination of total receptor expression and receptor–receptor interaction by ELISA

To detect total expression, cells were transfected with N-terminally HA- and C-terminally FLAG-tagged (HAF) constructs. To detect dimerization capacity, cells were co-transfected with equal amounts of N-terminally HA-tagged constructs and C-terminally FLAG-tagged constructs. Seventy-two hours after transfection, cells were washed twice with cold DPBS, harvested, and solubilized overnight at 4 °C in lysis buffer (10 mM Tris/HCl, 150 mM NaCl, 1 mM EDTA, 1 mM dithiothreitol, 1% desoxycholate Na, 1% NP-40, and 0.2 mM phenylmethylsulphonyl fluoride in water). The lysates were incubated in anti-FLAG antibody (Sigma–Aldrich)-coated 96-well plates for 2 h. Following five washing steps, the samples were incubated at 37 °C for 2 h in DPBS-T (DPBS with 0.05% Tween 20) with 1 μg/ml biotin-labeled anti-HA MAB (Roche). This step was followed by four washing steps with DPBS-T and incubation at 37 °C for 1 h in blocking buffer with 1 μg/ml streptavidin-labeled peroxidase (BioLegend). The color reaction was performed as described earlier. The protein concentration of cell lysates of each sample was measured with the BCA Protein Assay Reagent Kit (Thermo Scientific, Bonn, Germany), according to the manufacturer's protocol. Results for total receptor expression and receptor–receptor interaction were calculated in relation to protein content. Due to the determination of dimer formation with differentially tagged receptors, the following GPCR-tag interaction combinations are possible: GPCR-NHA + GPCR-NHA, GPCR-FLAG + GPCR-FLAG, and dimers with both GPCR-tags GPCR-NHA + GPCR-FLAG. The ELISA only detects one specific combination of the three: the GPCR-NHA + GPCR-FLAG dimers. Therefore, only one third of dimers were detectable in principle according to this method.

Measurement of cAMP accumulation

Forty-eight hours after transfection, cells were pre-incubated for 5 min with stimulation buffer (serum-free DMEM and 1 mM 3-isobutyl-1-methylxanthine (IBMX, Sigma–Aldrich). This stimulation buffer was used for all further steps. Cells were then stimulated for 45 min at 37 °C with 100 nM (Nle4, D-Phe7)-α-MSH (NDP-α-MSH, Sigma–Aldrich) or 1000 nM α-MSH (Sigma–Aldrich, in the case of His158Arg and His158Ala) in stimulation buffer. Ligands were dissolved in DPBS with 0.1% BSA. The reaction was stopped by aspiration of medium. Cells were lysed at 4 °C for 1 h on a shaking platform with cell lysis buffer containing 5 nM HEPES, 0.1% BSA, 0.3% Tween 20, and 1 mM IBMX. Each sample was transferred to a 384-well plate (Perkin-Elmer Life Science, Inc., Boston, MA, USA) and intracellular cAMP was determined using the AlphaScreen technology manufacturer's protocol (Perkin-Elmer; Staubert *et al.* 2007). The plate was measured with the Berthold Microplate Reader (Berthold Technologies GmbH & Co. KG, Bad Wildbad, Germany).

Structural MC4R homology model

A structural homology model of the monomeric MC4R was generated as described previously (Tarnow *et al.* 2008). Sequence alignment was used to define helical and loop regions – as presented in the supporting information (supporting information, Supplementary Figure S1, see section on supplementary data given at the end of this article), in combination with helix assignments in GPCR crystal structures (Worth *et al.* 2009). Structure images were produced using PyMOL software (DeLano WL, version 1.03, San Carlos, CA, USA).

Statistical analysis

Data and statistical analyses were performed using the statistical tools (unpaired two-tailed *t*-test, if necessary with Welch's correction) implemented in Graph Pad Prism Version 5 (GraphPad Software, San Diego, CA, USA).

Results

The general strategy used here was to inhibit MC4R dimerization by substituting different amino acids into the potential dimeric interface. This exploited the fact that the MC4R and the CB1R – which was used for constructing chimeric receptors – are not able to form dimers (Rediger *et al.* 2009). Chimeric MC4R/CB1R variants with specific multiple substitutions between transmembrane helix 3 (TMH3)-TMH4, including ICL2, were designed as described in Fig. 1. The structural dimensions of variations were derived from the sequence and by comparing the

http://jme.endocrinology-journals.org
DOI: 10.1530/JME-13-0061
© 2013 Society for Endocrinology
Printed in Great Britain
Published by Bioscientifica Ltd.

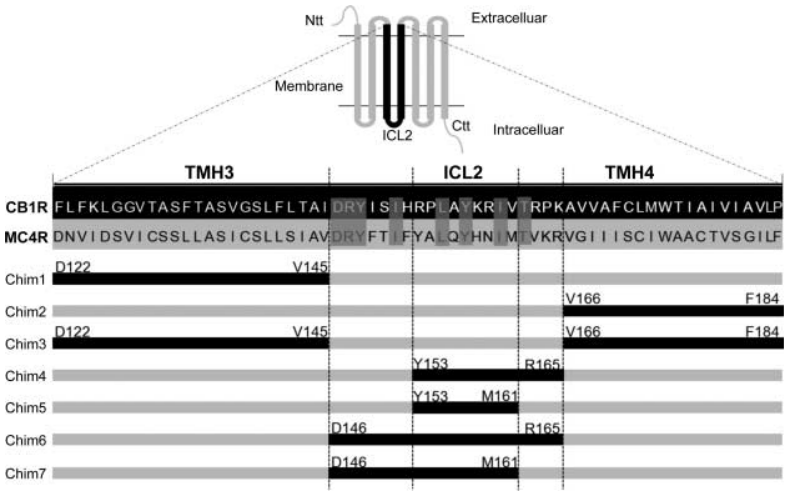

Figure 1

Assignment of chimeric MC4R/CB1R receptor constructs. MC4R/CB1R chimeric receptors were constructed via overlap PCR. The details of the MC4R (gray) regions substituted by the section of the CB1R (black) are described and shown in detail. The assigned amino acid regions are based on MC4R sequence alignment (supporting information, Supplementary Figure S1) and structural insights from GPCR crystal structures. Identical amino acids are shaded gray at the TMH3-ICL2-TMH4 junction, in order to highlight the 12 amino acids within this region that differ between the receptors. Chimera specification: chim1, substitution of TMH3 (Asp122–Val145); chim2, substitution of TMH4 (Val166–Phe184); chim3, substitution of TMH3 (Asp122–Val145) and TMH4 regions (Val166–Phe184); chim4, substitution of the ICL2 and intracellularly located regions of TMH4 (Tyr153–Arg165); chim5, substitution of ICL2 (Tyr153–Met161); chim6, substitution of the intracellularly located region of TMH3, ICL2, and intracellularly located region of TMH4 (Asp146–Arg165); and chim7, substitution of the intracellularly located TMH3 and intracellular loop 2 (Asp146–Met161).

structures of different GPCRs (supporting information, Supplementary Figure S1). The reason this experimental setup was chosen is that several GPCR–GPCR interfaces have been reported to be located in this region (Carrillo *et al.* 2004, Guo *et al.* 2008, Mancia *et al.* 2008). Furthermore, it has been shown that CB1R not only signals via Gi but also via Gs activation (Rhee *et al.* 1998), indicating that the substitutions performed most probably do not modify MC4R G-protein specificity. The signaling properties of our chimeric MC4R/CB1R constructs and two single side chain substitutions were tested in comparison with the WT MC4R (for an overview, all results are summarized in the supporting information, Supplementary Table S1, see section on supplementary data given at the end of this article).

Substitution of the entire TMH3 or TMH4 impair receptor cell surface expression levels

Despite the fact that chimeras 1, 2, and 3 (chim1, chim2, and chim3) with fully substituted TMH3 and/or TMH4 showed total expression levels comparable to WT MC4R, the cell surface expression of these constructs was greatly decreased (Fig. 2A and B). Functional characterization also showed that the signaling capacity was totally abrogated (supporting information, Supplementary Table S1). We therefore excluded these constructs from further experiments. Of note, it was reported in previous studies that specific amino acids in TMH3 are significant for MC4R function, including Asp122 and Asp125 (Pogozheva *et al.* 2005). Cell surface expression level of chim4 was moderately reduced in comparison to chim5, chim6, chim7 and MC4R-WT (Fig. 2B).

TMH3 and ICL2 constrain the inactive state

MC4R/CB1R chimeras were tested for their signaling properties (Fig. 3). All constructs exhibited elevated basal cAMP levels compared with WT. Chim6 and chim7 are combinations of TMH3 and ICL2 substitutions (Fig. 1) and expressed the greatest constitutive activation of fourfold compared with WT.

The chimeric receptors with increased basal signaling activity also exhibited hyperstimulation after ligand treatment – by around 160–210% compared with WT (Fig. 3). Moreover, chim4 exhibited decreased cell surface expression level and only slightly increased basal activity, as well as enhanced signaling capability comparable to WT. The typical concentration–response curve of chim7 revealed no shift in the EC_{50} value (supporting

http://jme.endocrinology-journals.org
DOI: 10.1530/JME-13-0061
© 2013 Society for Endocrinology
Printed in Great Britain
Published by Bioscientifica Ltd.

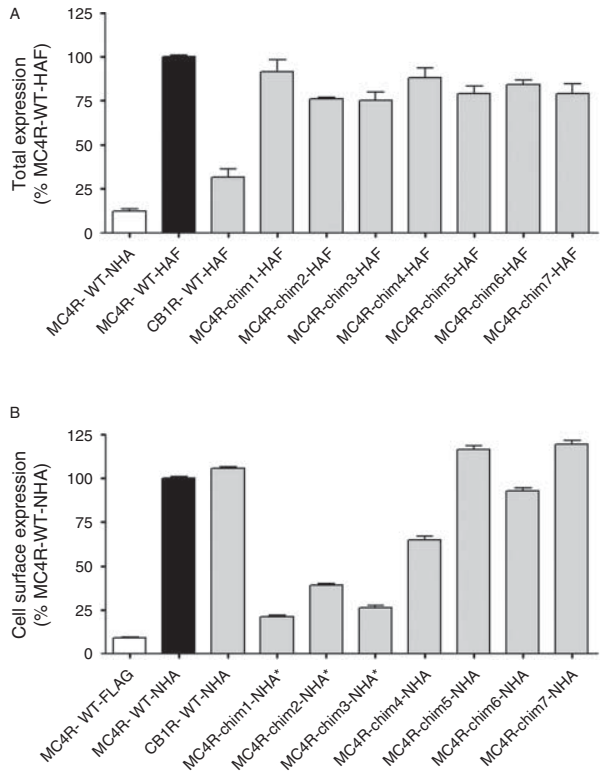

Figure 2
Expression of the chimeric MC4R/CB1R receptors. (A) Total receptor expression was determined in COS-7 cells with N-terminally HA- and C-terminally FLAG-tagged (HAF) constructs using a sandwich ELISA approach. N-terminally HA-tagged MC4R-WT served as negative control (MC4R-WT-NHA, white bar). The CB1R shows decreased total expression levels compared with the MC4R-WT (32%). The MC4R/CB1R chimeras have comparable total expression levels. The values are calculated per mg/ml protein and shown as percentage of the MC4R-WT expression (absorption (492/620) per mg/ml protein: 0.9±0.21). Data are means±s.e.m. of three or more independent experiments performed in triplicates. (B) For determination of cell surface expression, N-terminally HA-tagged receptors were measured in intact COS-7 cells. The MC4R-WT C-terminally FLAG-tagged served as negative control (MC4R-WT-FLAG, white bar). The chimeras chim1, chim2, and chim3 showed impaired and chim4 slightly decreased cell surface expression. We therefore excluded chim1, chim2, and chim3 from further functional experiments (marked with *). Values are given as percent of MC4R-WT expression (absorption (492/620): 0.6±0.18 set as 100%). Data are means±s.e.m. of three or more independent experiments performed in six replicates.

information, Supplementary Figure S2, see section on supplementary data given at the end of this article).

The enhanced signaling of chim5–chim7 might also be due to signaling from MC4R homodimer to PTX-sensitive G-proteins (Buch *et al.* 2009); however, signaling from MC4R to other G-proteins than Gs depends on the cell system used (Breit *et al.* 2011). In COS-7 cells, no reduction in basal activity was observed for the MC4R mutant Asp90Asn after NDP-α-MSH challenge (Biebermann *et al.* 2003), as has been found in HEK293 cells (Buch *et al.* 2009). We also tested PTX-sensitive signaling for MC4R-WT in COS-7 cells and found no enhancement of cAMP accumulation (supporting information, Supplementary Figure S3, see section on supplementary data given at the end of this article). Therefore, in the cell system used, we have been able to exclude the possibility that cAMP hyperstimulation of chim5–chim7 is due to loss of PTX-sensitive G-protein activation.

Specific regions of TMH3, TMH4, and ICL2 are important for MC4R homodimer formation

To investigate the interaction between chimeric receptors, we performed a sandwich ELISA. All tested constructs included ICL2 substitution from CB1R into the MC4R and gave rise to decreased or impaired dimerization capacity (dimer dissociation). Chim4 and chim6 showed significant decreases (69 and 67% dimerization of WT, $P<0.0001$) and chim5 and chim7 highly significant reductions (39 and 31% dimerization of WT, $P<0.0001$) in homodimerization capacities compared with WT (Fig. 4, in addition homodimerization capacities chim1–chim3 supporting information, Supplementary Figure S4, see section on supplementary data given at the end of this article). It is striking that chim4 and chim6, with the lowest suppression of dimer formation, included substitution of both CB1R ICL2 and the junction of TMH4. Chim5 and chim7 exhibited the maximum suppression of

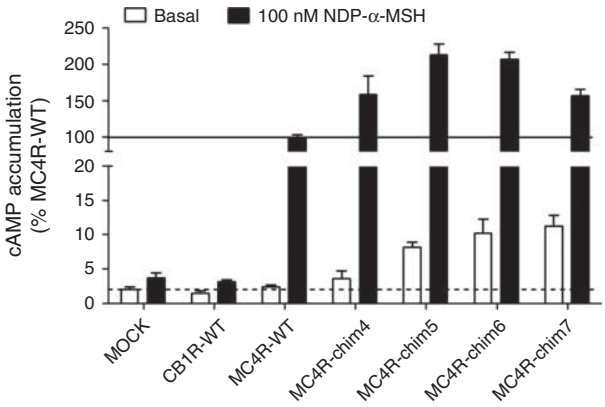

Figure 3
Signaling of the chimeric MC4R/CB1R receptors. cAMP accumulation was measured in COS-7 cells using the AlphaScreen technology. Cells were stimulated with 100 nM NDP-α-MSH. All tested chimeras show increased basal and ligand-induced cAMP accumulation compared with the MC4R-WT, with the exception of chim4, which had no significant increase in ligand-independent activity. The empty pcDps-vector served as negative control (MOCK) marked with dashed line. Values are given in percentage of MC4R-WT signaling marked with solid line (MC4R-WT 93.7±11.94 nM was set as 100%). Data are means±s.e.m. of three independent experiments performed in triplicates.

http://jme.endocrinology-journals.org
DOI: 10.1530/JME-13-0061
© 2013 Society for Endocrinology
Printed in Great Britain
Published by Bioscientifica Ltd.

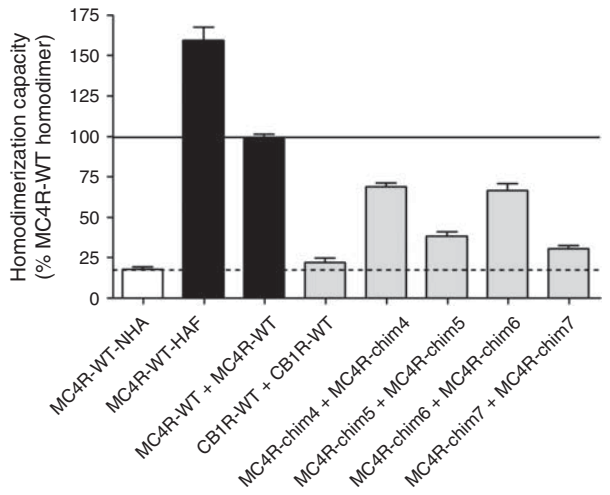

Figure 4
Dimerization of the chimeric MC4R/CB1R receptors. To investigate dimerization by sandwich ELISA, COS-7 cells were transiently co-transfected with equal amounts of N-terminally HA-tagged constructs and C-terminally FLAG-tagged constructs. The FLAG-tagged receptors attach to the FLAG-antibody-coated 96-well plate. The dimerization capacities were measured via the N-terminally HA-tagged receptor as an increase in optical density (mean absorption (492/620)). The N-terminally HA-tagged MC4R transfected alone served as negative control (MC4R-WT-NHA, white bar). N-terminally HA- and C-terminally FLAG-tagged MC4R (MC4R-WT-HAF) and the MC4R-WT homodimer (MC4R-WT-NHA + MC4R-WT-FLAG) served as positive controls (black bars). The CB1R is not able to form homodimers (Rediger *et al.* 2009). Chim4 and chim6 show slightly decreased (69 and 67%) and chim5 and chim7 greatly decreased (39 and 31%) dimerization capacity compared with WT. The values are calculated per mg/ml protein and shown as percentage of the MC4R-WT homodimer (absorption (492/620)/mg/ml protein: 0.6 ± 0.14). Data are means ± S.E.M. of four or more independent experiments performed in triplicates.

dimer formation and were modified either in ICL2 alone or in ICL2 and the proximate region to TMH3.

To ensure that the sandwich ELISA data are reproducible with a second method, we applied a YFP-based bimolecular fluorescence complementation assay (BiFC), which permits the determination of receptor interaction in living cells (supporting information, Supplementary Figure S5 and S6). As an example, we tested interactions for chim6 and chim7 and demonstrated once again that homodimerization of chim6 and chim7 is reduced compared with dimerization of MC4R-WT.

The naturally occurring MC4R mutation His158Arg in ICL2 exhibits enhanced signaling properties and reduced dimer formation

We also characterized the naturally occurring MC4R variant His158Arg in ICL2 (Hinney *et al.* 2006) with expression parameters comparable to WT (supporting information, Supplementary Table S1). This mutation revealed a threefold increased basal level of cAMP accumulation (Fig. 5A). Maximal ligand-induced signaling was increased to 168% of WT. To confirm the importance of this position and to investigate how these findings depend on side chain properties, we also designed and tested the His158Ala substitution. We detected a threefold increase in basal levels of cAMP accumulation and enhanced ligand-induced signaling.

In addition, the naturally occurring constitutively activating mutation (CAM) His158Arg and the variant His158Ala exhibited decreased homodimerization, corresponding to 56–64% of the value for the WT (Fig. 5B). On the one hand, this clearly indicates that inhibition of dimerization by modification at this position does not depend on the substituted side chain. On the other hand, it appears that the ICL2 is indeed a crucial key region for dimeric organization.

Discussion

In this study, we aimed to investigate two principle aspects of MC4R: i) the structural regions participating in dimerization and ii) the functional properties of receptor constructs with depressed dimerization capacity. We have found that both multiple and single substitutions in the intracellular region of the receptor of TMH3-ICL2-TMH4 inhibit MC4R dimerization (Fig. 6). From these results, we conclude that ICL2 makes the major contribution to the MC4R homodimerization process, with respect to our experimental setup. In accordance with this, our group has recently shown that disulphide bridges are not involved in MC4R dimerization (Elsner *et al.* 2006), which has been suggested for other GPCRs (Berthouze *et al.* 2007). However, we cannot exclude the possibility that TMH1 and TMH2, or TMH5–7, might play an additional role in MC4R–MC4R interactions, as was recently speculated for MC4R and as has been suggested for other GPCRs in general (Lee *et al.* 2003).

It is known that GPCRs probably exist in a monomer–dimer equilibrium ((Kasai *et al.* 2011), reviewed in Lambert (2010)), which raises the possibility that specific modifications in the receptors might shift the equilibrium toward one of these states. There have only been a few reports (Grant *et al.* 2004, Ravindran *et al.* 2009, Moreno *et al.* 2012) of GPCR dimer dissociation induced by ligand binding or mutations. Single side chain substitutions have been found to interrupt the dimer interface at TMH4, as in chemokine receptor CCR5 (one residue) or the heterodimer between the metabotropic glutamate-2 receptor and

http://jme.endocrinology-journals.org
DOI: 10.1530/JME-13-0061
© 2013 Society for Endocrinology
Printed in Great Britain
Published by Bioscientifica Ltd.

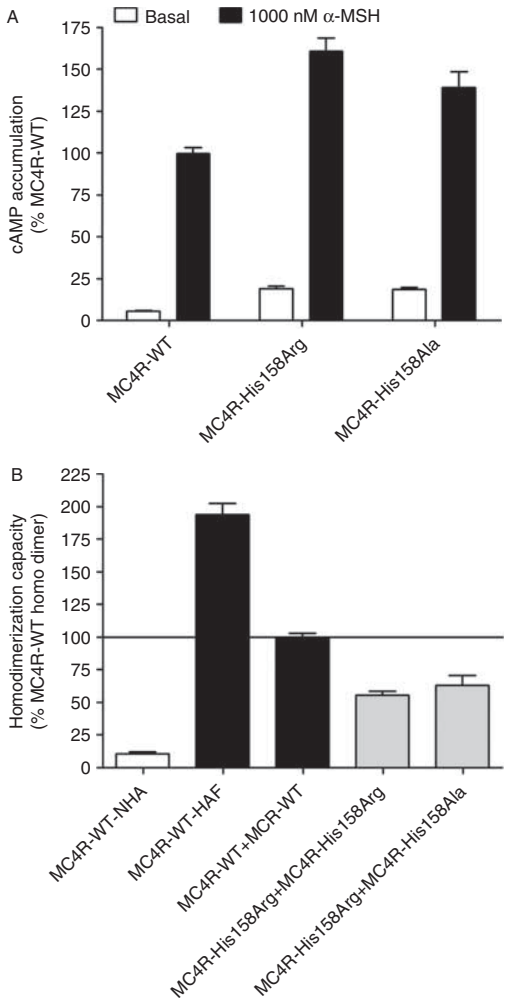

Figure 5
Functional investigation of the pathogenic MC4R mutation His158Arg and the artificial mutation His158Ala. (A) cAMP accumulation was measured in COS-7 cells using the AlphaScreen technology. Cells were stimulated with 1000 nM of the endogenous ligand α-MSH. Both mutants shows increased basal and ligand-induced cAMP accumulation compared with the MC4R-WT. Values are given in percentage of MC4R-WT signaling (MC4R-WT 153.5±34.10 nM was set as 100%). Data are means±s.e.m. of three independent experiments performed in triplicates. (B) Dimerization of MC4R mutant His158Arg and His158Ala was investigated using transiently co-transfected COS-7 cells with equal amounts of N-terminally HA-tagged constructs and C-terminally FLAG-tagged constructs. The FLAG-tagged receptor attached to the FLAG antibody-coated 96-well plate. The dimerization capacities were measured via the N-terminally HA-tagged receptor as an increase in optical density (mean absorption (492/620)). The N-terminally HA-tagged MC4R served as negative control (MC4R-WT-NHA, white bar). N-terminally HA- and C-terminally FLAG-tagged MC4R (MC4R-WT-HAF) and the MC4R-WT homodimer (MC4R-WT-NHA+MC4R-WT-FLAG) served as positive controls (black bars). Both MC4R-His158Arg and MC4R-His158Ala show decreased (56 and 64%) dimerization capacity compared with MC4R-WT. The values are calculated per mg/ml protein and shown as percentage of the MC4R-WT homodimer (absorption (492/620)/mg/ml protein: 0.3±0.03). Data are means±s.e.m. of four independent experiments performed in triplicates.

the serotonin-5 receptor (three residues) (Hernanz-Falcon *et al.* 2004, Moreno *et al.* 2012).

We also detected an increase in the permanent (basal) signaling activity for single and multiple substitutions in ICL2 and adjacent helices. It is well known for MC4R that particular mutations are able to increase the constitutive (ligand independent) basal tone of signaling (cAMP accumulation), such as mutations at Leu140 in TMH3 (Mo *et al.* 2012). It has also been reported that specific mutations may induce biased signals, whereby cAMP accumulation related to Gs and to the pERK1/2 pathway can be differentially modified (Mo *et al.* 2012). Moreover, a systematic and comprehensive mutagenesis study on amino acids of TMH6 revealed further significant insights into signaling regulation at MC4R (Huang & Tao 2012). Several specific mutations in TMH6 induced constitutive activation of pERK1/2 phosphorylation, or constitutive activation of Gs, as well as inactivating mutations were identified. Taken together, these findings provide detailed information on the determinants of the MC4R mechanism in the transmembrane region (Huang & Tao 2012). Finally, such systematic approaches help to elucidate intramolecular interaction networks and help us to understand in detail how the receptor switches between the different activity states. In addition, the N-terminus of MC4R is also important in the regulation of ligand-independent signaling. The results of mutagenesis at specific residues in the N-terminal MC4R region had suggested that this region acts as an intramolecular, tethered agonist (partial) and maintains a basal signaling tone (Srinivasan *et al.* 2004). Specific naturally occurring mutations at the N-terminal tail decreased the level of basal cAMP accumulation, which also highlights the importance of this signaling capacity under pathophysiological conditions.

Our current study is compatible with the concept that the degree of oligomerization could also be involved in the regulation of the basal signaling activity. This is indicated by the simultaneous occurrence of dimer separation and increased basal activity. For further studies, it might be of interest to investigate the function of the N-terminus in combination with CAMs at other parts of the receptor. In summary, the important basal activity level of MC4R can be regulated at different receptor regions and tuned up or down, probably by a variety of mechanisms.

It is striking that ligand-induced Gs-mediated signaling capacity was enhanced in our constructs with dissociated dimers. This may be caused by synergy between the increased basal activity and the capacity of ligand-induced stimulation. Alternatively, this finding

http://jme.endocrinology-journals.org
DOI: 10.1530/JME-13-0061
© 2013 Society for Endocrinology
Printed in Great Britain
Published by Bioscientifica Ltd.

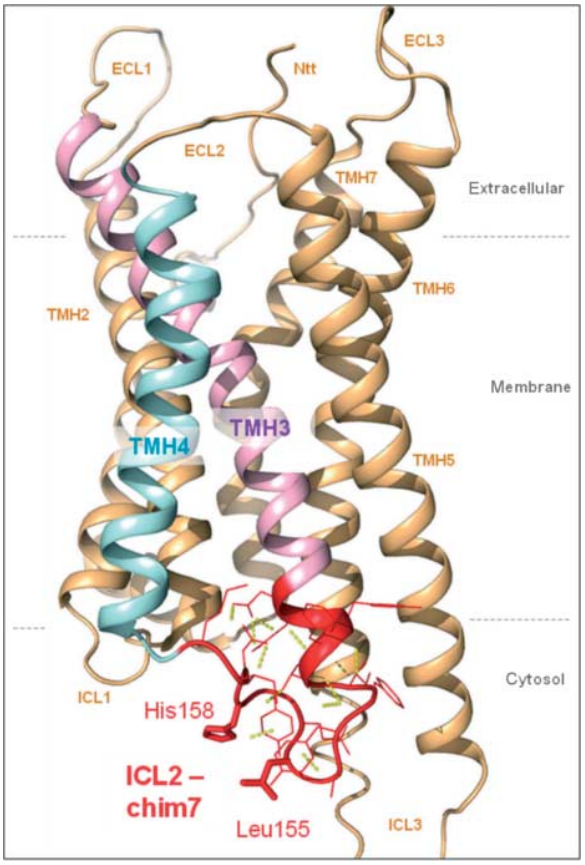

Figure 6
Structural implications from a MC4R homology model. Our aim was to induce MC4R dimer dissociation by substituting specific CB1R fragments into the potential MC4R–MC4R dimer interface, in order to identify protomer–protomer contacts and to compare functional properties between monomeric vs dimeric MC4R. Therefore, it was important to maintain the capacity of chimeric receptors to couple Gs such as wild-type MC4R and to avoid modifying the coupling specificity of MC4R for Gs by constructing chimeric receptors. The CB1R is a Gi- and Gs protein coupling GPCR (Howlett *et al.* 1986) and is known from GPCRs such as the β-adrenergic receptor 2 (ADRB2) that the essential amino acids for Gi and Gs coupling are similar. One of these residues is Phe139 at the ICL2 of ADRB2, which is leucine 155 at the corresponding position of MC4R. Both amino acids are hydrophobic and conservation of Phe/Leu residues at this position has been reported, based on comparison of different family A GPCRs (Rasmussen *et al.* 2011). In the chimeric receptor variants MC4R/CB1R, a leucine is also localized at the corresponding position (supporting information, Supplementary Figure S1). This indicates that the Gs coupling capacity at this position is also probably maintained in the chimeric receptors. Substituted helices or receptor regions (e.g. MC4R chim7) are highlighted by different colors in the structural MC4R homology model. Our experimental data suggest that the MC4R homodimeric constellation is partially inhibited by substitutions at the transition between ICL2 and TMH3 (red). In the natural MC4R variant His158Arg tested here, it is of special note that the corresponding CB1R amino acid is Lys225 (CB1R sequence number), which is also positively charged like the arginine MC4R variant. The solid line marked homodimer formation of the MC4R-WT. This single substitution, as well as the variant His158Ala, leads to partial dissociation of MC4R dimers, thus confirming the importance of MC4R ICL2 for dimeric organization.

might also be explained by the receptor:G-protein ratio of 2:1 in the homodimeric WT, in contrast to the ratio of 1:1 between increased levels of MC4R monomers and G-proteins. However, our data and experimental setup do not provide clear evidence that there is a direct relationship between homodimerization/monomerization and the capacity for signaling. This question can be studied in future with heterodimeric MC4R/GPCR complexes. Several studies on different GPCRs have found significant differences between GPCR–GPCR dimers and monomers with respect to structure–function relationships: i) for homodimers of dopamine receptors, it has been shown (Guo *et al.* 2005) that TMH4 orientation is modified during (dimeric) receptor activation; ii) studies on homodimeric GPCRs have found that, after agonist-mediated activation, G-protein coupling may occur at only one protomer (Damian *et al.* 2006); and iii) conformational changes between α_2A-adrenergic and μ-opioid receptor heterodimers have been reported, whereby the propagated conformational change from one activated receptor caused inactivation of the second receptor (Vilardaga *et al.* 2008).

In summary, these findings support a concept whereby the ICL2, together with specific adjacent regions of TMH3 and TMH4, is important for constituting a dimeric MC4R constellation. Modifications here lead to dissociation of the dimers into receptor monomers. Furthermore, this region is also important for maintaining an inactive state and for determining signaling capacity. In conclusion, the conformation and interplay of the entire intracellular TMH3-ICL2-TMH4 region is a regulating element in signaling and receptor organization. Our findings add to the few known examples of GPCR dimer dissociation induced by ligand binding or mutations (Grant *et al.* 2004, Ravindran *et al.* 2009, Moreno *et al.* 2012).

Supplementary data
This is linked to the online version of the paper at http://dx.doi.org/10.1530/JME-13-0061.

Declaration of interest
The authors declare that there is no conflict of interest that could be perceived as prejudicing the impartiality of the research reported.

Funding
This work was funded by the Deutsche Forschungsgemeinschaft (BI 893/2-1, BI893/5-1, BI893/6-2) and graduate school 1208: Hormonal Regulation of Energy Metabolism, Body Weight and Growth, TP1.

http://jme.endocrinology-journals.org
DOI: 10.1530/JME-13-0061
© 2013 Society for Endocrinology
Printed in Great Britain
Published by Bioscientifica Ltd.

Author contribution statement
C L P, H B, G K, and A R were involved in conception and design of the experiments. C L P, A R, C L, J M, P T, and A M were involved in performance of the experiments. C L P, H B, G K, J P, A M, A G, and H K were involved in data analysis. All authors were involved in writing the paper and were responsible for the final approval of the submitted and published versions.

Acknowledgement
The authors are grateful for the important contributions of Lara Zajic.

References

Berthouze M, Rivail L, Lucas A, Ayoub MA, Russo O, Sicsic S, Fischmeister R, Berque-Bestel I, Jockers R & Lezoualc'h F 2007 Two transmembrane Cys residues are involved in 5-HT4 receptor dimerization. *Biochemical and Biophysical Research Communications* **356** 642–647. (doi:10.1016/j.bbrc.2007.03.030)

Biebermann H, Krude H, Elsner A, Chubanov V, Gudermann T & Gruters A 2003 Autosomal-dominant mode of inheritance of a melanocortin-4 receptor mutation in a patient with severe early-onset obesity is due to a dominant-negative effect caused by receptor dimerization. *Diabetes* **52** 2984–2988. (doi:10.2337/diabetes.52.12.2984)

Biebermann H, Kuhnen P, Kleinau G & Krude H 2012 The neuroendocrine circuitry controlled by POMC, MSH, and AGRP. *Handbook of Experimental Pharmacology* **209** 47–75. (doi:10.1007/978-3-642-24716-3_3)

Breit A, Buch TR, Boekhoff I, Solinski HJ, Damm E & Gudermann T 2011 Alternative G protein coupling and biased agonism: new insights into melanocortin-4 receptor signalling. *Molecular and Cellular Endocrinology* **331** 232–240. (doi:10.1016/j.mce.2010.07.007)

Buch TR, Heling D, Damm E, Gudermann T & Breit A 2009 Pertussis toxin-sensitive signaling of melanocortin-4 receptors in hypothalamic GT1–7 cells defines agouti-related protein as a biased agonist. *Journal of Biological Chemistry* **284** 26411–26420. (doi:10.1074/jbc.M109.039339)

Carrillo JJ, Lopez-Gimenez JF & Milligan G 2004 Multiple interactions between transmembrane helices generate the oligomeric α1b-adrenoceptor. *Molecular Pharmacology* **66** 1123–1137. (doi:10.1124/mol.104.001586)

Cone RD 2006 Studies on the physiological functions of the melanocortin system. *Endocrine Reviews* **27** 736–749. (doi:10.1210/er.2006-0034)

Damian M, Martin A, Mesnier D, Pin JP & Baneres JL 2006 Asymmetric conformational changes in a GPCR dimer controlled by G-proteins. *EMBO Journal* **25** 5693–5702. (doi:10.1038/sj.emboj.7601449)

Elsner A, Tarnow P, Schaefer M, Ambrugger P, Krude H, Gruters A & Biebermann H 2006 MC4R oligomerizes independently of extracellular cysteine residues. *Peptides* **27** 372–379. (doi:10.1016/j.peptides.2005.02.027)

Farooqi IS, Yeo GS & O'Rahilly S 2003 Binge eating as a phenotype of melanocortin 4 receptor gene mutations. *New England Journal of Medicine* **349** 606–609 author reply 606–609. (doi:10.1056/NEJM200308073490615)

George SR, O'Dowd BF & Lee SP 2002 G-protein-coupled receptor oligomerization and its potential for drug discovery. *Nature Reviews. Drug Discovery* **1** 808–820. (doi:10.1038/nrd913)

Grant M, Collier B & Kumar U 2004 Agonist-dependent dissociation of human somatostatin receptor 2 dimers: a role in receptor trafficking. *Journal of Biological Chemistry* **279** 36179–36183. (doi:10.1074/jbc.M407310200)

Guo W, Shi L, Filizola M, Weinstein H & Javitch JA 2005 Crosstalk in G protein-coupled receptors: changes at the transmembrane homodimer interface determine activation. *PNAS* **102** 17495–17500. (doi:10.1073/pnas.0508950102)

Guo W, Urizar E, Kralikova M, Mobarec JC, Shi L, Filizola M & Javitch JA 2008 Dopamine D2 receptors form higher order oligomers at physiological expression levels. *EMBO Journal* **27** 2293–2304. (doi:10.1038/emboj.2008.153)

Hernanz-Falcon P, Rodriguez-Frade JM, Serrano A, Juan D, del Sol A, Soriano SF, Roncal F, Gomez L, Valencia A, Martinez AC *et al.* 2004 Identification of amino acid residues crucial for chemokine receptor dimerization. *Nature Immunology* **5** 216–223. (doi:10.1038/ni1027)

Hinney A, Bettecken T, Tarnow P, Brumm H, Reichwald K, Lichtner P, Scherag A, Nguyen TT, Schlumberger P, Rief W *et al.* 2006 Prevalence, spectrum, and functional characterization of melanocortin-4 receptor gene mutations in a representative population-based sample and obese adults from Germany. *Journal of Clinical Endocrinology and Metabolism* **91** 1761–1769. (doi:10.1210/jc.2005-2056)

Howlett AC, Qualy JM & Khachatrian LL 1986 Involvement of Gi in the inhibition of adenylate cyclase by cannabimimetic drugs. *Molecular Pharmacology* **29** 307–313.

Huang H & Tao YX 2012 Pleiotropic functions of the transmembrane domain 6 of human melanocortin-4 receptor. *Journal of Molecular Endocrinology* **49** 237–248. (doi:10.1530/JME-12-0161)

Kasai RS, Suzuki KG, Prossnitz ER, Koyama-Honda I, Nakada C, Fujiwara TK & Kusumi A 2011 Full characterization of GPCR monomer-dimer dynamic equilibrium by single molecule imaging. *Journal of Cell Biology* **192** 463–480. (doi:10.1083/jcb.201009128)

Krishna R, Gumbiner B, Stevens C, Musser B, Mallick M, Suryawanshi S, Maganti L, Zhu H, Han TH, Scherer L *et al.* 2009 Potent and selective agonism of the melanocortin receptor 4 with MK-0493 does not induce weight loss in obese human subjects: energy intake predicts lack of weight loss efficacy. *Clinical Pharmacology and Therapeutics* **86** 659–666. (doi:10.1038/clpt.2009.167)

Lambert NA 2010 GPCR dimers fall apart. *Science Signaling* **3** pe12. (doi:10.1126/scisignal.3115pe12)

Lee SP, O'Dowd BF, Rajaram RD, Nguyen T & George SR 2003 D2 dopamine receptor homodimerization is mediated by multiple sites of interaction, including an intermolecular interaction involving transmembrane domain 4. *Biochemistry* **42** 11023–11031. (doi:10.1021/bi0345539)

Levoye A, Dam J, Ayoub MA, Guillaume JL, Couturier C, Delagrange P & Jockers R 2006 The orphan GPR50 receptor specifically inhibits MT1 melatonin receptor function through heterodimerization. *EMBO Journal* **25** 3012–3023. (doi:10.1038/sj.emboj.7601193)

Mancia F, Assur Z, Herman AG, Siegel R & Hendrickson WA 2008 Ligand sensitivity in dimeric associations of the serotonin 5HT2c receptor. *EMBO Reports* **9** 363–369. (doi:10.1038/embor.2008.27)

Mo XL, Yang R & Tao YX 2012 Functions of transmembrane domain 3 of human melanocortin-4 receptor. *Journal of Molecular Endocrinology* **49** 221–235. (doi:10.1530/JME-12-0162)

Moreno JL, Muguruza C, Umali A, Mortillo S, Holloway T, Pilar-Cuellar F, Mocci G, Seto J, Callado LF, Neve RL *et al.* 2012 Identification of three residues essential for 5-HT2A-mGlu2 receptor heteromerization and its psychoactive behavioral function. *Journal of Biological Chemistry* **287** 44301–44319. (doi:10.1074/jbc.M112.413161)

Nickolls SA & Maki RA 2006 Dimerization of the melanocortin 4 receptor: a study using bioluminescence resonance energy transfer. *Peptides* **27** 380–387. (doi:10.1016/j.peptides.2004.12.037)

Nijenhuis WA, Oosterom J & Adan RA 2001 AgRP(83–132) acts as an inverse agonist on the human-melanocortin-4 receptor. *Molecular Endocrinology* **15** 164–171. (doi:10.1210/me.15.1.164)

Pogozheva ID, Chai BX, Lomize AL, Fong TM, Weinberg DH, Nargund RP, Mulholland MW, Gantz I & Mosberg HI 2005 Interactions of human melanocortin 4 receptor with nonpeptide and peptide agonists. *Biochemistry* **44** 11329–11341. (doi:10.1021/bi0501840)

Rasmussen SG, DeVree BT, Zou Y, Kruse AC, Chung KY, Kobilka TS, Thian FS, Chae PS, Pardon E, Calinski D *et al.* 2011 Crystal structure of the β2 adrenergic receptor-Gs protein complex. *Nature* **477** 549–555. (doi:10.1038/nature10361)

http://jme.endocrinology-journals.org
DOI: 10.1530/JME-13-0061
© 2013 Society for Endocrinology
Printed in Great Britain
Published by Bioscientifica Ltd.

Ravindran A, Joseph PR & Rajarathnam K 2009 Structural basis for differential binding of the interleukin-8 monomer and dimer to the CXCR1 N-domain: role of coupled interactions and dynamics. *Biochemistry* **48** 8795–8805. (doi:10.1021/bi901194p)

Rediger A, Tarnow P, Bickenbach A, Schaefer M, Krude H, Gruters A & Biebermann H 2009 Heterodimerization of hypothalamic G-protein-coupled receptors involved in weight regulation. *Obesity Facts* **2** 80–86. (doi:10.1159/000209862)

Rediger A, Piechowski CL, Habegger K, Gruters A, Krude H, Tschop MH, Kleinau G & Biebermann H 2012 MC4R dimerization in the paraventricular nucleus and GHSR/MC3R heterodimerization in the arcuate nucleus: is there relevance for body weight regulation. *Neuroendocrinology* **95** 277–288. (doi:10.1159/000334903)

Rhee MH, Bayewitch M, Avidor-Reiss T, Levy R & Vogel Z 1998 Cannabinoid receptor activation differentially regulates the various adenylyl cyclase isozymes. *Journal of Neurochemistry* **71** 1525–1534. (doi:10.1046/j.1471-4159.1998.71041525.x)

Rozenfeld R & Devi LA 2010 Receptor heteromerization and drug discovery. *Trends in Pharmacological Sciences* **31** 124–130. (doi:10.1016/j.tips.2009.11.008)

Rozenfeld R & Devi LA 2011 Exploring a role for heteromerization in GPCR signalling specificity. *Biochemical Journal* **433** 11–18. (doi:10.1042/BJ20100458)

Srinivasan S, Lubrano-Berthelier C, Govaerts C, Picard F, Santiago P, Conklin BR & Vaisse C 2004 Constitutive activity of the melanocortin-4 receptor is maintained by its N-terminal domain and plays a role in energy homeostasis in humans. *Journal of Clinical Investigation* **114** 1158–1164. (doi:10.1172/JCI21927)

Staubert C, Tarnow P, Brumm H, Pitra C, Gudermann T, Gruters A, Schoneberg T, Biebermann H & Rompler H 2007 Evolutionary aspects in evaluating mutations in the melanocortin 4 receptor. *Endocrinology* **148** 4642–4648. (doi:10.1210/en.2007-0138)

Tao YX 2010 The melanocortin-4 receptor: physiology, pharmacology, and pathophysiology. *Endocrine Reviews* **31** 506–543. (doi:10.1210/er.2009-0037)

Tarnow P, Rediger A, Brumm H, Ambrugger P, Rettenbacher E, Widhalm K, Hinney A, Kleinau G, Schaefer M, Hebebrand J *et al*. 2008 A heterozygous mutation in the third transmembrane domain causes a dominant-negative effect on signalling capability of the MC4R. *Obesity Facts* **1** 155–162. (doi:10.1159/000138251)

Van der Ploeg LH, Martin WJ, Howard AD, Nargund RP, Austin CP, Guan X, Drisko J, Cashen D, Sebhat I, Patchett AA *et al*. 2002 A role for the melanocortin 4 receptor in sexual function. *PNAS* **99** 11381–11386. (doi:10.1073/pnas.172378699)

Vilardaga JP, Nikolaev VO, Lorenz K, Ferrandon S, Zhuang Z & Lohse MJ 2008 Conformational cross-talk between α2A-adrenergic and mu-opioid receptors controls cell signaling. *Nature Chemical Biology* **4** 126–131. (doi:10.1038/nchembio.64)

Worth CL, Kleinau G & Krause G 2009 Comparative sequence and structural analyses of G-protein-coupled receptor crystal structures and implications for molecular models. *PLoS ONE* **4** e7011. (doi:10.1371/journal.pone.0007011)

Received in final form 10 May 2013
Accepted 14 May 2013
Accepted Preprint published online 14 May 2013

http://jme.endocrinology-journals.org
DOI: 10.1530/JME-13-0061
© 2013 Society for Endocrinology
Printed in Great Britain
Published by Bioscientifica Ltd.

9.3 Publikation 3: Differential Modulation of Beta-Adrenergic Receptor Signaling by Trace Amine-Associated Receptor 1 Agonists

G. Kleinau*, J. Pratzka*, D. Nürnberg, A. Grüters, D. Führer-Sakel, H. Krude, J. Köhrle, T. Schöneberg, H. Biebermann.
PLoS One. 6(10): e27073.
doi:10.1371/journal.pone.0027073. Epub 2011 Oct 31.

***gleichberechtigte Erstautoren**

OPEN ACCESS Freely available online

PLoS one

Differential Modulation of Beta-Adrenergic Receptor Signaling by Trace Amine-Associated Receptor 1 Agonists

Gunnar Kleinau[1❍], Juliane Pratzka[1❍], Daniela Nürnberg[1], Annette Grüters[1], Dagmar Führer-Sakel[3], Heiko Krude[1], Josef Köhrle[2], Torsten Schöneberg[4], Heike Biebermann[1]*

1 Institute of Experimental Pediatric Endocrinology, Charité-Universitätsmedizin Berlin, Berlin, Germany, **2** Institute of Experimental Endocrinology, Charité-Universitätsmedizin Berlin, Berlin, Germany, **3** Klinik für Endokrinologie, Zentrum für Innere Medizin, Universitätsklinikum Essen, Essen, Germany, **4** Institute of Biochemistry, Medical Faculty, University of Leipzig, Leipzig, Germany

Abstract

Trace amine-associated receptors (TAAR) are rhodopsin-like G-protein-coupled receptors (GPCR). TAAR are involved in modulation of neuronal, cardiac and vascular functions and they are potentially linked with neurological disorders like schizophrenia and Parkinson's disease. Subtype TAAR1, the best characterized TAAR so far, is promiscuous for a wide set of ligands and is activated by trace amines tyramine (TYR), phenylethylamine (PEA), octopamine (OA), but also by thyronamines, dopamine, and psycho-active drugs. Unfortunately, effects of trace amines on signaling of the two homologous β-adrenergic receptors 1 (ADRB1) and 2 (ADRB2) have not been clarified yet in detail. We, therefore, tested TAAR1 agonists TYR, PEA and OA regarding their effects on ADRB1/2 signaling by co-stimulation studies. Surprisingly, trace amines TYR and PEA are partial allosteric antagonists at ADRB1/2, whereas OA is a partial orthosteric ADRB2-antagonist and ADRB1-agonist. To specify molecular reasons for TAAR1 ligand promiscuity and for observed differences in signaling effects on particular aminergic receptors we compared TAAR, tyramine (TAR) octopamine (OAR), ADRB1/2 and dopamine receptors at the structural level. We found especially for TAAR1 that the remarkable ligand promiscuity is likely based on high amino acid similarity in the ligand-binding region compared with further aminergic receptors. On the other hand few TAAR specific properties in the ligand-binding site might determine differences in ligand-induced effects compared to ADRB1/2. Taken together, this study points to molecular details of TAAR1-ligand promiscuity and identified specific trace amines as allosteric or orthosteric ligands of particular β-adrenergic receptor subtypes.

Citation: Kleinau G, Pratzka J, Nürnberg D, Grüters A, Führer-Sakel D, et al. (2011) Differential Modulation of Beta-Adrenergic Receptor Signaling by Trace Amine-Associated Receptor 1 Agonists. PLoS ONE 6(10): e27073. doi:10.1371/journal.pone.0027073

Editor: Rakesh K. Srivastava, The University of Kansas Medical Center, United States of America

Received August 2, 2011; **Accepted** October 9, 2011; **Published** October 31, 2011

Copyright: © 2011 Kleinau et al. This is an open-access article distributed under the terms of the Creative Commons Attribution License, which permits unrestricted use, distribution, and reproduction in any medium, provided the original author and source are credited.

Funding: This work was supported by the Deutsche Forschungsgemeinschaft (DFG): Graduate College 1208 (Hormonal Regulation of Energy Metabolism, Body Weight and Growth) TP1 and TP3, and grant KL2334/2-1. The funders had no role in study design, data collection and analysis, decision to publish, or preparation of the manuscript.

Competing Interests: The authors have declared that no competing interests exist.

* E-mail: heike.biebermann@charite.de

❍ These authors contributed equally to this work.

Introduction

The group of trace amine-associated receptors (TAAR) [1] belongs to the rhodopsin-like family of G protein-coupled receptors (GPCRs) and is of importance for several physiological aspects such as proper cardiac and vascular functions (reviews [2,3,4,5]). It has also been proposed that TAAR are involved as neuromodulators in brain [2,6]. In accordance, TAAR are postulated to be linked with neurological disorders like bipolar disease [7,8], schizophrenia [9,10], depression and Parkinson's disease [11,12]. In consequence, TAAR are potential new important therapeutic targets for several pathological situations [13,14]. The first human member of this receptor group (TAAR5) was identified in 1998 [15,16] and the term TAAR was introduced when TAAR1, TAAR8 and TAAR9 were discovered [17]. Three out of the nine hTAAR members are pseudogenes [18]. TAAR1 is activated by trace amines [6] such as tyramine (TYR), β-phenylethylamine (PEA) or octopamine (OA) [17,19] and signals via the Gs protein/adenylyl cyclase system. In addition, it was reported that a thyroid hormone derivative, 3-thyronamine (T_1AM) [20,21,22,23,24,25,26,27,28,29] activates TAAR1. Remarkable differences in efficacies of T_1AM between hTAAR1 and rodent Taar1 were observed [30]. In addition, ligands of the dopamine-, serotonine-, histamine-, or adrenergic receptors are able to induce TAAR1 mediated signaling [17,19,31,32]. Surprisingly, antagonists of the serotonin receptor like cyproheptadine as well as antagonists of adrenergic receptors like phentolamine are Taar1 agonists [19]. Besides trace amines and biogenic amines also volatile amines activate human TAAR1 and murine Taar 3, 5, and 7 [33], characterizing these TAAR additionally as odorant receptors [34,35,36]. Finally, TAAR1 responds to psycho-active drugs [19,37]. This points, altogether, to an enormous TAAR1 ligand-binding promiscuity that might reflect also the evolutionary link between TAAR and homologous vertebrate aminergic receptors [2,17,18,38,39,40] or invertebrate tyramine receptors (TAR) and octopamine receptors (OAR).

Trace amines in mammalians are suggested to function as endogenous neuromodulators of classical monoamine neurotransmitters [41,42]. In contrast, in the tyramine/octopamine system in invertebrates, the homologue to the mammalian adrenergic system [43,44], trace amines are acting as direct neurotransmitters. Trace amines and their invertebrate receptors are involved in regulation of metabolism and of sensory and behavioral functions [44]. Several tyramine and octopamine receptors were identified in invertebrates like insects [44,45,46,47] or mollusks [48]. Of note, the overlap in homologous receptor-ligand systems has also unexpected consequences. For example TAR and OAR are targets for insecticid development [44] and these substances could potentially affect TAAR or other aminergic receptors. In reverse, β-blockers have an endocrine-disrupting potential on organisms with TAR and OAR expression [49]. It is well known that particular ligands interact with several different aminergic receptors or modulate different physiological systems. Octopamine has been shown previously to be an agonist at the α-adrenergic receptor [50,51] and the β3-adrenergic receptor [52]. Substance PEA may act as an α-adrenergic receptor antagonist [53]. The OAR of *Lymnaea stagnalis* was found to be activated by α2-adrenergic receptor ligands, which leads in case of OAR to activation of both Gs- and Gq-mediated pathways [48]. Furthermore, it can be postulated from several studies that TAAR1 function might be related with the dopamine-2 receptor [54,55,56,57,58] as well as with the serotonin receptor 5-HT(1A) [59]. Recently published evidence points to a physiological role for T_1AM as an endogenous adrenergic-blocking neuromodulator in the central noradrenergic system [22]. In conclusion, a wide spectrum of potential ligand-aminergic receptor combinations or modulation of different physiological systems by specific ligands has been recognized. But, reflecting possible cross-combinations of the huge number of potential interaction partners this complex system is only recognized fragmentarily.

Herein we tested particular trace amines acting as agonists on hTAAR1 regarding their direct effects on hADRB1 and hADRB2 signaling. We found allosteric and orthosteric antagonistic effects of particular trace amines on ADRB1 and ADRB2. Octopamine induced different signaling effects on ADRB1 and ADRB2. Based on these findings we investigated the structural basis of TAAR ligand-promiscuity by comparative studies to other aminergic receptors and found similarities and differences between aminergic receptors which help to explain differential modification of signaling induced by trace amines.

Results

Different effects of trace amines at hTAAR1 and human β-adrenergic receptors

Ligands PEA, TYR and OA (figure 1) activate hTAAR1 [17,19] with subsequent stimulation of adenylyl cyclase and cAMP formation (figure 2, supplemental figure S1). Of note, hTAAR1 exhibits a high level of basal constitutive (ligand independent) signaling activity (73±14 nM cAMP) compared to mock transfected cells (figure 2). This hTAAR1 characteristic is in accordance to the reported effects of inverse agonists effecting ligand independent signaling activity of TAAR1 [60,61].

For describing the functional effects of PEA, TYR and OA we use the following terms: allosteric antagonist if a non-competitive effect on ISOP is observed and orthosteric antagonist if a competitive effect occurs. The most potent agonist tested was PEA (Emax = 403±54 nM), followed by TYR (Emax = 219±67 nM) and OA (Emax = 172±42 nM) (figure 2 and supplemental figure S1).

Isoprenaline (ISOP) is a full agonist to β-adrenergic receptors and was also reported as an agonist to TAAR1 [19]. We functionally tested the effects of particular trace amines at the human ADRB1 and ADRB2 (figure 3). Therefore, HEK293 cells (ATCC-LGC, Wesel, Germany) were transiently transfected with hADRB1 or hADRB2 and incubated with TYR, PEA or OA alone or in presence of ISOP. For competition experiments we prestimulated ADRB1 and ADRB2 with each trace amine TYR, PEA and OA in concentrations ranging from 6.7 nM to 6700 nM [17,19]. Then, ISOP in concentrations from 1 nM up to 10000 nM was added and cAMP accumulation was measured. Controls were stimulated with each trace amine and ISOP alone, respectively.

As shown in figure 3A-B, TYR acted as an allosteric antagonist at both, ADRB1 and ADRB2, by decreasing the E_{max} values to 30% and 60% of the wild type receptor, respectively, when compared to ISOP alone. A small increase of ADRB2 signaling at highest TYR concentrations was not significant. The concentration-response curves revealed no shift in the EC_{50} value (figure 3A, table 1) indicating a non-competitive allosteric effect of TYR on ISOP-stimulated ADRB1 and ADRB2. Similarly, PEA non-competitively antagonized signaling of both ADRB1 and ADRB2 (figure 3C, D).

In contrast, OA acted as an agonist to hADRB1 (figure 3E), but with lower potency (EC_{50} 3129±461 nM) than ISOP (EC_{50} = 61±10 nM) (table 1). OA together with ISOP showed slightly differences in their EC_{50} values. Nevertheless, there were no changes in E_{max} values (table 1, figure 3E) detectable. Interestingly, OA did not activate ADRB2 but acted as an orthosteric antagonist by inhibiting ISOP activation competitively (figure 3F).

Structural similarities and differences between hTAAR and homologous aminergic receptors

Our knowledge concerning ligand binding at β-adrenergic receptors and other members of the rhodopsin-like GPCR family has been dramatically increased since crystal structures of ADRB1, ADRB2, and dopamine-3 receptor (DRD3) in complex with antagonists or agonists recently became available [62,63,64,65]. These crystal structures provide molecular details of intermolecular interaction between receptor proteins and small molecules with respect to the location of ligands, their orientation and intermolecular interaction partners (figure 4A–C). TAAR, OAR/TAR of invertebrates and classical aminergic receptors show high amino acid sequence identities (supplemental material figure S2). To compare hTAAR with aminergic receptors we analyzed determinants of the β2-adrenergic ligand-binding region (figure 4 and figure 5) and designed human TAAR homology models based on the β2-adrenergic receptor conformation (figure 6A, supplemental material figure S3). This is reasonable because TAAR1 shows highest sequence similarity to ADRB1 (~35%) and ADRB2 (~39%) and TAAR1 is activated by adrenergic receptor agonists such as isoprenaline [19,30].

Structural properties and specificities of TAAR. TAAR are structurally constituted by an extracellular N-terminal tail (Ntt), seven transmembrane helices (TMH1-7), three extracellular loops (ECL1-3), three intracellular loops (ICL1-3) and an intracellular C-terminal part (Ctt). TAAR share specific highly conserved amino acids in the TMH with all rhodopsin-like GPCR [66]. One of the main structural difference between GPCR is the conformation and spatial localization of ECL2 [67]. While in rhodopsin a β-sheet like fold is observable, crystal structures of adrenergic receptors show a helical ECL2 conformation. We suggest based on the sequence alignment that ECL2 of TAAR is in

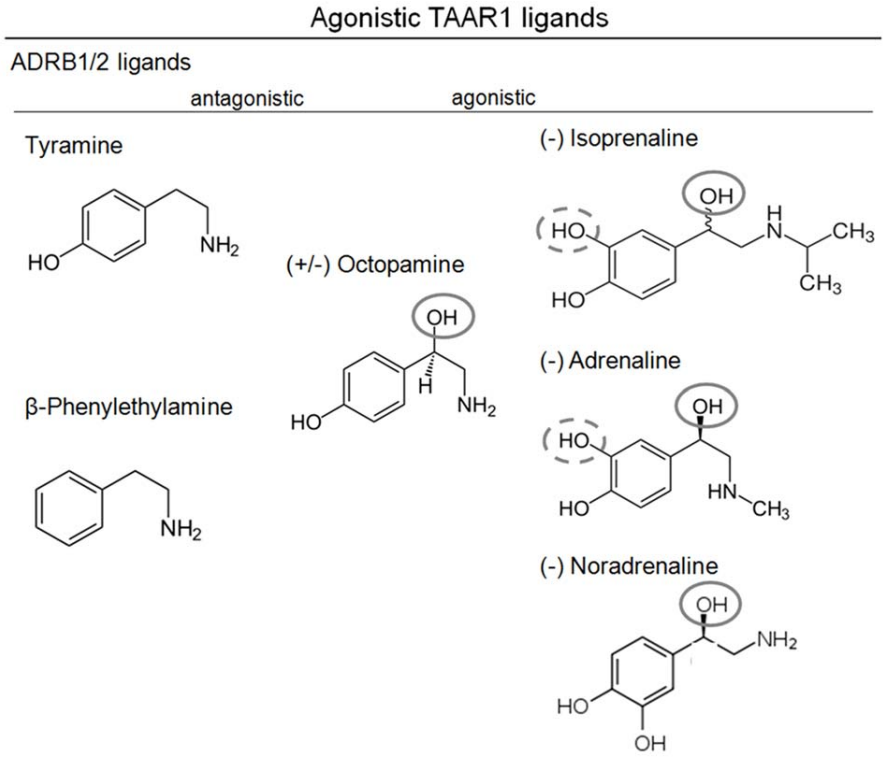

Figure 1. Molecular structures of ADRB1/2 and TAAR1 ligands. The trace amines TYR, PEA and OA are agonists of TAAR1. In contrast, TYR and PEA are antagonists on ADRB1/2, most likely due to less hydroxyl groups compared OA or already known agonistic beta-adrenergic ligands (grey circles). OA has an additional hydroxyl group (grey circle), but yet a hydroxyl group less (dashed grey circle) compared to full ADRB1/2 agonists isoprenaline, adrenaline and noradrenaline.
doi:10.1371/journal.pone.0027073.g001

an adrenergic-receptor-like helical conformation, fixed by two cysteine-bridges: i. the highly conserved cysteine bridge between ECL2 and TMH3, and ii. between ECL2 and ECL1 (figure 6A).

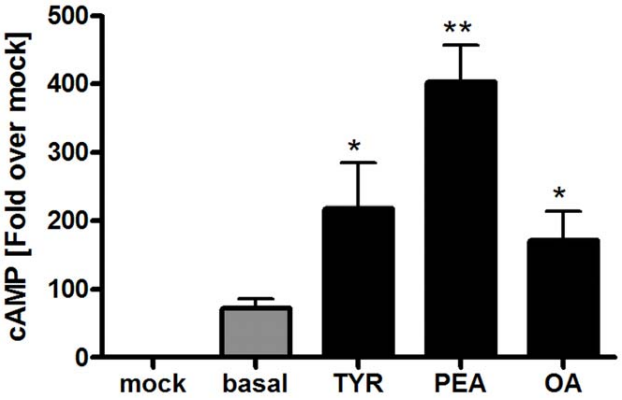

Figure 2. Functional characterization of hTAAR1 interacting with different trace amines. HEK293 cells transiently transfected with hTAAR1 and were incubated for 45 minutes with 10 mM of PEA, OA and TYR. Basal signaling activity as well as activation of the Gs protein/adenylyl cyclase pathway was determined by AlphaScreen technology. Data represent mean ± SEM of cAMP accumulation after stimulation from 4–5 independent experiments performed in triplicates. TAAR1 showed an elevated ligand independent basal activity. PEA was the most potent agonist ($p<0.01$), followed by TYR ($p<0.05$) and OA ($p<0.05$). Data were analyzed using a paired one-tailed t-test.
doi:10.1371/journal.pone.0027073.g002

Disulphide-bridged extracellular loops 1 and 2 are also observable in the crystal structure of adenosine-2A receptor (pdb entry code 3EML [68]) and this interaction is of structural and functional relevance [69,70].

Defining the ligand binding region of aminergic receptors. As shown in figure 4 the ligand binding region of adrenergic receptors is located between the extracellular ends of the transmembrane helices. This pocket-like crevice is covered by specific amino acids [71] which are predestinated for interaction with ligands in different particular modes [72]. For comparison of amino acids (figure 5) which are potentially important for ligand binding at different aminergic receptors we depicted those amino acids of ADRB2 that are determinants of this spatial region (figure 4, figure 6A). We found that most of the ligand binding-sensitive side chains in aminergic receptors (e.g. positions 2.57, 3.32, 6.48, 6.51, 7.53) are also conserved in TAAR. This is also reflected by our homology model of hTAAR1 compared with the crystal structure of ADRB1 (figure 6A). hTAAR1 is, in contrast to other TAAR, characterized by six additional residues which are similar to the binding pocket of β-adrenergic receptors (figure 5), including specific amino acids at TMH5 positions 5.42 and 5.46. Their side chains are known to be important for signaling and ligand specific signaling effects [73,74]. These two residues are also conserved in DRD3 and TAR/OAR. However, the observable high sequence similarity might explain TAAR1 ligand promiscuity. In contrast, also significant differences between ADRB1/ADRB2 compared to hTAAR1 are observable by comparison of amino acids in the ligand binding region. Especially the asparagines at positions 6.55 (TMH6) and 7.39 (TMH7) are known to be important for ligand binding at

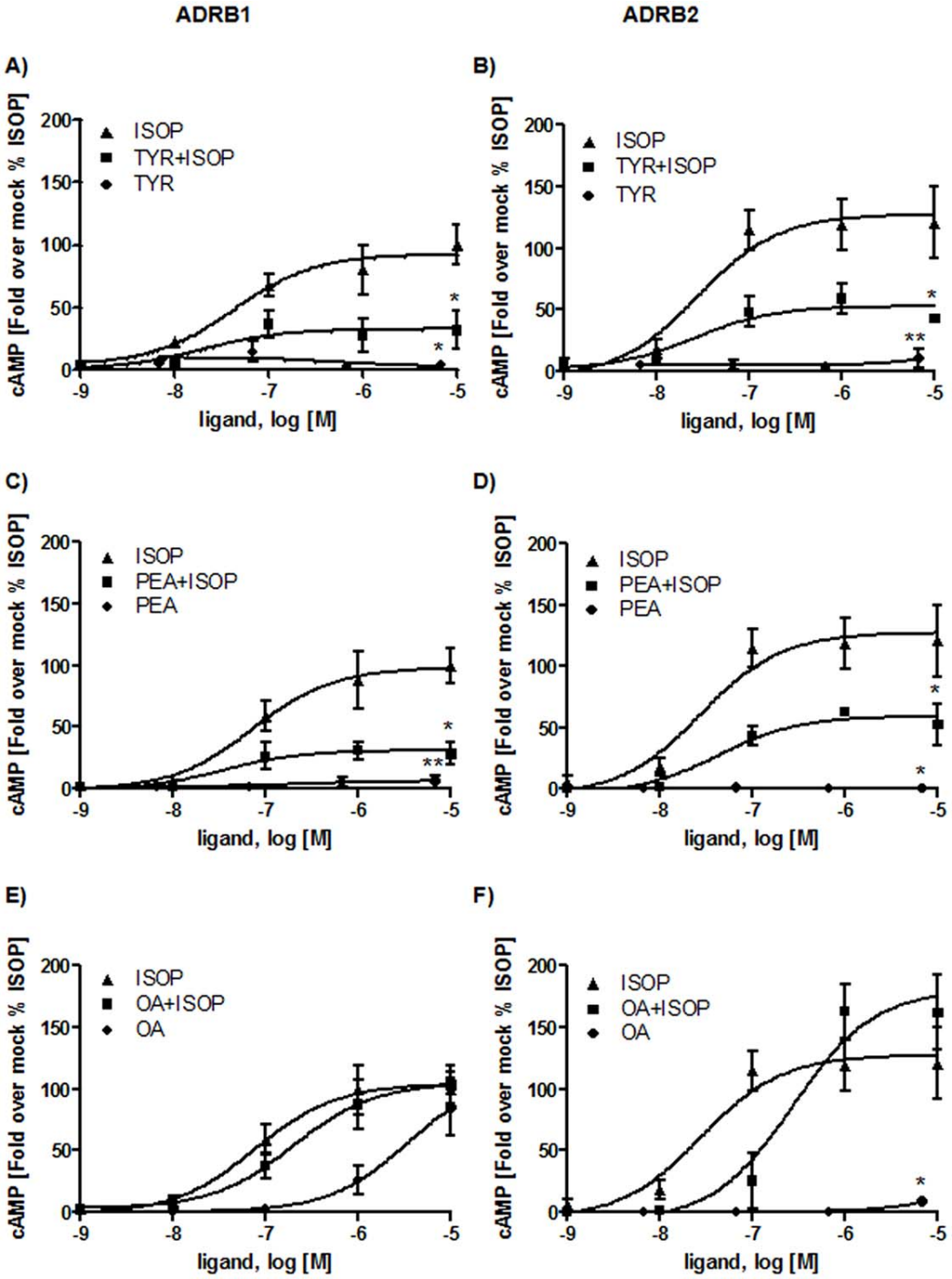

Figure 3. Characterization of hADRB1 and hADRB2 after trace amine challenge. HEK293 cells were transiently transfected with hADRB1 and hADRB2, respectively. Cells were pre-incubated with increasing concentrations of the trace amines TYR, PEA or OA (6.7 nM to 6700 nM) for 15 minutes. For competition studies ISOP with increasing concentrations (10000 nM to 1 nM) was added and incubated for additional 30 minutes. As controls hADRB1 and hADRB2 were incubated with each substance alone with the same concentration for 45 minutes. Three to four independent experiments measured in duplex or tripletts mean ± SEM are depicted here. Fold over mock was calculated and expressed as percentage of ISOP stimulation (100%). Maximal values were statistically analyzed using paired one-tail t-test compared to ISOP maximal stimulation. **A-B**) hADRB1 and hADRB2 were stimulated with ISOP and TYR alone and with both substances simultaneously. TYR shows no agonistic effect on hADRB1 ($p<0.05$) and hADRB2 ($p<0.01$), but acts as an allosteric antagonist on hADRB1/2, indicated by a decreased maximum of stimulation ($p<0.05$) with comparable EC_{50} values. **C-D**) PEA shows no agonistic effects on both hADRB1 ($p<0.01$) and hADRB2 ($p<0.05$) but leads to a decreased maximum of stimulation by ISOP when pre-incubated with PEA ($p<0.05$). The EC_{50} value is similar to stimulation with ISOP alone. **E**) OA acts as an agonist on hADRB1 but with a decreased efficacy. Simultaneous incubation with ISOP and OA reveals no antagonistic effect of OA on hADRB1 (table 1). **F**) OA is an orthosteric antagonist on hADRB2, indicated by a right shift of the EC_{50} value. OA however showed no agonistic effect on hADRB2 ($p<0.05$).
doi:10.1371/journal.pone.0027073.g003

Table 1. EC_{50} values of different agonists at hTAAR1, hADRB1 and hADRB2.

Receptor	Ligand	EC_{50} [nM] [nM]	Emax [nM]
ADRB1	ISOP	61±10	270±47
	TYR	-	*
	PEA	-	*
	OA	3129±461	217±30
	TYR+ISOP	39±22	82±15
	PEA+ISOP	41±9	87±8
	OA+ISOP	210±74	270±104
ADRB2	ISOP	29±5	328±44
	TYR	-	*
	PEA	-	*
	OA	-	*
	TYR+ISOP	20±3	167±35
	PEA+ISOP	44±9	162±52
	OA+ISOP	249±70	443±50
hTAAR1	TYR	1540±251	219±67
	PEA	260±16	403±54
	OA	4170±1470	172±42

EC_{50} values were calculated using GraphPadPrism from concentration response curves of measured cAMP accumulation. Displayed is the mean ± SEM from n≥3 independent experiments. Emax values mean ± SEM from n≥3 independent experiments were calculated from fold over mock data. "–"not determinable with sufficient accuracy, "*" not determinable due to extremely low stimulation.

doi:10.1371/journal.pone.0027073.t001

adrenergic-receptors (figure 6B), but they are absent in hTAAR or OAR and TAR.

Comparison of hTAAR subtypes. On note, there are also molecular differences in the ligand-binding region between hTAAR1 and further hTAAR group members (figure 5). Mapping amino acids that are different between TAAR1 and other hTAAR subtypes to the structural homology models of all hTAAR members a particular spatial region between TMH3, TMH5 and TMH6 is most diverse in biophysical properties (supplemental material figure S3). Such region with divergent properties might cause differences of TAAR subtype-ligand sensitivity or induced effects of ligands [3,18,75,76]. Despite these differences between hTAAR a specific set of identical amino acids in the ligand binding region of TAAR is constituted by residues S2.61, R2.64 (TMH2); H3.28, S/C3.36 (TMH3); F/Y4.56 (TMH4); D6.58 (TMH6); and D7.36 (TMH7). These amino acids with few exceptions are not found in DRD3, ADRB1/2 or TAR and OAR. In conclusion, those residues and spatial potential ligand-binding region between TMH2, TMH3, TMH6 and TMH7 (supplemental material figure S3) are predestinated to interact with so far unknown TAAR-selective ligands.

Discussion

A diverse spectrum of ligands including trace amines interacts with aminergic receptors and modulates different physiological functions. We show here, that the ligand-binding region of TAAR1 is characterized by high similarity to other aminergic GPCR like ADRB1, DRD3 or TAR/OAR. Trace amines such as PEA, TYR and OA (figure 1) can activate hTAAR1 via the Gs protein/adenylyl cyclase pathway. Human TAAR1 possesses a ligand independent basal activity and PEA is the most potent agonist, followed by TYR and OA (figure 2, supplemental material figure S1). In accordance, a previous experimental study demonstrated that ligands on hTAAR1 interact with typical binding-motifs of aminergic receptors [77]. Of note, also for non-human TAAR3 and TAAR4 subtypes (e.g. TAAR orthologs from rat and mouse) ligand promiscuity was reported, but for different ligands compared to hTAAR1. TAAR3 and TAAR4 are pseudogenes in humans [18].

We here tested TAAR1 agonists TYR, PEA and OA regarding their effects on ADRB1/2 signaling. We found that TYR and PEA are allosteric antagonists at both tested β-adrenergic receptors, whereas OA was a weak orthosteric ADRB2-antagonist and a weak ADRB1-agonist. This finding revealed trace amines TYR, PEA and OA as potential endogenous ligands for ADRB1 and ADRB2, but primarily as partial antagonists. Secondly, despite high similarities between the hTAAR1 and ADRB1/2, allosteric modification of isoprenaline induced activation of ADRB1 and ADRB2 by TYR and PEA points to differences in details of ligand binding and action. The ligands PEA and TYR are distinguished from OA and ISOP by a lower number of hydroxyl-groups at the aliphatic chain (figure 1). The additional hydroxyl-group of OA and ISOP interacts via H-bond with an asparagine (position 7.39) at TMH7 as observed in the ADRB1 crystal structure (figure 6B). Of special note, amino acids side chains at this position were already identified being involved in determination of binding properties and selectivity of ligands on rat and mouse TAAR1 [78]. This anchor-contact towards TMH7 (H-bond to 7.39) can not be assumed for TYR and PEA due to a lack of this specific hydroxyl-group (figure 1). In consequence, differences in the orientation of TYR and PEA at ADRB1/2 compared to observed localization of ISOP in the orthosteric binding pocket of ADRB1 between TMH3, TMH5, TMH6, and TMH7 are likely. In conclusion, allosteric effects of PEA or TYR for co-stimulation with ISOP can be explained by a different orientation of both ligand subtypes in the ligand-binding region. The ADRB1 crystal structure co-crystallized with ISOP reveals a spatial region for potential binding of allosteric antagonists TYR and PEA close to the binding site of agonist ISOP (figure 6B). Based on our findings we assume a second binding site at ADRB1 and ADRB2 which can be occupied by small molecule antagonists.

OA with a hydroxyl-group at the phenyl ring and at the hydrophilic side chain (figure 1) is able to interact with N7.39 at TMH7 like ISOP at ADRB1 and is therefore likely localized similarly to other adrenergic ligands and induces orthosteric effects. Studies on invertebrate adrenergic receptor-like trace amine receptors point indeed to similar or identical details of octopamine/receptor interactions compared to adrenergic receptors. Huang and co-workers [79] provided evidence for participation of serine D3.32 (TMH3) and S5.42 (TMH5) for activation of octopamine receptor by OA. However, the different effects of OA at ADRB1 (agonistic) versus ADRB2 (neutral in the basal state and antagonistic for ISOP treatment) are likely related to peculiarity of interaction between the hydroxyl-group at the phenylic ring system with hydrophilic residues at TMH5 (positions 5.42, 5.46) as suggested for other ligands [80]. Alternatively, differences to other adrenergic-ligands might be caused by changed interactions to the asparagine at position 6.55 which is observable at ADRB1 complexed with ISOP (figure 6B). Of note, an aromatic residue at TMH6 at position Y6.55 was found as a molecular switch for G-protein preference of OAR [81].

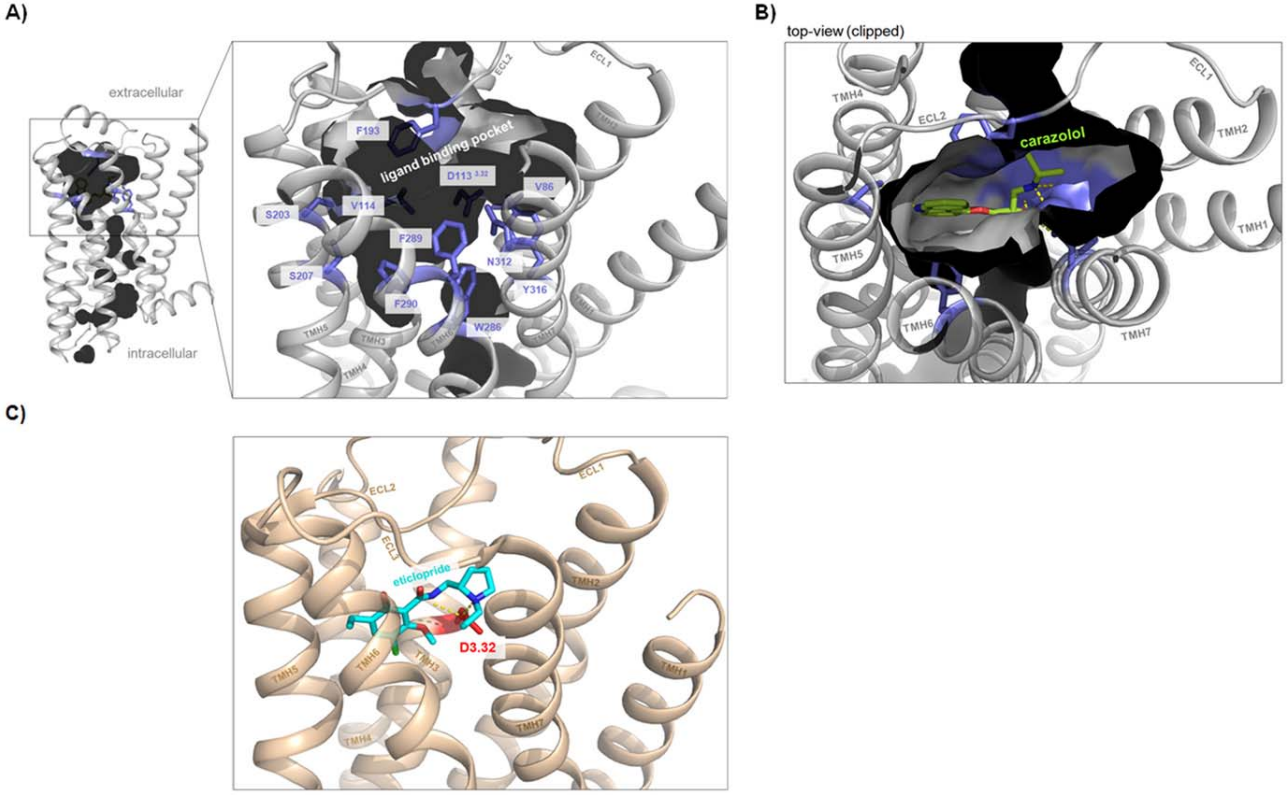

Figure 4. Defining the ligand binding region of aminergic receptors. A) The pocket-like ligand binding region (inner crevice surface) of the human β2-adrenergic receptor (pdb entry code 2RH1) is surrounded by amino acids (lilac sticks, labeled) which are also known from mutagenesis studies to be important for ligand binding and signal transduction. **B**) The inverse agonist carazolol is embedded tightly in this pocket of the β2-adrenergic receptor (top-view) and interacts with residues of TMH 3, 5, and 7 by hydrogen bonds [62]. Differences in binding and effects on receptor conformation compared to agonists were found to be relatively small, mainly manifested in the interaction pattern to TMH5 or induced side chain rotamer conformations at TMH5 (amino acids at positions 5.41, 5.42 and 5.46) [80]. **C**) The crystal structure of dopamine-3 receptor (pdb entry code 3PBL) with the antagonist eticlopride [65] shows a similar localization between the transmembrane helices compared to carazolol in the adrenergic receptor (B). An aspartate (red stick) at position 3.32 in helix 3 is well known to function as an anchor point for binding of ligands at aminergic receptors.
doi:10.1371/journal.pone.0027073.g004

Based on analyses of TAAR homology models and sequence comparison we showed that the general ligand binding region of hTAARs is characterized by high amino acid conservation specifically in a crevice between the interfaces of TMH 2, 3, 6 and 7 (figure 5 and supplemental figure S3). This region is termed *minor pocket* [82] as part of the entire ligand binding region known for family A GPCRs [72]) and is not occupied by isoprenaline in the ADRB1 crystal structure (figure 6B), nor by carazolol in ADRB2 (figure 4B). Therefore we here hypothesize a preference of this pocket for a shared endogenous and also so far unknown TAAR ligand(s). In addition, our comparative studies also revealed that hTAAR1 is significantly different from all other hTAAR group members in the general ligand binding region. This likely would explain non-responsiveness of other hTAARs to particular ligands of TAAR1.

Taken together, we here present molecular details causing TAAR1 ligand promiscuity. We also found different effects of trace amines at hTAAR1 versus hADRB1 and hADRB2 which can be explained by complementary properties at ligands and receptors. Particular TAAR1 agonists are inhibitors of β-adrenergic receptor subtypes. These differences in ligand-induced effects are caused by specific properties of TAAR1 compared to ADRB1 and ADRB2 in the ligand binding region. Interestingly, an antagonistic effect on β-adrenergic signaling was reported in the early 80′s for several thyronamines. T_3AM, 3,5-T2AM, and T_0AM interfere with ligand binding to adrenergic receptors expressed at the plasma membrane of turkey erythrocytes and inhibited the activation of cAMP synthesis [83,84]. Of special note, octopamine acts as an orthosteric ligand for ADRB1 and is an ADRB2-antagonist. These findings are also interesting under aspects of ligand development for TAAR [3,60,78,85,86,87,88,89,90], which has to be carefully explored concerning their potential interactions to other aminergic receptors.

Materials and Methods

Cloning of hTAAR1 and β-adrenergic receptors

Full length human TAAR1 (hTAAR1, NM_138327.1) was subcloned into the eukaryotic expression vector pcDps, N-terminally tagged with an hemagglutinin (5′ YPYDVPDYA 3′) epitope via *Kpn*I and *Spe*I restriction sites. For better cell surface expression hTAAR1 was additionally N-terminally fused with the first 20 amino acids of the bovine Rhodopsin [18,33]. The human β1-adrenergic receptor (hADRB1, NM_000684.2)-pcDps construct cloned via *Kpn*I/*Spe*I containing N-terminal (HA)-tag and C-terminal Flag-tag (5′ DYKDDDDK 3′).

Human β2-adrenergic receptor (ADRB2, NM_000024.5) was subcloned via *EcoR*I and SpeI with an N-terminal (HA)-tag as well. All constructs in the eukaryotic expression vector (pcDps) were

Sub-structure	Ball. & Weinst.	hTAAR1	hTAAR2	hTAAR5	hTAAR6	hTAAR8	hTAAR9	hADRB1	hADRB2	hDRD3	OAR	TAR
TMH2	2.53	L72	L92	L83	V81	V80	V81	M107	M82	V78	V72	V85
	2.57*	V76	I96	V87	V85	V84	V85	V111	V86	V82	V76	V89
	2.61	*S80*	*S100*	*S91*	*S89*	*S88*	*S89*	G115	G90	V86	*S80*	N93
	2.64	*R83*	*R103*	*R94*	*R92*	*R91*	*R92*	I118	H93	L89	*R83*	Y96
TMH3	3.28	*H99*	Y119	*H110*	*H108*	*H107*	*H108*	W134	W109	F106	W99	W112
	3.29	T100	Y120	T111	T109	S108	T109	T135	T110	V107	L100	L113
	3.32*	D103	D123	D114	T112	D111	D112	D138	D113	D110	D103	D116
	3.33	I104	L124	T115	V113	V112	T113	V139	V114	V111	V104	V117
	3.36	S107	S127	*C118*	*C116*	*C115*	*C116*	V142	V117	*C114*	*C107*	*C120*
	3.37	**S108**	I128	L119	Y117	Y116	F117	**T143**	**T118**	**T115**	**T108**	**T121**
TMH4	4.56	*F154*	*F174*	*Y165*	*Y163*	*Y162*	*Y163*	V189	T164	V164	I154	I167
	4.61	**I159**	V179	L170	F168	F167	F168	**I194**	**I169**	L169	L159	L172
ECL2		N164	Y184	C175	Y173	N172	N173	W199	Y174	T174	D164	D177
		V184	V203	-	-	-	-	F218	F193	-	-	L190
		F185	M204	L194	T192	I191	A192	V219	**F194**	L183	L188	T191
		F186	F205	L195	V193	I192	P193	T220	T195	S184	N189	R192
TMH5	5.38	S190	W209	F199	N197	G196	N197	Y224	Y199	F188	Y193	Y196
	5.42*	**T194**	L213	L203	**T201**	I200	L201	**S228**	**S203**	**S192**	**S197**	**S200**
	5.46*	**S198**	G217	L207	**S205**	L204	L205	**S232**	**S207**	**S196**	**S201**	**S204**
TMH6	6.48*	W264	W275	W265	W271	W270	W271	W337	W286	W342	W404	W340
	6.51*	F267	C278	F268	Y274	Y273	Y274	F340	F289	F345	F407	F343
	6.52*	**F268**	**F279**	T269	S275	T274	L275	**F341**	**F290**	**F346**	**F408**	**F344**
	6.55*	T271	I282	T272	S278	I277	A278	N344	N293	H349	Y412	Y347
	6.58	*D274*	*D285*	*D275*	*D281*	*D280*	*D281*	K347	H296	N352	R414	V350
TMH7	7.35	N286	F297	F287	Y293	Y292	Y293	F359	Y308	Y365	F427	V363
	7.36	*D287*	*D298*	*D288*	*E294*	*E293*	*E294*	V360	I309	S366	S428	Y364
	7.39*	I290	T301	I291	C297	C296	V297	N363	N312	T368	F430	T367
	7.40	W291	W302	W292	W298	W297	W298	W364	W313	W369	W431	W368
	7.43*	Y294	Y305	Y295	Y301	Y300	Y301	Y367	Y316	Y373	Y434	Y371

Figure 5. Amino acids covering the ligand binding region of β-adrenergic receptors and TAARs. Amino acids covering the ligand binding regions of β-adrenergic receptors 1 and 2 are compared with corresponding residues of human TAAR subtypes, dopamine-3 receptor and invertebrate tyramine (*Apis*) (TAR) or octopamine receptor (*Bombyx*) (OAR) (see also amino acid sequence alignment figure S2). This comparison reveals potential overlapping binding determinants which are predestinated to interact with shared ligands. The amino acids of ADRB1 and ADRB2 ligand binding region are identified by analyzing solved crystal structures complexed with different ligands (figure 4). Residues which are directly involved in ligand binding at adrenergic receptors are marked by a star-symbol (*). The numbering is provided by the *Ballesteros and Weinstein* numbering scheme [66] and consecutively to the entire amino acid sequence. Especially TAAR1 shows similar or even identical side chains (bold) with the adrenergic receptors, dopamine-3 receptor and OAR or TAR. Highly conserved amino acids between all receptors are marked by a gray background. Conserved residues within hTAAR subtypes are in italic with a partial gray background. These five residues are located at TMH 2, 3, 6 and 7 and likely encode TAAR specificities compared to other aminergic receptors.
doi:10.1371/journal.pone.0027073.g005

sequenced for verification with BigDye-terminator sequencing (Perkin-Elmer, Weiterstadt, Germany) and an automatic sequencer (ABI 3710xl; Applied Biosystems, Foster City, CA).

Cell culture, cAMP assay and ligand induced effects

Human embryonic kidney cells (HEK293) were cultured in Minimum Essential Medium (MEM) Earle's (Biochrom AG) supplemented with 10% FBS (PAA Laboratories GmbH), 100 U/ml penicillin, and 100 µg/ml streptomycin (Biochrom AG) and 2 mM L-glutamine (Invitrogen) at 37°C with 5% CO_2. 48 well plates were coated with Poly-L-Lysine (Biochrom) and HEK293 cells were seeded with 37,500 cells per well. Transient transfection in triplicates with 84 ng DNA/well using metafectene according to manufactures instructions (Biontex, Munich, Germany) was performed 28 hours later. 40 hours after transfection cells were pre-incubated for 5 minutes with stimulation buffer containing of MEM Earle's media and 1 mM 3-isobutyl-1-methylxanthine (IBMX, Sigma). This stimulation buffer was used for all further steps. For ligand competition experiments cells were incubated with tyramine, 2-phenylethylamine or (±) octopamine ranging from 6.7 nM to 6700 nM, diluted in stimulation buffer for 15 minutes followed by a stimulation with (-) isoprenaline in concentrations ranging from 1 nM to 10000 nM for 30 minutes. Ligands were all purchased from Sigma, Munich. Controls were incubated with tyramine, β-phenylethylamine, octopamine or isoprenaline for 45 minutes. All reactions were performed at 37°C with 5% CO_2 saturated air and stopped by aspirating medium. Cells were lysed at 4°C for 2 h on a shaking platform with cell lysis buffer containing 5 nM HEPES, 0.1% BSA, 0.3% Tween20 and 1 mM IBMX.

The competitive cyclic adenosine-monophosphate (cAMP) assay via Alphascreen (Perkin Elmer Life Science, Inc., Boston, MA) was carried out according to the manufacturers' protocol. Briefly, 5 µl of each sample were transferred to a 384 well plate. Acceptor beads were diluted in 1X HBSS with 1M HEPES, 0.1% BSA, pH 7.4 and incubated for 30 minutes at room temperature. Then donor beads and 50 µM biotinylated cAMP diluted in the same way were added and incubated for an hour at room temperature. Measurement of the plate was performed using Berthold Microplate Reader (Berthold Technologies GmbH & Co. KG). Results are expressed in fold over mock (unstimulated empty vector). Dose response curves and bar graphs with mean ± SEM as well as statistical analysis (paired one-tailed t-test) were generated using GraphPad Prism Version 4.03.

Structural homology models of hTAARs

Crystal structures of inactive receptor conformations serving for GPCR homology modeling have been published for several family A GPCR members like rhodopsin, adenosine- or β-adrenergic receptors (reviewed in [67]). For modeling of the human TAARs 1, 2, 5, 6, 8, and 9 we used the inactive structural conformation of the β-2 adrenergic receptor (pdb entry 2RH1, [62]), based on high sequence similarity between hTAAR1 and β-adrenergic receptor 2 (39% similarity, Blosum62 matrix).

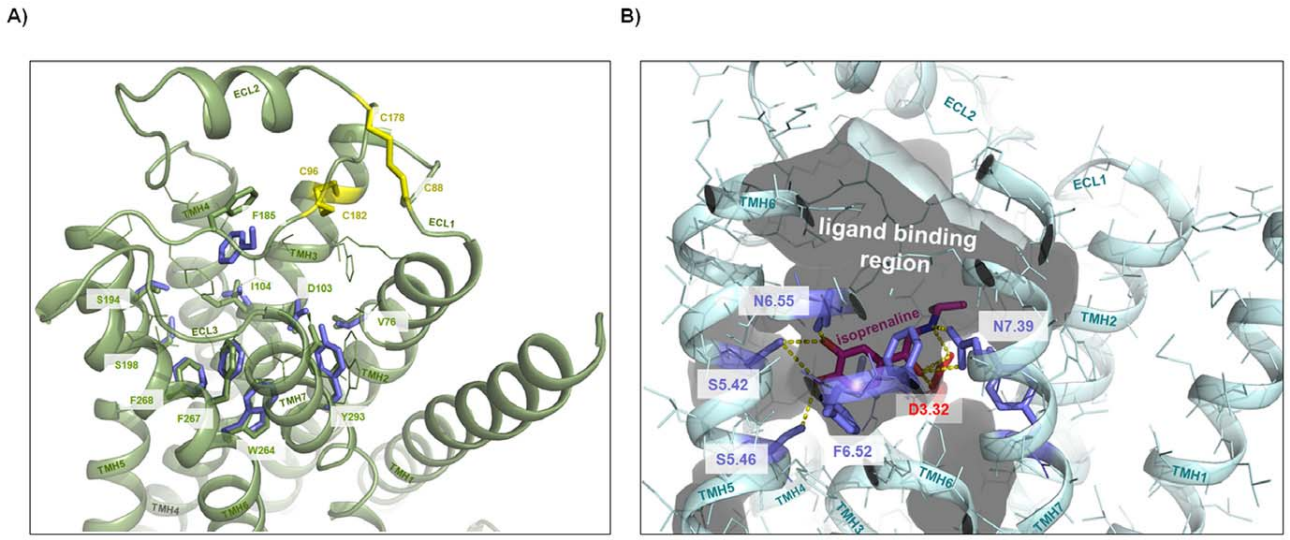

Figure 6. TAAR1 shows similarity in the ligand binding region compared with β-adrenergic receptors. A) Superimposition of the hTAAR1 homology model (extracellular top-side view, green backbone) and the hADRB2 crystal structure (lilac sticks hADRB2, backbone not shown) reveals similarities of residues which are known to be important for ligand binding and signal transduction in adrenergic receptors (figure 4 and figure 5). These identical amino acids (sticks) should be involved in binding of shared ligands like isoprenaline. Additional side chains of hTAAR1 covering the putative ligand binding region (figure 5) are represented as green lines. Cysteine bridges (yellow) between loops 1 and 2 or loop 2 and TMH3 are highlighted and labeled. **B**) The recently published crystal structure of the turkey β1-adrenergic receptor co-crystallized with the agonist isoprenaline (pdb entry code 2Y03 [80]) shows main key players for intermolecular hydrogen bonding (yellow dotted lines) at aminergic receptors like side chains at positions D3.32 (TMH3) (red stick); S5.42, S5.46 (TMH5); and N7.39 (TMH7) (lilac sticks). Interestingly, the inner-pocket surface (translucent) between the extracellular ends of the helices and ECL2 shows an unoccupied volume which might form a second binding site for small molecules.
doi:10.1371/journal.pone.0027073.g006

The amino acid sequence alignment (supplemental material figure S2) for assignment of corresponding amino acid positions was made by usage of the Hidden-Markov algorithm derived for several GPCRs in comparison to the available GPCRs structures [67]. Refinements of the loop regions were made manually.

The software package Sybyl 7.3.5 (Tripos Inc., St. Louis, Missouri, 63144, USA) was used for structural modeling approaches. Gaps of missing residues in the loops of the template structure were closed by the 'Loop Search' tool in Sybyl. Substituted side chains and loops of each homology model were subjected to conjugate gradient minimizations until converging at a termination gradient of 0.05 kcal/(mol*Å)) and molecular dynamics simulation (4 ns) by fixing the backbone of the transmembrane helices. The AMBER 7.0 force field was used. Finally, the models were minimized without constraints for 2ns using the AMBER 7.0 force field. Stability of the models was validated by checking the geometry using PROCHECK.

Structure images were produced using PyMOL Molecular Graphics System, version 1.3, Schrödinger, LLC. To facilitate comparison of different GPCRs we used both the amino acid numbering of the entire TAARs with their signal peptides and the Ballesteros-Weinstein numbering scheme [66].

Supporting Information

Figure S1 Dose response curves of hTAAR1 agonists. The trace amines tyramine (TYR), beta-phenylethylamine (PEA) and octopamine (OA) activate hTAAR1 via Gs/adenylate cyclase signaling. HEK293 transiently expressing hTAAR1 were stimulated with each trace amine in concentrations ranging 0.1 mM to 10 nM. Shown are dose response curves fold over basal means ± SEM from n≥4 independent experiments of measured cAMP in triplicates as described in *Material and Methods*. PEA was the most potent agonist ($p<0.01$), followed by TYR ($p<0.05$) and OA ($p<0.05$) for 10 μM each ligand. Data were analyzed using paired one-tailed t-test tested against basal value of hTAAR1.
(TIF)

Figure S2 Amino acid sequence alignment of hTAAR1 and homologous receptors. The alignment compares amino acids of ADRB1, ADRB2, human TAAR, invertebrate octopamine (OAR) and tyramine (TAR) receptors and the human dopamine-3 receptor (DRD3). Particular background colors indicating conservation among different receptors and reflecting biophysical properties of the amino acid side chains: black – proline, blue – positively charged, cyan/green – aromatic and hydrophobic, green – hydrophobic, red – negatively charged, gray – hydrophilic, dark-red – cysteines, magenta – histidine. The putative helix dimensions and loop regions are assigned according to observable features in the crystal structure of the inactivated β2-adrenergic receptor (pdb entry code 2RH1). Furthermore, in homology to the ligand binding regions of β-adrenergic receptors amino acid positions covering the putative ligand binding region of TAARs are marked with a plus (+). Highly conserved amino acids of family A GPCRs are marked by a star-symbol (*).
(TIF)

Figure S3 Differences between amino acids in the putative ligand binding region of human TAARs 2, 5, 6, 8 and 9 compared with hTAAR1. Amino acids constituting the ligand binding region (side chains as sticks) of hTAAR1 (green) are highlighted at the molecular homology model (backbone, top view). For the hTAAR subtypes 2, 5, 6, 8 and 9 only side chains are shown which are different compared to TAAR1 residues. This comparison reveals that most of the differences are located spatially between TMH3, TMH5 and TMH6 (red translucent circles). In other words, between the interfaces of TMH 2-3-6-7 a

region of high similarity for all hTAAR subtypes might exist (green translucent circle).
(TIF)

Author Contributions

Conceived and designed the experiments: GK JP DN HK HB. Performed the experiments: JP DN HB. Analyzed the data: GK JP AG DF-S HK JK TS HB. Contributed reagents/materials/analysis tools: GK HB. Wrote the paper: GK JP DN AG DF-S HK JK TS HB.

References

1. Maguire JJ, Parker WAE, Foord SM, Bonner TI, Neubig RR, et al. (2009) International Union of Pharmacology. LXXII. Recommendations for Trace Amine Receptor Nomenclature. Pharmacological Reviews 61: 1–8.
2. Grandy DK (2007) Trace amine-associated receptor 1--Family archetype or iconoclast? Pharmacology & Therapeutics 116: 355–390.
3. Lewin A (2006) Receptors of mammalian trace amines. The AAPS Journal 8: E138–E145.
4. Lindemann L, Hoener MC (2005) A renaissance in trace amines inspired by a novel GPCR family. Trends in Pharmacological Sciences 26: 274–281.
5. Zucchi R, Chiellini G, Scanlan TS, Grandy DK (2006) Trace amine-associated receptors and their ligands. Br J Pharmacol 149: 967–978.
6. Burchett SA, Hicks TP (2006) The mysterious trace amines: Protean neuromodulators of synaptic transmission in mammalian brain. Progress in Neurobiology 79: 223–246.
7. Pae CU, Drago A, Mandelli L, De Ronchi D, Serretti A (2009) TAAR 6 and HSP-70 variations associated with bipolar disorder. Neurosci Lett 465: 257–261.
8. Vanti WB, Nguyen T, Cheng R, Lynch KR, George SR, et al. (2003) Novel human G-protein-coupled receptors. Biochem Biophys Res Commun 305: 67–71.
9. Duan J, Martinez M, Sanders AR, Hou C, Saitou N, et al. (2004) Polymorphisms in the Trace Amine Receptor 4 (TRAR4) Gene on Chromosome 6q23.2 Are Associated with Susceptibility to Schizophrenia. The American Journal of Human Genetics 75: 624–638.
10. Bly M (2005) Examination of the trace amine-associated receptor 2 (TAAR2). Schizophrenia Research 80: 367–368.
11. D'Andrea G, Nordera G, Pizzolato G, Bolner A, Colavito D, et al. (2010) Trace amine metabolism in Parkinson's disease: Low circulating levels of octopamine in early disease stages. Neuroscience Letters 469: 348–351.
12. Pae CU, Drago A, Kim JJ, Patkar AA, Jun TY, et al. (2010) TAAR6 variations possibly associated with antidepressant response and suicidal behavior. Psychiatry Res 180: 20–24.
13. Branchek TA, Blackburn TP (2003) Trace amine receptors as targets for novel therapeutics: legend, myth and fact. Current Opinion in Pharmacology 3: 90–97.
14. Sotnikova TD, Caron MG, Gainetdinov RR (2009) Trace amine-associated receptors as emerging therapeutic targets. Mol Pharmacol 76: 229–235.
15. Liu IS, Kusumi I, Ulpian C, Tallerico T, Seeman P (1998) A serotonin-4 receptor-like pseudogene in humans. Brain Res Mol Brain Res 53: 98–103.
16. Zeng Z, Fan P, Rand E, Kyaw H, Su K, et al. (1998) Cloning of a Putative Human Neurotransmitter Receptor Expressed in Skeletal Muscle and Brain. Biochemical and Biophysical Research Communications 242: 575–578.
17. Borowsky B, Adham N, Jones KA, Raddatz R, Artymyshyn R, et al. (2001) Trace amines: Identification of a family of mammalian G protein-coupled receptors. Proceedings of the National Academy of Sciences of the United States of America 98: 8966–8971.
18. Stäubert C, Böselt I, Bohnekamp J, Römpler H, Enard W, et al. (2010) Structural and Functional Evolution of the Trace Amine-Associated Receptors TAAR3, TAAR4 and TAAR5 in Primates. PLoS ONE 5: e11133.
19. Bunzow JR, Sonders MS, Arttamangkul S, Harrison LM, Zhang G, et al. (2001) Amphetamine, 3,4-Methylenedioxymethamphetamine, Lysergic Acid Diethylamide, and Metabolites of the Catecholamine Neurotransmitters Are Agonists of a Rat Trace Amine Receptor. Molecular Pharmacology 60: 1181–1188.
20. Piehl S, Hoefig CS, Scanlan TS, Kohrle J (2010) Thyronamines--Past, Present, and Future. Endocr Rev. er.2009–0040.
21. Ghelardoni S, Suffredini S, Frascarelli S, Brogioni S, Chiellini G, et al. (2009) Modulation of cardiac ionic homeostasis by 3-iodothyronamine. Journal of Cellular and Molecular Medicine 13: 3082–3090.
22. Gompf HS, Greenberg JH, Aston-Jones G, Ianculescu AG, Scanlan TS, et al. (2010) 3-Monoiodothyronamine: the rationale for its action as an endogenous adrenergic-blocking neuromodulator. Brain Res 1351: 130–140.
23. Ianculescu AG, Scanlan TS (2010) 3-Iodothyronamine (T(1)AM): a new chapter of thyroid hormone endocrinology? Mol Biosyst 6: 1338–1344.
24. Panas HN, Lynch LJ, Vallender EJ, Xie Z, Chen GL, et al. (2010) Normal thermoregulatory responses to 3-iodothyronamine, trace amines and amphetamine-like psychostimulants in trace amine associated receptor 1 knockout mice. J Neurosci Res 88: 1962–1969.
25. Piehl S, Heberer T, Balizs G, Scanlan TS, Kohrle J (2008) Development of a validated liquid chromatography/tandem mass spectrometry method for the distinction of thyronine and thyronamine constitutional isomers and for the identification of new deiodinase substrates. Rapid Commun Mass Spectrom 22: 3286–3296.
26. Pietsch CA, Scanlan TS, Anderson RJ (2007) Thyronamines are substrates for human liver sulfotransferases. Endocrinology 148: 1921–1927.
27. Saba A, Chiellini G, Frascarelli S, Marchini M, Ghelardoni S, et al. (2010) Tissue Distribution and Cardiac Metabolism of 3-Iodothyronamine. Endocrinology 151: 5063–5073.
28. Scanlan TS (2009) Minireview: 3-Iodothyronamine (T1AM): a new player on the thyroid endocrine team? Endocrinology 150: 1108–1111.
29. Zucchi R, Ghelardoni S, Chiellini G (2010) Cardiac effects of thyronamines. Heart Failure Reviews 15: 171–176.
30. Wainscott DB, Little SP, Yin T, Tu Y, Rocco VP, et al. (2007) Pharmacologic characterization of the cloned human trace amine-associated receptor1 (TAAR1) and evidence for species differences with the rat TAAR1. J Pharmacol Exp Ther 320: 475–485.
31. Wolinsky TD, Swanson CJ, Smith KE, Zhong H, Borowsky B, et al. (2007) The Trace Amine 1 receptor knockout mouse: an animal model with relevance to schizophrenia. Genes, Brain and Behavior 6: 628–639.
32. Lindemann L, Ebeling M, Kratochwil NA, Bunzow JR, Grandy DK, et al. (2005) Trace amine-associated receptors form structurally and functionally distinct subfamilies of novel G protein-coupled receptors. Genomics 85: 372–385.
33. Liberles SD, Buck LB (2006) A second class of chemosensory receptors in the olfactory epithelium. Nature 442: 645–650.
34. Fleischer J, Breer H, Strotmann J (2009) Mammalian olfactory receptors. Front Cell Neurosci 3: 9.
35. Krautwurst D (2008) Human Olfactory Receptor Families and Their Odorants. Chemistry & Biodiversity 5: 842–852.
36. Liberles SD (2009) Trace Amine-associated Receptors Are Olfactory Receptors in Vertebrates. Annals of the New York Academy of Sciences 1170: 168–172.
37. Wallach JV (2009) Endogenous hallucinogens as ligands of the trace amine receptors: a possible role in sensory perception. Med Hypotheses 72: 91–94.
38. Gloriam DEI, Bjarnadóttir TK, Yan Y-L, Postlethwait JH, Schiöth HB, et al. (2005) The repertoire of trace amine G-protein-coupled receptors: large expansion in zebrafish. Molecular Phylogenetics and Evolution 35: 470–482.
39. Hussain A, Saraiva LR, Korsching SI (2009) Positive Darwinian selection and the birth of an olfactory receptor clade in teleosts. Proceedings of the National Academy of Sciences 106: 4313–4318.
40. Vallender EJ, Xie Z, Westmoreland SV, Miller GM (2010) Functional evolution of the trace amine associated receptors in mammals and the loss of TAAR1 in dogs. BMC Evol Biol 10: 51.
41. Berry MD (2004) Mammalian central nervous system trace amines. Pharmacologic amphetamines, physiologic neuromodulators. J Neurochem 90: 257–271.
42. Zucchi R, Chiellini G, Scanlan TS, Grandy DK (2006) Trace amine-associated receptors and their ligands. British Journal of Pharmacology 149: 967–978.
43. David JC, Coulon JF (1985) Octopamine in invertebrates and vertebrates. A review. Prog Neurobiol 24: 141–185.
44. Roeder T (2005) Tyramine and octopamine: ruling behavior and metabolism. Annu Rev Entomol 50: 447–477.
45. Arakawa S, Gocayne JD, McCombie WR, Urquhart DA, Hall LM, et al. (1990) Cloning, localization, and permanent expression of a Drosophila octopamine receptor. Neuron 4: 343–354.
46. Cazzamali G, Klaerke DA, Grimmelikhuijzen CJ (2005) A new family of insect tyramine receptors. Biochem Biophys Res Commun 338: 1189–1196.
47. Saudou F, Amlaiky N, Plassat JL, Borrelli E, Hen R (1990) Cloning and characterization of a Drosophila tyramine receptor. EMBO J 9: 3611–3617.
48. Gerhardt CC, Bakker RA, Piek GJ, Planta RJ, Vreugdenhil E, et al. (1997) Molecular cloning and pharmacological characterization of a molluscan octopamine receptor. Mol Pharmacol 51: 293–300.
49. Massarsky A, Trudeau VL, Moon TW (2011) beta-blockers as endocrine disruptors: the potential effects of human beta-blockers on aquatic organisms. J Exp Zool A Ecol Genet Physiol 315: 251–265.
50. Airriess CN, Rudling JE, Midgley JM, Evans PD (1997) Selective inhibition of adenylyl cyclase by octopamine via a human cloned alpha 2A-adrenoceptor. Br J Pharmacol 122: 191–198.
51. Brown CM, McGrath JC, Midgley JM, Muir AG, O'Brien JW, et al. (1988) Activities of octopamine and synephrine stereoisomers on alpha-adrenoceptors. Br J Pharmacol 93: 417–429.
52. Carpene C, Galitzky J, Fontana E, Atgie C, Lafontan M, et al. (1999) Selective activation of beta3-adrenoceptors by octopamine: comparative studies in mammalian fat cells. Naunyn Schmiedebergs Arch Pharmacol 359: 310–321.
53. Ma G, Bavadekar SA, Schaneberg BT, Khan IA, Feller DR (2010) Effects of synephrine and beta-phenethylamine on human alpha-adrenoceptor subtypes. Planta Med 76: 981–986.
54. Lindemann L, Meyer CA, Jeanneau K, Bradaia A, Ozmen L, et al. (2008) Trace Amine-Associated Receptor 1 Modulates Dopaminergic Activity. Journal of Pharmacology and Experimental Therapeutics 324: 948–956.

55. Miller GM, Verrico CD, Jassen A, Konar M, Yang H, et al. (2005) Primate Trace Amine Receptor 1 Modulation by the Dopamine Transporter. Journal of Pharmacology and Experimental Therapeutics 313: 983–994.
56. Xie Z, Miller GM (2007) Trace amine-associated receptor 1 is a modulator of the dopamine transporter. J Pharmacol Exp Ther 321: 128–136.
57. Xie Z, Westmoreland SV, Bahn ME, Chen GL, Yang H, et al. (2007) Rhesus monkey trace amine-associated receptor 1 signaling: enhancement by monoamine transporters and attenuation by the D2 autoreceptor in vitro. J Pharmacol Exp Ther 321: 116–127.
58. Xie Z, Westmoreland SV, Miller GM (2008) Modulation of monoamine transporters by common biogenic amines via trace amine-associated receptor 1 and monoamine autoreceptors in human embryonic kidney 293 cells and brain synaptosomes. J Pharmacol Exp Ther 325: 629–640.
59. Revel FG, Moreau JL, Gainetdinov RR, Bradaia A, Sotnikova TD, et al. (2011) TAAR1 activation modulates monoaminergic neurotransmission, preventing hyperdopaminergic and hypoglutamatergic activity. Proc Natl Acad Sci U S A. 108(20): 8485–90.
60. Bradaia A, Trube G, Stalder H, Norcross RD, Ozmen L, et al. (2009) The selective antagonist EPPTB reveals TAAR1-mediated regulatory mechanisms in dopaminergic neurons of the mesolimbic system. Proc Natl Acad Sci U S A 106: 20081–20086.
61. Stalder H, Hoener MC, Norcross RD (2011) Selective antagonists of mouse trace amine-associated receptor 1 (mTAAR1): discovery of EPPTB (RO5212773). Bioorg Med Chem Lett 21: 1227–1231.
62. Cherezov V, Rosenbaum DM, Hanson MA, Rasmussen SG, Thian FS, et al. (2007) High-resolution crystal structure of an engineered human beta2-adrenergic G protein-coupled receptor. Science 318: 1258–1265.
63. Rasmussen SG, Choi HJ, Rosenbaum DM, Kobilka TS, Thian FS, et al. (2007) Crystal structure of the human beta2 adrenergic G-protein-coupled receptor. Nature 450: 383–387.
64. Rosenbaum DM, Zhang C, Lyons JA, Holl R, Aragao D, et al. (2011) Structure and function of an irreversible agonist-beta(2) adrenoceptor complex. Nature 469: 236–240.
65. Chien EY, Liu W, Zhao Q, Katritch V, Han GW, et al. (2010) Structure of the human dopamine D3 receptor in complex with a D2/D3 selective antagonist. Science 330: 1091–1095.
66. Ballesteros JA, Weinstein H, Stuart CS (1995) [19] Integrated methods for the construction of three-dimensional models and computational probing of structure-function relations in G protein-coupled receptors. Methods in Neurosciences: Academic Press. pp 366–428.
67. Worth CL, Kleinau G, Krause G (2009) Comparative sequence and structural analyses of G-protein-coupled receptor crystal structures and implications for molecular models. PLoS One 4: e7011.
68. Jaakola VP, Griffith MT, Hanson MA, Cherezov V, Chien EY, et al. (2008) The 2.6 angstrom crystal structure of a human A2A adenosine receptor bound to an antagonist. Science 322: 1211–1217.
69. Peeters MC, van Westen GJ, Guo D, Wisse LE, Muller CE, et al. (2011) GPCR structure and activation: an essential role for the first extracellular loop in activating the adenosine A2B receptor. FASEB J 25: 632–643.
70. Peeters MC, van Westen GJ, Li Q, AP IJ (2011) Importance of the extracellular loops in G protein-coupled receptors for ligand recognition and receptor activation. Trends Pharmacol Sci 32: 35–42.
71. Kratochwil NA, Malherbe P, Lindemann L, Ebeling M, Hoener MC, et al. (2005) An Automated System for the Analysis of G Protein-Coupled Receptor Transmembrane Binding Pockets:â€‰ Alignment, Receptor-Based Pharmacophores, and Their Application. Journal of Chemical Information and Modeling 45: 1324–1336.
72. Wichard JD, Ter Laak A, Krause G, Heinrich N, Kuhne R, et al. (2011) Chemogenomic analysis of G-protein coupled receptors and their ligands deciphers locks and keys governing diverse aspects of signalling. PLoS One 6: e16811.
73. Strader CD, Fong TM, Tota MR, Underwood D, Dixon RA (1994) Structure and function of G protein-coupled receptors. Annu Rev Biochem 63: 101–132.
74. Vilar S, Karpiak J, Berk B, Costanzi S (2011) In silico analysis of the binding of agonists and blockers to the beta2-adrenergic receptor. J Mol Graph Model 29: 809–817.
75. Hu LA, Zhou T, Ahn J, Wang S, Zhou J, et al. (2009) Human and mouse trace amine-associated receptor 1 have distinct pharmacology towards endogenous monoamines and imidazoline receptor ligands. Biochemical Journal 424: 39–45.
76. Revel FG, Moreau JL, Gainetdinov RR, Bradaia A, Sotnikova TD, et al. (2011) TAAR1 activation modulates monoaminergic neurotransmission, preventing hyperdopaminergic and hypoglutamatergic activity. Proc Natl Acad Sci U S A 108: 8485–8490.
77. Huang ES (2003) Construction of a sequence motif characteristic of aminergic G protein-coupled receptors. Protein Sci 12: 1360–1367.
78. Tan ES, Groban ES, Jacobson MP, Scanlan TS (2008) Toward deciphering the code to aminergic G protein-coupled receptor drug design. Chem Biol 15: 343–353.
79. Huang J, Hamasaki T, Ozoe F, Ohta H, Enomoto K, et al. (2007) Identification of critical structural determinants responsible for octopamine binding to the alpha-adrenergic-like Bombyx mori octopamine receptor. Biochemistry 46: 5896–5903.
80. Warne T, Moukhametzianov R, Baker JG, Nehme R, Edwards PC, et al. (2011) The structural basis for agonist and partial agonist action on a beta(1)-adrenergic receptor. Nature 469: 241–244.
81. Huang J, Hamasaki T, Ozoe F, Ozoe Y (2008) Single amino acid of an octopamine receptor as a molecular switch for distinct G protein couplings. Biochem Biophys Res Commun 371: 610–614.
82. Rosenkilde MM, Benned-Jensen T, Frimurer TM, Schwartz TW (2010) The minor binding pocket: a major player in 7TM receptor activation. Trends Pharmacol Sci 31: 567–574.
83. Cody V, Meyer T, Dohler KD, Hesch RD, Rokos H, et al. (1984) Molecular structure and biochemical activity of 3,5,3′-triiodothyronamine. Endocr Res 10: 91–99.
84. Meyer T, Hesch RD (1983) Triiodothyronamine--a beta-adrenergic metabolite of triiodothyronine? Horm Metab Res 15: 602–606.
85. Hart ME, Suchland KL, Miyakawa M, Bunzow JR, Grandy DK, et al. (2006) Trace Amine-Associated Receptor Agonists: Synthesis and Evaluation of Thyronamines and Related Analogues. Journal of Medicinal Chemistry 49: 1101–1112.
86. Lewin AH, Navarro HA, Gilmour BP (2009) Amiodarone and its putative metabolites fail to activate wild type hTAAR1. Bioorganic & Medicinal Chemistry Letters 19: 5913–5914.
87. Snead AN, Miyakawa M, Tan ES, Scanlan TS (2008) Trace amine-associated receptor 1 (TAAR1) is activated by amiodarone metabolites. Bioorg Med Chem Lett 18: 5920–5922.
88. Stalder H, Hoener MC, Norcross RD (2011) Selective antagonists of mouse trace amine-associated receptor 1 (mTAAR1): Discovery of EPPTB (RO5212773). Bioorganic & Medicinal Chemistry Letters In Press, Corrected Proof.
89. Tan ES, Miyakawa M, Bunzow JR, Grandy DK, Scanlan TS (2007) Exploring the structure-activity relationship of the ethylamine portion of 3-iodothyronamine for rat and mouse trace amine-associated receptor 1. J Med Chem 50: 2787–2798.
90. Tan ES, Naylor JC, Groban ES, Bunzow JR, Jacobson MP, et al. (2009) The Molecular Basis of Species-Specific Ligand Activation of Trace Amine-Associated Receptor 1 (TAAR1). ACS Chemical Biology 4: 209–220.

10 Curriculum Vitae

Mein Lebenslauf wird aus datenschutzrechtlichen Gründen in der elektronischen Version meiner Arbeit nicht veröffentlicht.

11 Publikationsliste

1. Dinter J*, Khajavi N*, Mühlhaus J, Wienchol CL, Grüters A, Krude H, Cöster M, Schöneberg T, Köhrle J, Mergler S, Kleinau G, Biebermann H. (2015)
The multi-target molecule 3-iodothyronamine is a modulator of beta-adrenergic receptor 2 mediated signaling which affects conjunctival epithelial cell *Europ. Thyroid J*, 2015, in press

2. Dinter J, Mühlhaus J, Jacobi SF, Wienchol CL, Cöster M, Meister J, Hoefig CS, Müller A, Josef Köhrle J, Grüters A, Krude H, Mittag J, Schöneberg T, Kleinau G, Biebermann H. (2015)
3-iodothyronamine differentially modulates alpha-2A adrenergic receptor-mediated signaling *J Mol Endocrinol.* 2015 Apr 15. pii: JME-15-0003. [Epub ahead of print]

3. Dinter J*, Mühlhaus J*, Wienchol CL, Yi CX, Nürnberg D, Morin S, Grüters A, Köhrle J, Schöneberg T, Tschöp M, Krude H, Kleinau G, Biebermann H. (2015)
Inverse agonistic action of 3-iodothyronamine at the human trace amine-associated receptor 5 *PLos One.* 2015 Feb 23;10(2):e0117774. doi: 10.1371/journal.pone.0117774.

4. Mühlhaus J*, Dinter J*, Nürnberg D*, Rehders M, Depke M, Golchert J, Homuth G, Yi CX, Morin S, Köhrle J, Brix K, Tschöp M, Kleinau G, Biebermann H. (2014)
Analysis of Human TAAR8 and Murine Taar8b Mediated Signaling Pathways and Expression Profile. *International journal of molecular sciences* 15, 20638-20655

5. Piechowski CL, Rediger A, Lagemann C, Mühlhaus J, Müller A, Pratzka J, Tarnow P, Grüters A, Krude H, Kleinau G, Biebermann H. (2013)
Inhibition of melanocortin-4 receptor dimerization by substitutions in intracellular loop 2. *Journal of molecular endocrinology* 51, 109-118

6. Müller TD, Müller A, Yi CX, Habegger KM, Meyer CW, Gaylinn BD, Finan B, Heppner K, Trivedi C, Bielohuby M, Abplanalp W, Meyer F, Piechowski CL, Pratzka J, Stemmer K, Holland J, Hembree J, Bhardwaj N, Raver C, Ottaway N, Krishna R, Sah R, Sallee FR, Woods SC, Perez-Tilve D, Bidlingmaier M, Thorner MO, Krude H, Smiley D, DiMarchi R, Hofmann S, Pfluger PT, Kleinau G, Biebermann H, Tschöp MH. (2013)
The orphan receptor Gpr83 regulates systemic energy metabolism via ghrelin-dependent and ghrelin-independent mechanisms. *Nature communications* 4, 1968

7. Müller A, Kleinau G, Piechowski CL, Müller TD, Finan B, Pratzka J, Grüters A, Krude H, Tschöp M, Biebermann H. (2013)
G-protein coupled receptor 83 (GPR83) signaling determined by constitutive and zinc(II)-induced activity. *PloS one* 8, e53347

8. Kleinau G*, Pratzka J*, Nürnberg D, Grüters A, Führer-Sakel D, Krude H, Köhrle J, Schöneberg T, Biebermann H. (2011)
Differential modulation of Beta-adrenergic receptor signaling by trace amine-associated receptor 1 agonists. *PLoS One* 6, e27073

9. Kurischko C, Kim HK, Kuravi VK, Pratzka J, Luca FC. (2011)
The yeast Cbk1 kinase regulates mRNA localization via the mRNA-binding protein Ssd1. *The Journal of cell biology* 192, 583-598

***gleichberechtigte Erstautoren**

12 Eidesstattliche Erklärung

„Ich, Juliane Dinter, versichere an Eides statt durch meine eigenhändige Unterschrift, dass ich die vorgelegte Dissertation mit dem Thema „Funktionelle Selektivität von G-Protein gekoppelten Rezeptoren in der Energiehomöostase“ selbstständig und ohne nicht offengelegte Hilfe Dritter verfasst und keine anderen als die angegebenen Quellen und Hilfsmittel genutzt habe.
Alle Stellen, die wörtlich oder dem Sinne nach auf Publikationen oder Vorträgen anderer Autoren beruhen, sind als solche in korrekter Zitierung (siehe „Uniform Requirements for Manuscripts (URM)“ des ICMJE - *www.**icmje**.org*) kenntlich gemacht. Die Abschnitte zu Methodik (insbesondere praktische Arbeiten, Laborbestimmungen, statistische Aufarbeitung) und Resultaten (insbesondere Abbildungen, Graphiken und Tabellen) entsprechen den URM (s. o.) und werden von mir verantwortet.
Meine Anteile an den ausgewählten Publikationen entsprechen denen, die in der untenstehenden gemeinsamen Erklärung mit der Betreuerin, angegeben sind. Sämtliche Publikationen, die aus dieser Dissertation hervorgegangen sind und bei denen ich Autor bin, entsprechen den URM (s. o.) und werden von mir verantwortet. Die Bedeutung dieser eidesstattlichen Versicherung und die strafrechtlichen Folgen einer unwahren eidesstattlichen Versicherung (§156,161 des Strafgesetzbuches) sind mir bekannt und bewusst.

Datum Juliane Dinter

13 Danksagung

An dieser Stelle möchte ich mich mit tiefer Hochachtung und Respekt bei Frau PD Dr. Heike Biebermann für die Betreuung und Begleitung meiner Dissertation bedanken.

Frau Prof. Dr. Annette Grüters-Kieslich und Herrn Prof. Dr. Heiko Krude danke ich für die freundliche Aufnahme in das Institut für Experimentelle Pädiatrische Endokrinologie.

Mein Dank richtet sich an Dr. Gunnar Kleinau für seine wertvolle Hilfestellung und seine inspirierenden Anregungen.

Desweiteren gebührt Herrn Prof. Dr. Josef Köhrle mein Dank für seine fachlich anregenden Impulse im Rahmen des Graduierten Kollegs 1208 „Hormonal Regulation of Energy Metabolism, Body Weight and Growth“.

Dankeschön an meine Kollegen des Instituts für ihre fachlichen und labortechnischen Hilfestellungen und die stets kollegiale und freundliche Atmosphäre.

Vielen Dank an alle Kooperationspartner und Ko-Autoren für die kreative fachliche Interaktion.

Außerdem danke ich allen, die mir direkt oder indirekt Wissen, Anregungen oder Inspirationen vermittelt haben.

Nicht zu vergessen sind meine dankbaren Empfindungen gegenüber meiner Familie für die allumfassende Unterstützung.